

THREE-DIMENSIONAL NUMERICAL STUDY OF FLAMES SUPPORTED BY A
ROTATING BURNER

BY

KISHWAR N. HOSSAIN

B.S., Lafayette College, 2000

M.S., University of Illinois at Urbana-Champaign, 2003

DISSERTATION

Submitted in partial fulfillment of the requirements
for the degree of Doctor of Philosophy in Aerospace Engineering
in the Graduate College of the
University of Illinois at Urbana-Champaign, 2008

Urbana, Illinois

Doctoral Committee:

Adjunct Professor Thomas Jackson, Chair

Professor John Buckmaster

Associate Professor Gregory Elliott

Assistant Professor Dimitrios Kyritsis

Abstract

In this study non-uniform methane diffusion flames, formed from a porous plug burner spinning in quiescent air are investigated numerically in a three-dimensional context. Flames are simulated for Damköhler numbers on the upper branch of the S-response curve close to the extinction point. Multi-dimensional instabilities appear at these near extinction Damköhler numbers, as observed in experimental studies of flames sustained by a rotating fuel disk [1] and by a rotating porous burner[2], [3].

Simulation results from the constant density and constant viscosity model suggest that the non-uniform flames are a result of thermodiffusional instabilities and are a function of the Damköhler number. Non-uniform flames simulated in this study include flame holes, single armed spirals and double armed spirals. The flame holes have stationary edges and the radius of these holes is found to increase as the Damköhler number is lowered. The single and double spirals have edges that rotate about the axis of the burner. It is found that the velocity of the single spiral relative to the flow is considerably higher than that of the double spiral. It is also found that the shapes of the spirals are affected by the velocity vectors and by interactions between distinct spiral arms. Analyses of the scalar dissipation and cross-scalar dissipation rates of these flames show that the flames are primarily diffusion flames with some premixing near the edges.

Factors, other than the Damköhler number, that are found to significantly affect the stability of the spinning porous plug burner include the mixture strength and the exit velocity at the burner surface. The range of Damköhler number within which the system exhibits non-uniform behaviour is larger at higher values of exit velocity and lower values of mixture strength.

Acknowledgments

I would like to express my gratitude to all those who have contributed to the completion of this thesis. Firstly, I would like to thank my husband, Peshala, for his unrelenting support, encouragement, love and affection. In addition, I would like to thank my parents and my brother for their love and patience. I would also like to thank my father-in-law and mother-in-law for their encouragement.

I wish to acknowledge the continued guidance of my advisors, Professor Thomas L. Jackson and Professor John D. Buckmaster. I am forever indebted to them for providing me with the opportunity to pursue a Ph.D. and I will treasure the knowledge that I have gained from working with them. I would also like to thank Professor Gregory Elliott of the Department of Aerospace Engineering and Professor Dimitrios Kyritsis of the Department of Mechanical Science and Engineering for serving on my thesis committee.

I would like to acknowledge the support of this work by the Center for Simulation of Advanced Rockets (CSAR) at the University of Illinois which is supported by the U.S. Department of Energy under contract number B523819, as a part of its Advanced Simulation and Computing Program (ASC). I would also like to acknowledge the support of Computer Sciences and Engineering (CSE) and the support of AFOSR contract number AF FA9550-06-1-0332, A. Nachman, program manager, for computer time on the Air Force cluster located

at Illinois.

I would like to acknowledge the support of the Champaign Simulation Center, CAT Inc., through Enterprise Works. I would particularly like to thank Mr. Walt Lohmann, Dr. Christopher Ha and Dr. One-Chul Lee from the Champaign Simulation Center.

I would like to give special thanks to Staci Tankersley of AE and Jodi Gritten-Dorsett of CSAR for their continued help. In addition, I would like to thank Diane Jeffers and Kendra Lindsey of AE and Sheryl Hembrey of CSAR. I am also indebted to the Turing support staff, especially Michael Campbell, for all their help with queuing issues on the cluster. I would also like to thank Dr. Luca Massa for his help.

I owe many thanks to Bill Mason, Bill and Kris Hartmann, Jennifer and Filip Rysanek, Jason and Cindy Kamphaus, Chet Hammill, Jim Wrzosek and many others for their friendship and support. Finally, I would like to add that I will always cherish the time I have spent at the University, and for that I thank all those who have contributed to this memorable experience.

Table of Contents

List of Tables.....	viii
List of Figures.....	ix
List of Symbols.....	xii
Chapter 1 Introduction.....	1
Chapter 2 Governing Equations and Boundary Conditions.....	9
2.1 The Constant-Density Model	13
2.2 The Porous Plug Burner	14
2.3 Non-dimensional Equations	17
Chapter 3 Numerical Method.....	20
3.1 One-Dimensional Validation	23
3.2 Parallel Implementation	28
3.3 Solution Methodology	31
3.4 Grid Convergence	32
Chapter 4 Results.....	35
4.1 The Burke-Schumann Flame Sheet	35
4.2 Non-uniform Flames at a Mixture Strength Value of 2.0	39
4.3 Flame Hole	45
4.3.1 Effect of Damköhler Number on Flame Hole Radius	48
4.4 Single Spiral	56
4.4.1 Comparison with Experiment	61
4.4.2 Effect of Damköhler Number on the Single Spiral	62
4.5 Double Spiral	64
4.6 Non-uniform Flames at a Mixture Strength Value of 5.0	67
4.7 Effect of Parameters of Study on the Stability of the System	71
4.8 Scalar and Cross Scalar Dissipation Rates of the Non-uniform Flames	73
4.9 Conclusion	79
Appendix A Nondimensionalizing the Governing Equations.....	80

Appendix B Code Verification	86
B.0.1 Grid Refinement Study	86
B.0.2 Benchmark Studies	88
Appendix C Normal Mode Analysis	94
Appendix D Eigenvalue Problem: Separation of Variables	99
Appendix E Source Code	104
References	171
Curriculum Vitae	174

List of Tables

3.1	Coefficients for optimal (5, 4), $2N$ -storage RK scheme, solution 3 of Carpenter and Kennedy [4]	22
3.2	Comparison of the sum of reaction rates	32
4.1	Damköhler number and flame hole radii	48
4.2	Effect of Parameters of Study on D^*	72
C.1	Transition Damköhler Numbers from the eigenvalue problem and from 3-D simulations for $k = 1$ to $k = 7$	98

List of Figures

1.1	Sketch of a diffusion flame supported by a rotating burner	3
1.2	The S-shaped sesponse curve	6
3.1	Sketch describing the one-dimensional diffusion problem used for code validation [5]	23
3.2	Leading two eigenvalues for one-dimensional code validation problem for $Le = 2.0$, $T_a = 4.0$, $Pe = 0.0$, $T_0 = 0.05$ [5]	25
3.3	Transient solution for one-dimensional code validation problem $Le = 2.0$, $Pe = 0.0$, $T_a = 4.0$, $T_0 = 0.05$ [5]	25
3.4	Steady state solutions for $Le = 2.0$, $Pe = 0.0$, $T_a = 4.0$, $T_0 = 0.05$, a. $D = 1.955e6$, b. $D = 2.050e6$	26
3.5	Transient solution for $Le = 2.0$, $Pe = 0.0$, $T_a = 4.0$, $T_0 = 0.05$, $D = 1.955e6$	27
3.6	Transient solution for $Le = 2.0$, $Pe = 0.0$, $T_a = 4.0$, $T_0 = 0.05$, $D = 2.050e6$	27
3.7	Speedup as a function of the problem size	29
3.8	Efficiency as a function of the number of processors	29
3.9	Scalability of the parallel code	30
3.10	Temperature and reaction rate contours for a 32 x 32 x 32 grid	33
3.11	Temperature and reaction rate contours for a 64 x 64 x 64 grid	33
3.12	Temperature and reaction rate contours for a 96 x 96 x 96 grid	33
3.13	Temperature and reaction rate contours for a 128 x 128 x 64 grid	34
4.1	Burke-Schumann solution, Schvab-Zeldovich variables	37
4.2	Burke-Schumann solution, temperature and species profiles	38
4.3	Non-dimensional velocities	40
4.4	S-shaped response	40
4.5	Temperature contour of a flame hole for $\phi = 2.0$, $Y_{o\infty} = 0.2$, $H_0 = 0.1$, $T_s = 1.0$, $\beta = 25$, $Z_e = 40$ and $D = 1.96$	41
4.6	Temperature contour of a flame hole for $\phi = 2.0$, $Y_{o\infty} = 0.2$, $H_0 = 0.1$, $T_s = 1.0$, $\beta = 25$, $Z_e = 40$ and $D = 1.96$	41
4.7	Temperature contour of a single spiral for $\phi = 2.0$, $Y_{o\infty} = 0.2$, $H_0 = 0.1$, $T_s = 1.0$, $\beta = 25$, $Z_e = 40$ and $D = 1.91$	42
4.8	Temperature contour of a single spiral for $\phi = 2.0$, $Y_{o\infty} = 0.2$, $H_0 = 0.1$, $T_s = 1.0$, $\beta = 25$, $Z_e = 5.43$ and $D = 1.91$	42
4.9	Temperature contour of a double spiral for $\phi = 2.0$, $Y_{o\infty} = 0.2$, $H_0 = 0.1$, $T_s = 1.0$, $\beta = 25$, $Z_e = 40$ and $D = 1.85$	43

4.10	Temperature contour of a double spiral for $\phi = 2.0$, $Y_{\infty} = 0.2$, $H_0 = 0.1$, $T_s = 1.0$, $\beta = 25$, $Z_e = 5.43$ and $D = 1.85$	43
4.11	Temperature and species contours of a flame hole for $\phi = 2.0$, $Y_{\infty} = 0.2$, $H_0 = 0.1$, $T_s = 1.0$, $\beta = 25$, $Z_e = 5.43$ and $D = 1.96$	45
4.12	Temperature and species contours of a flame hole for $\phi = 2.0$, $Y_{\infty} = 0.2$, $H_0 = 0.1$, $T_s = 1.0$, $\beta = 25$, $Z_e = 5.43$ and $D = 1.96$	46
4.13	Radial temperature profile at $\theta = 0rad$	47
4.14	Flame hole radius as a function of Damköhler number	49
4.15	Temperature contours of the flame hole in the xy and the rz planes at $D = 1.96$	50
4.16	Temperature contours of the flame hole in the xy and the rz planes at $D = 1.955$	51
4.17	Temperature contours of the flame hole in the xy and the rz planes at $D = 1.95$	51
4.18	Temperature contours of the flame hole in the xy and the rz planes at $D = 1.945$	52
4.19	Temperature contours of the flame hole in the xy and the rz planes at $D = 1.94$	52
4.20	Reaction rate contours at $D=1.96$	53
4.21	Reaction rate contours at $D=1.955$	53
4.22	Reaction rate contours at $D=1.95$	54
4.23	Reaction rate contours at $D=1.945$	54
4.24	Reaction rate contours at $D=1.94$	55
4.25	Curvature of flame front in the rz plane at stoichiometric vs the radial velocity	55
4.26	Temperature and species contours of a single spiral for $\phi = 2.0$, $Y_{\infty} = 0.2$, $H_0 = 0.1$, $T_s = 1.0$, $\beta = 25$, $Z_e = 5.43$ and $D = 1.91$ at <i>time</i> = 300, 320, 340	58
4.27	Temperature and species contours in the $z\theta$ plane of a single spiral for $\phi = 2.0$, $Y_{\infty} = 0.2$, $H_0 = 0.1$, $T_s = 1.0$, $\beta = 25$, $Z_e = 5.43$ and $D = 1.91$ at <i>time</i> = 340	59
4.28	Single spiral contours and relative velocity vectors for case 1, $D = 1.91$. Contour Values:4, 6, 8.	59
4.29	Slope of leading edge as function of r	60
4.30	Single spiral observed in the experiments of Nayagam and Williams (Printed with permission).	61
4.31	Temperature contours of single spirals for $\phi = 2.0$, $Y_{\infty} = 0.2$, $H_0 = 0.1$, $T_s = 1.0$, $\beta = 25$, $Z_e = 40$ at a. $D = 1.91$, b. $D = 1.88$ and c. $D = 1.86$	62
4.32	Overlay of spirals for $D = 1.90$, $D = 1.88$ and $D = 1.86$	63
4.33	Temperature and species contours of a double spiral for $\phi = 2.0$, $Y_{\infty} = 0.2$, $H_0 = 0.1$, $T_s = 1.0$, $\beta = 25$, $Z_e = 5.43$ and $D = 1.85$ at <i>time</i> = 120, 140, 160	65
4.34	Temperature and species contours in the $z\theta$ plane of a double spiral for $\phi = 2.0$, $Y_{\infty} = 0.2$, $H_0 = 0.1$, $T_s = 1.0$, $\beta = 25$, $Z_e = 5.43$ and $D = 1.85$ at <i>time</i> = 160	66
4.35	Non-dimensional Velocities	68
4.36	S-shaped Response	68
4.37	Temperature contour of a flame hole for $\phi = 5.0$, $Y_{\infty} = 0.2$, $H_0 = 0.1$, $T_s = 1.0$, $\beta = 50$, $Z_e = 5.43$ and $D = 6.7$	69
4.38	Temperature contour of a single spiral for $\phi = 5.0$, $Y_{\infty} = 0.2$, $H_0 = 0.1$, $T_s = 1.0$, $\beta = 50$, $Z_e = 5.43$ and $D = 6.6$	69
4.39	Temperature contour of a double spiral for $\phi = 5.0$, $Y_{\infty} = 0.2$, $H_0 = 0.1$, $T_s = 1.0$, $\beta = 50$, $Z_e = 5.43$ and $D = 6.2$	70

4.40	Temperature, scalar and cross scalar contours in the xy plane of a flame hole for $\phi = 2.0$, $Y_{o\infty} = 0.2$, $H_0 = 0.1$, $T_s = 1.0$, $\beta = 25$, $Z_e = 5.43$ and $D = 1.95$.	77
4.41	Temperature, scalar and cross scalar contours in the xy plane of a single spiral for $\phi = 2.0$, $Y_{o\infty} = 0.2$, $H_0 = 0.1$, $T_s = 1.0$, $\beta = 25$, $Z_e = 5.43$ and $D = 1.9$.	77
4.42	Temperature, scalar and cross scalar contours in the xy plane of a double spiral for $\phi = 2.0$, $Y_{o\infty} = 0.2$, $H_0 = 0.1$, $T_s = 1.0$, $\beta = 25$, $Z_e = 5.43$ and $D = 1.85$	77
B.1	Order of Grid Convergence	87
B.2	Benchmark Problem 1, Grid=16 cubed	89
B.3	Benchmark Problem 1, Grid = 32 cubed	90
B.4	Temperature Profile for Benchmark Problem 2	91
B.5	Error for Benchmark Problem 2	92
B.6	Benchmark Problem 3, Error in the Temperature, Grid = 16 cubed	93
B.7	Benchmark Problem 3, Error in the Species, Grid = 16 cubed	93
C.1	The first eigenvalue as a function of D for several k's, $N = 50$	98

List of Symbols

English Symbols

A_i, B_i, C_i	Runge-Kutta coefficients
b	Angular velocity
B	Pre-exponential factor
C_p	Specific heat
D	Damköhler number
D^*	Highest Damköhler number at which non-uniform flames can be sustained
D_E	Extinction Damköhler number
\bar{D}	Scaling factor for the Damköhler number
D_i	Diffusion coefficient for species i
E	Internal energy; average error
$L2$	Average error
E_p	Parallel efficiency
F, G, H	Similarity variables for the Von Karman spinning disk solution
h	Grid spacing
k	Wave number
Le_i	Lewis number of species i
n	Problem size
N	Total number of grid points
P	Pressure
p	Pressure; number of processors; order of convergence
Pe	Peclet number
Pr	Prandtl number
Q	Heat release
r, θ, z	Cylindrical coordinates
R_u	Universal gas constant
S_p	Speed-up
Sc_i	Schmidt number for species i
T	Temperature
t	Time
T^*	Burke-Schumann flame temperature

u	Radial velocity
v	Tangential velocity
w	Axial velocity
x, y, z	Cartesian coordinates
Y_i	Species i
Z	Mixture fraction
z^*	Burke-Schumann flame location
Z_e	Zeldovich number

Greek Symbols

α_i	Ratio of stoichiometric mass fraction for species i
β	Non-dimensional heat release parameter
χ	Scalar dissipation rate
χ_c	Cross-scalar dissipation rate
χ_s	Scalar dissipation rate at the stoichiometric surface
κ	Curvature
λ	Thermal conductivity
Λ	Reaction rate
μ	Viscosity
ν	Dynamic viscosity
ν_i	Stoichiometric coefficient of species i
ω	Growth rate
ϕ	Mixture strength
ρ	Density
τ	Non-dimensional time
τ_χ	Diffusive time

Chapter 1

Introduction

The evolution of non-uniform flames is typically a manifestation of the intrinsic instabilities of the system. These instabilities lead to dynamics that are unique and offer insight into the conditions necessary for the sustainability of the flame. An understanding of these instabilities can also be of importance to turbulence modeling. The flame supported by a rotating porous plug burner offers a suitable platform for the study of such an instability. Here the non-uniformity appears in the form of flame holes and spirals. The spirals are particularly interesting because they are distinct flames that rotate about the axis of the burner, and thus simultaneously support an ignition front and a trailing extinction front. An instantaneous representation of such a flame in terms of the scalar dissipation rate is characterized by distinct regions separated by edges representing propagation and recession of the flame. This study aims to identify the conditions that render the diffusion flame formed on a rotating porous plug burner unstable, and to analyze the features of the resulting non-uniform flame such as the dynamic edges, the characteristics of which may be of some importance to the study of turbulent flames. We begin our discussion with a more detailed

look at the configuration we are considering and a review of other studies that provide information on the onset of instabilities in diffusion flames.

Rotation of the porous plug causes a flow of the ambient air toward the burner, while there is a steady flow of fuel from the burner exit. Consequently, the fuel and air mix at a finite distance above the burner surface and a diffusion flame is formed, as sketched in figure 1.1. Here, the injection velocity of the fuel is w_0 and the angular velocity of the burner is b_0 . If $b_0 > 0$ then the burner rotates counterclockwise. In this study the fuel is taken to be methane and the oxidizer is air. The viscosity, thermal conductivity, and the specific heat at constant pressure are taken to be constants. The density is also taken to be constant, uncoupling the mass and momentum equations from the energy and species equations. This is a standard modeling approach in combustion and has proven to be robust in identifying important parameters and their effect on stability [6]. The flow is solved, independently of the combustion equations, using the similarity solution for the Von Karman swirling flow [7]. For the combustion equations, a one-step global irreversible reaction is considered and the reaction rate is taken to be of the Arrhenius type. The system of unsteady, three-dimensional equations is then solved numerically using the velocity profiles as inputs.

Experimental studies using the rotating burner configuration show the evolution of non-uniform flames with variations in the rotational speeds of the burner [2], [3]. The experiments commence at low rotational speeds that sustain a steady flat flame. As the rotational speed is increased a pulsating flame hole, characterized by a flame sheet with a circular extinguished region in the center, forms. The hole expands outward until it reaches a critical radius, and then propagates inward to reestablish the flat flame; the cycle continues with frequencies

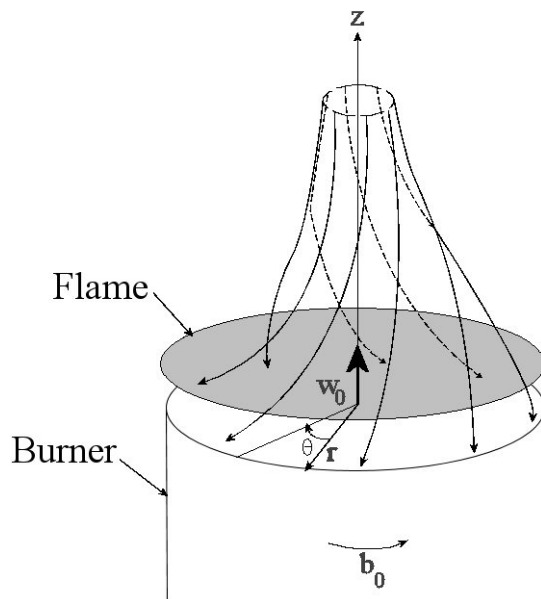


Figure 1.1: Sketch of a diffusion flame supported by a rotating burner

ranging from $1 - 4 \text{ Hz}$. As the rotational speed is increased further this pulsating hole transitions into single-armed, and then multi-armed, spiral flames.

Another set of experiments that use a similar configuration are those performed using a rotating PMMA disk, facing downward, burning in air. These show that steadily burning diffusion flames last for 15 to 20 s at low rotation speeds and high flow rates [1]. In these experiments two distinct flame configurations are observed. In one configuration a circular flame sheet of finite radius is formed and undergoes symmetric shrinking until it is extinguished. In the other, the initial circular flame disintegrates asymmetrically, forms spirals and is extinguished. In a related study Nayagam and Williams [8] investigate the inflammability limits of a stagnation point flow impinging on a spinning fuel disk. Here the authors consider a stagnation point flow with an external radial velocity gradient and a spinning

fuel disk with Arrhenius pyrolysis. This asymptotic study shows that the inflammability boundaries for the one-dimensional system are a function of the strain-rate parameter, a combination of the external radial velocity and the angular velocity of the disk. Thus, the strain-rate is an important parameter and may also have an effect on the stability of the system.

The influence of the strain-rate on the stability of diffusion flames is evidenced by a study of flames formed between opposed slot jet burners [9]. In these experiments a strain-rate gradient along the length of the burners is introduced by a slight misalignment of the burner exits. There is a threshold for the local strain-rate value below which the spatially uniform diffusion flame is replaced by a stable edge flame configuration [10], [11].

An experimental study by Pellet et al. [12] of diffusion flames formed between opposed jet burners shows that increases in the flow velocities causes a disk flame to “rupture” from the center outward. The resulting annular flame shifts axially until it reaches a stable location at the stagnation point of the flow. A reduction of the mass flow rate from the value where the ring flame is observed, leads to a shrinking and shifting of the ring until the disk flame is restored. The subsequent two-dimensional numerical study of Frouzakis et al. [13], reproduces the qualitative results of Pellet et al. [12], and shows that an increase in the Reynolds number of the flow leads to the local extinction of the flat diffusion flame and the formation of an edge-flame. The authors identify a range of Reynolds numbers within which either a diffusion flame or an edge-flame can form. Within this range of Reynolds numbers the type of flame that is obtained is dependent on the initial conditions; however, a mechanism for the transition of a diffusion flame to an edge flame is not established.

In another two-dimensional numerical study, Lu and Ghoshal [14] show that the dynamic behavior of a hole is dependent on the strain rate and the hole radius; for every strain rate there is a critical hole radius that is a bifurcation point and separates the expanding and shrinking behavior.

These destabilizing effects of the strain rate on diffusion flames are reminiscent of the transition from a stable to an unstable branch along the S-shaped response curve shown in figure 1.2. The S-shaped curve represents the typical response of a one-dimensional diffusion flame to variations in Damköhler number (D), the ratio of the chemical reaction rate to the rate of diffusion. Here, D_E represents the extinction point while D_I represents the ignition point. An investigation of the fast-time instability of a counterflow system shows that the top branch of the S-response curve is stable while most of the middle branch is unstable, and that the extinction point is where the flame sheet transitions from a stable to an unstable solution [15]. Sustainable non-uniform flame patterns are typically observed within a narrow range of Damköhler numbers on the upper branch of the S-response curve [16], [17], [18]. Buckmaster and Jackson [19], in their investigation of the propensity of flame holes to close in a zero velocity field, identify detachment Damköhler numbers, the maximum Damköhler number for which a hole will close. Thus, the S-response curve can provide a relatively clear visualization of parameters where the system is unstable.

Although the onset of instability in a system is typically a function of the Damköhler number, there are other parameters that affect the range of Damköhler numbers within which the system is unstable. A theoretical study by Kukuck and Matalon [18], on oscillations in a diffusion flame formed in a semi-infinite domain, shows that increases in the

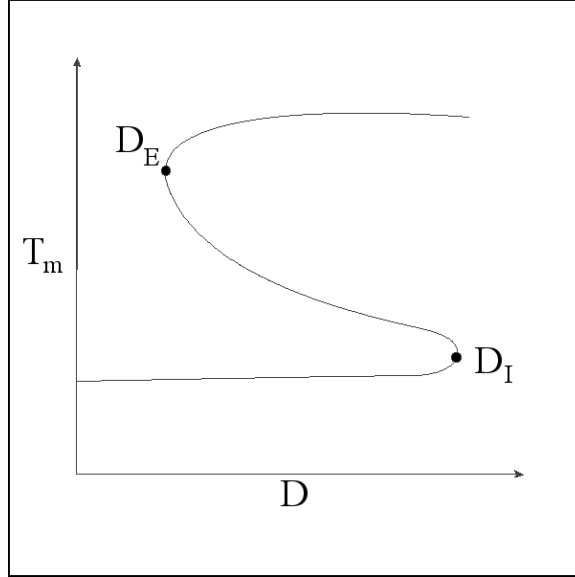


Figure 1.2: The S-shaped response curve

mixture strength (defined as the ratio of the fuel and oxidizer mass fractions at the boundaries normalized by the stoichiometric coefficients), results in an increase in the range of Damköhler numbers where oscillations occur. This study also shows that an increase in the fuel supply temperature relative to the temperature of the oxidizer also promotes the onset of oscillations. The importance of these boundary conditions is also highlighted in a study of a counterflow in a rectangular channel closed at one end [20]. Here the authors show that stable flames formed in the channel consist of an edge near the closed end of the channel and a trailing diffusion flame. From a large Damköhler number analysis on the quasi one dimensional diffusion flame far from the edge they find that the wall boundary conditions have a significant effect on the strength of the diffusion flame. It is shown that there exists a range for the supply mixture strength beyond which a solution for the diffusion flame does not exist. The imposition of the diffusive fluxes at the boundaries leads to weaker flames, which in turn are prone to oscillations if the supply mixture strength has a low enough value.

Heat losses to the channel wall also have an effect on the onset of stability. The effect of heat loss is considered in detail in the context of a premixed flame anchored to a porous plug burner by Margolis [21] and by Buckmaster [22]. These studies show that heat loss to the burner has a stabilizing effect on the left stability boundary of the premixed flame. In terms of the right stability boundary, increases in the heat loss lead to a destabilizing shift till a threshold is reached, beyond which the burner is stabilizing. For high enough values of the activation energy, a Lewis number stability band does not exist.

Another parameter which affects the stability of diffusion flames is the Lewis number. The Lewis number has an affect, primarily, on the type of instability exhibited by a system. Chen et al. [23] observe that cellular flames can only be established close to extinction and for low effective Lewis numbers (Le_{eff}), defined as the Lewis number for the more completely consumed reactant. Cheatham and Matalon [17], in a theoretical study of cellular instabilities in a diffusion flame formed in a semi-infinite domain, show that for $Le_i \leq 1$ there exist unstable modes at D higher than the extinction value. For sufficiently large D the flame is stable. As D is lowered the flame becomes unstable before the extinction value, D_E , is reached. The growth rate for the instabilities increases as D is lowered further. The stability boundaries for different Lewis numbers indicate that, as the Lewis number for the oxidant is lowered, the boundaries shift toward higher values of Le_f making the cellular instability more accessible.

The effect of Lewis numbers on pulsating instabilities for the same configuration is given by Kukuck and Matalon [18]. They show that for a fixed mixture strength and fixed oxidant Lewis number there is a range of fuel Lewis numbers $1 < Le_f < Le_{f*}$ within which

oscillations can occur. An increase in the oxidant Lewis number leads to an expansion of this range and an increase in the range of Damköhler numbers within which the system can support oscillations.

From the discussion above it is evident that the key parameters for the onset of instabilities, and the consequent spatially non-uniform flame structures, in diffusion flames are Damköhler number, Lewis number, the boundary conditions at the injection surface, and the strain rate. In this study we analyze the affect of some of these parameters on the stability of the flame supported by a rotating porous plug burner. We begin with a detailed account of the formulation in section 2 and a discussion of the numerical method in section 3. A discussion of the results is given in section 4.

Chapter 2

Governing Equations and Boundary Conditions

In this study the density is taken to be constant. This facilitates the numerical solution by uncoupling the transport equations from the combustion equations. In doing so the effect of the temperature increase, due to reaction, on the flow is ignored. Consequently, the flow is modeled using the Von Karman spinning disk similarity solution [7]. The dimensional governing equations for a constant density and constant viscosity axisymmetric flow in cylindrical coordinates (r, θ, z) are given by

$$\frac{1}{r} \frac{\partial(ru)}{\partial r} + \frac{\partial w}{\partial z} = 0, \quad (2.1)$$

$$u \frac{\partial u}{\partial r} - \frac{v^2}{r} + w \frac{\partial u}{\partial z} = -\frac{1}{\rho} \frac{\partial p}{\partial r} + \nu \left[\frac{\partial}{\partial r} \left(\frac{1}{r} \frac{\partial ru}{\partial r} \right) + \frac{\partial^2 u}{\partial z^2} \right], \quad (2.2)$$

$$u \frac{\partial v}{\partial r} + w \frac{\partial v}{\partial z} + \frac{1}{r} uv = \nu \left[\frac{\partial^2}{\partial r} \left(\frac{1}{r} \frac{\partial rv}{\partial r} \right) + \frac{\partial^2 v}{\partial z^2} \right], \quad (2.3)$$

$$u \frac{\partial w}{\partial r} + w \frac{\partial w}{\partial z} = -\frac{1}{\rho} \frac{\partial p}{\partial z} + \nu \left[\frac{1}{r} \frac{\partial}{\partial r} \left(r \frac{\partial w}{\partial r} \right) + \frac{\partial^2 w}{\partial z^2} \right], \quad (2.4)$$

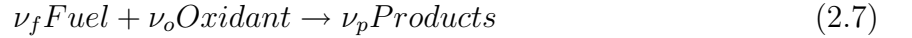
where (u, v, w) are the radial, tangential and axial velocities, respectively. The appropriate boundary conditions are,

$$\text{At } z = 0, \quad u_0 = 0, \quad v_0 = b_0 r, \quad w_0 = w_0, \quad P_0 = 0, \quad (2.5)$$

$$\text{At } z = \infty, \quad u_\infty = 0, \quad v_\infty = 0 \quad \text{and} \quad w_\infty = C. \quad (2.6)$$

At $z = 0$ the burner rotates with an angular velocity of b_0 while fuel is injected from the porous surface. The vertical velocity at the surface is given by, w_0 . The constant C is to be determined as a part of the solution.

A one-step irreversible reaction of the form,



is considered, where ν_f and ν_o are the stoichiometric coefficients of the fuel and oxidant, respectively. The chemical reaction rate is assumed to be Arrhenius. The Mach number is assumed to be low and so the effect of pressure is negligible in the energy and species equations. The unsteady, three-dimensional energy and species equations for constant density and constant viscosity are given by

$$\mathbf{L}[\rho C_p T, \rho Y_i] - \mathbf{M}[\lambda T, \rho D_i Y_i] = \Omega[Q, -\alpha_i], \quad (2.8)$$

where

$$\mathbf{L} = \frac{\partial}{\partial t} + u \frac{\partial}{\partial r} + \frac{v}{r} \frac{\partial}{\partial \theta} + w \frac{\partial}{\partial z},$$

$$\mathbf{M} = \frac{1}{r} \frac{\partial}{\partial r} + \frac{\partial^2}{\partial r^2} + \frac{1}{r^2} \frac{\partial}{\partial \theta^2} + \frac{\partial^2}{\partial z^2}.$$

Here, T is the temperature, Y_i the species mass fraction, Q the heat release, α_i the ratio of

stoichiometric mass fractions, and D_i the diffusion coefficient for species i . Ω is the reaction rate and has the form, $\Omega = BY_oY_f \exp\{-E/R_u T\}$, where B is the pre-exponential factor and E/R_u is the gas phase activation temperature. The boundary conditions are

$$\begin{aligned}
 \text{At } z = 0 : \quad T &= T_s, \quad \frac{\partial Y_f}{\partial z} = \frac{w_o}{D_f}(Y_f - Y_{f0}), \quad Y_o = \frac{w_o}{D_o}Y_o, \\
 \text{At } z = \infty : \quad T &= T_\infty, \quad Y_o = Y_{o\infty}, \quad Y_f = 0, \\
 \text{At } r = \delta : \quad T &= T_{avg}, \quad Y_i = Y_{i_{avg}}, \\
 \text{At } r = \infty : \quad \frac{\partial T}{\partial r} &= 0, \quad \frac{\partial Y_i}{\partial r} = 0, \\
 \text{Periodic in } \theta : \quad T|_{\theta=0} &= T|_{\theta=2\pi}, \quad Y_i|_{\theta=0} = Y_i|_{\theta=2\pi}, \\
 \frac{\partial T}{\partial \theta}|_{\theta=0} &= \frac{\partial T}{\partial \theta}|_{\theta=2\pi}, \quad \frac{\partial Y_i}{\partial \theta}|_{\theta=0} = \frac{\partial Y_i}{\partial \theta}|_{\theta=2\pi}.
 \end{aligned} \tag{2.9}$$

At the burner surface the temperature is set to a constant, T_s . As discussed earlier, this is an important parameter because increases in the temperature differential between the burner exit and the ambient increases the range of Damköhler number within which the system is unstable [18]. Flux conditions are used for the species at the burner surface. At $z = \infty$ the temperature is set to the ambient temperature, T_∞ , while the fuel mass fraction is set to zero and the oxidizer mass fraction is set to the appropriate value for air. Neumann boundary conditions are applied at $r = \infty$, while at $r = 0$ dirichlet conditions derived from averages of the field variables from adjacent θ s are used, that is,

$$T_{avg} = \int_{\theta-a}^{\theta+a} T(\delta, \theta, z) d\theta \tag{2.10}$$

$$Y_{i_{avg}} = \int_{\theta-a}^{\theta+a} Y_i(\delta, \theta, z) d\theta \tag{2.11}$$

with $\delta \ll 1$ and $a = \pi/8$. The temperature and species are taken to be periodic in θ .

2.1 The Constant-Density Model

The constant-density approximation is crucial in rendering combustion problems manageable for analysis. Burke-Schumann in effect introduced this approximation in their pioneering analysis of diffusion flames [24]. The justification for it can be derived from the notion that variations in temperature are a result of combustion and the heat release is small compared to the energy of the mixture, hence, the density variations are small and the velocity field can be approximated to be that of a constant-density fluid to leading order [6]. In most combustion phenomena, however, there are large increases in temperature and its primary effect on the flow is in the form of thermal expansion. Thermal expansion plays a crucial role in premixed flames in terms of promoting an intrinsic hydrodynamic instability, but it does not have a similar effect on diffusion flames. Thus, the constant-density model has been used prudently in numerous studies to model diffusion flames. In a constant-density model, the density is taken to be a constant everywhere, thus neglecting any effects of thermal expansion. In recent years the validity of the constant-density model, in terms of its effect on diffusion flames, has been explored through numerical studies [25], [26], [27].

These studies suggest that although thermal expansion affects flame stability it does not play as crucial a role in diffusion flames as it does in premixed flames. It is found that oscillatory or cellular diffusion flames are typically not driven by hydrodynamic instabilities but are thermo-diffusional in nature [26]. A comparison of growth rates for a planar unstrained flame produced by one reactant introduced at one end of a tubular domain diffusing against a stream of the other reactant at the opposite end, shows that thermal expansion results in a widening of the range of Damköhler numbers, within which cellular instabilities occur

while shrinking the range within which oscillatory instabilities occur [25].

A study of edge flames formed by introducing two streams, one of fuel and the other oxidizer, through porous plugs shows that the effect of thermal expansion is primarily on the standoff of distance of the flame [27]. At low values of axial velocity this effect is small however at higher velocities it is significant.

These studies show that the onset of oscillations in diffusion flames is not a result of the constant-density model. Thermal expansion does have an effect on the quantitative nature of the instabilities in terms of ranges of parameters and stand-off distances, however, the constant-density model generally provides a good approximation to the qualitative results. In terms of the current study, it is expected that thermal expansion would result in the widening of the range of Damköhler numbers within which the instabilities manifest themselves, while having little effect on the qualitative nature of the instabilities.

2.2 The Porous Plug Burner

A porous plug burner is considered in this study primarily for ease of numerical representation. In a porous plug burner the reactant is injected through the burner tube at a controlled rate and a constant temperature; the backflow of products is prevented by the porous plug. It is assumed that the heat conducted back to the burner is removed by cooling coils such that the surface temperature is constant. Thus, the temperature, mass flux and the composition of the reactants can be prescribed at the burner exit. These boundary conditions at the burner exit are expected to affect both the structure and the stability of the diffusion flame. As mentioned earlier, heat loss to the burner affects the stability boundaries

of a premixed flame anchored to a porous plug [21], [22]. Similar effects are expected in the current configuration as evidenced by the experimental studies of Nayagam [3]. Here, a 17.78 *cm* diameter burner is considered and the injection velocity is varied from 0 *cm/s* to 0.20 *cm/s*. In the corresponding map of flame patterns it is shown that for a rotation rate of around 3 *rps* the flame can transition from a single spiral to a semi-circular flame with a straight edge, to a pulsating flame hole as the fuel flow rate increases. Thus, the value of the mass flux is an important parameter of study.

The temperature at the burner exit is also expected to affect the nature of the flame supported by the rotating porous plug. Studies by Kukuck and Matalon [18] and Short and Liu [20] show that an increase in the temperature differential between the reactants has an adverse effect on the stability of the diffusion flame. In the current study the temperature at infinity is set to the ambient, thus the parameter of interest in terms of the temperature differential is T_s . Since the burner exit cannot be cooler than the ambient the minimum possible temperature at the burner exit is T_∞ . This is also expected to be the most stable exit temperature as indicated by [18] and [20]. Previous studies using burners show that under experimental settings, the temperature at the burner exit is likely to be slightly higher than the ambient. Smooke et al [28] find that taking an exit temperature of $1.4T_\infty$ improves correlation of the flame structure and temperature between experiments and two-dimensional numerical simulations. In a more recent numerical study of an axisymmetric counterflow diffusion flame formed between opposing jets, the temperatures at the jet exits were set to 345 *K* at the oxidizer boundary, 315 *K* at the fuel boundary and 350 *K* at the cooling flange boundaries surrounding the burner exits [29]. The results from these numerical sim-

ulations correlated well with the experimental values as well. This suggests, however, that the temperature in the vicinity of the burner exit is likely to be higher than the ambient even when cooling mechanisms are utilized. Thus, in this study two exit temperatures will be considered to evaluate the affect of this boundary condition on the stability of the flame. The ideal case where the exit temperature is set to the value of the ambient, T_∞ , and a case where the exit temperature is $1.4T_\infty$.

2.3 Non-dimensional Equations

For non-dimensionalization, the lengths are scaled by $\sqrt{\nu/b_0}$, time by the reciprocal of b_0 , temperature by T_∞ , and the species by Y_{f0} , the mass fraction of the fuel at the burner exit.

The similarity variables for the velocities are

$$F = \frac{u}{b_0 r}, \quad G = \frac{v}{b_0 r}, \quad H = \frac{w}{\sqrt{b_0 \nu}}, \quad P = \frac{p}{\rho b_0 \nu}, \quad (2.12)$$

where F, G, H and P are functions of z . The resulting non-dimensional equations are

$$H' = -2F, \quad (2.13)$$

$$F'' = F^2 + F'H - G^2, \quad (2.14)$$

$$G'' = 2FG + HG', \quad (2.15)$$

$$P' = 2HF - 2F'. \quad (2.16)$$

Here, one boundary condition is needed for H , two for F , two for G , and one for P. Also, the equation for P is uncoupled from the rest and may be ignored in the simulation. The boundary conditions are given by

$$\begin{aligned} F(0) = 0, \quad G(0) = G_0 = 1, \quad H(0) = H_0, \quad P(0) = 0, \\ F(\infty) = 0, \quad G(\infty) = 0. \end{aligned} \quad (2.17)$$

The non-dimensional unsteady energy and species equations are given by

$$L[T, Y_i] - M[T, Le_i Y_i] = \Omega[\beta, -\alpha_i], \quad (2.18)$$

where

$$\mathbf{L} = \partial/\partial t + rF\partial/\partial r + G\partial/\partial \theta + H\partial/\partial z,$$

$$\mathbf{M} = r^{-1} \partial/\partial r + \partial^2/\partial r^2 + r^{-2} \partial^2/\partial \theta^2 + \partial^2/\partial z^2.$$

Here, $Le_i = \rho C_p D_i / \lambda$, is the Lewis number for species i , $\beta = QY_{f0}/C_p T_0$, the heat release parameter, $\Omega = D\bar{D}Y_o Y_f \exp\{Ze(1 - T^*/T)\}$, the reaction rate, $D = Bb_0^{-1}\rho^{-1}Y_{f0}$, the Damköhler number, the ratio of the chemical reaction rate to the diffusion rate, $Z_e = E/(R_u T_0 T^*)$ the Zeldovich number, $\bar{D} = Ze^3 T^*/z^{*2}$, a scaling factor, and, T^* and z^* the Burke-Schumann flame temperature and flame location, respectively, for the baseline parameters listed in section 4.1. The Prandtl number, $Pr = \nu\rho C_p/\lambda$, is set to 1.0. The boundary conditions are

$$z = 0 : \quad T_0 = T_s, \quad Y_{f_z} = H_0 Le_f (Y_f - 1),$$

$$Y_{o_z} = H_0 Le_o Y_o,$$

$$z = \infty : \quad T_\infty = 1, \quad Y_f = 0, \quad Y_o = \phi^{-1},$$

$$r = \delta : \quad T = T_{avg}, \quad Y_i = Y_{i,avg}$$

$$r = \infty : \quad T_r = 0, \quad Y_{i_r} = 0,$$

and periodic in θ

$$T_\theta|_{\theta=0} = T_\theta|_{\theta=2\pi}, \quad Y_{i_\theta}|_{\theta=0} = Y_{i_\theta}|_{\theta=2\pi},$$

$$T_\theta|_{\theta=0} = T_\theta|_{\theta=2\pi}, \quad Y_{i_\theta}|_{\theta=0} = Y_{i_\theta}|_{\theta=2\pi}.$$

Here, ϕ is the mixture strength defined as the ratio of the fuel mass fraction at the burner surface to the oxidizer mass fraction at infinity. This definition of the mixture strength is not normalized by the stoichiometric coefficients and is thus different from the one used by Kukuck and Matalon [18]. At the burner surface the non-dimensional temperature is set to a constant, T_s , and at $z = \infty$ the temperature is set to the ambient temperature, unity, while

the fuel mass fraction is set to zero. Neumann boundary conditions are applied at the outer radial boundary and Dirichlet conditions at the inner boundary, while the temperature and species are taken to be periodic in θ .

For the current study the fuel is taken to be methane, and the oxidizer is air; thus, $Le_f = 1.0$, $Le_o = 1.0$ $\alpha_f = 0.25$ and $\alpha_o = 1.0$. The mass fraction of air at infinity, $Y_{o\infty}$ is taken to be 0.2. The parameters of study are D , T_s , H_0 , and ϕ while β and Ze are kept constant.

Chapter 3

Numerical Method

The one-dimensional similarity equations of the Von Karman spinning disk flow, given by equations (D.2-D.4), are solved using the COLSYS package [30]. Colsys is a robust collocation package used for solving mixed-order systems of multipoint boundary value problems. It employs a method of spline collocation at Gaussian points [30].

The energy and species equations, (D.7), are solved using a fourth-order centered finite difference scheme in space and a $2N$ -storage, five-stage, fourth-order Runge-Kutta scheme, (5,4) *RK*, in time [4]. The fourth order centered difference schemes is used because it provides high accuracy and is relatively easy to implement on a parallel platform. Section B.0.1 gives a summary of the grid refinement study that shows that the centered difference scheme is fourth order accurate.

The $2N$ -storage (5,4) *RK* scheme is used due to its high accuracy and low storage requirements. The low-storage feature is especially relevant due to the relatively large problem sizes being considered in this study. The $2N$ -storage method for an initial value problem

$$U_t = F[t, U(t)]; \quad U(t_0) = U_0, \quad (3.1)$$

is given by

$$\begin{aligned}
 t_j &= t^N + C_j * h, \\
 dU_j &= A_j dU_{j-1} + hF(U_j), \\
 U_j &= U_{j-1} + B_j dU_j, \quad j = 1, \dots, M,
 \end{aligned} \tag{3.2}$$

where, h is the time step and j is a step in the *RK* scheme. Also, $U_1 \equiv U^N$, $U_M \equiv U^{N+1}$, $t_M \equiv t^{N+1}$, and the scheme is self-starting so that $A_1 = 0$. Thus, in a 2N storage scheme only the dU and U vectors need to be stored. The coefficients, A_j , B_j and C_j of the 2N storage (5,4) RK scheme used in this study are given in table 3. Carpenter and Kennedy [4] have shown that the non-linear accuracy for the (5,4) *RK* is higher than that for the (4,4) *RK* and that in terms of the work ratio the (5,4) *RK* is nearly as efficient. In comparison to the Williamson (3,3) *RK*, 2N storage[31] the (5,4) *RK* has higher accuracy for a given step size and greater stability boundaries [4]. Section B.0.2 also gives results from benchmark studies used to verify the capabilities of the code in solving simplified problems, the analytical solutions of which are known.

Coefficient	Value
A_1	0.0
A_2	-0.4178904745
A_3	-1.192151694643
A_4	-1.697784692471
A_5	-1.514183444257
B_1	0.1496590219993
B_2	0.3792103129999
B_3	0.8229550293869
B_4	0.6994504559488
B_5	0.1530572479681
C_1	0.0
C_2	0.1496590219993
C_3	0.3704009573644
C_4	0.6222557631345
C_5	0.9582821306748

Table 3.1: Coefficients for optimal $(5, 4)$, $2N$ -storage RK scheme, solution 3 of Carpenter and Kennedy [4]

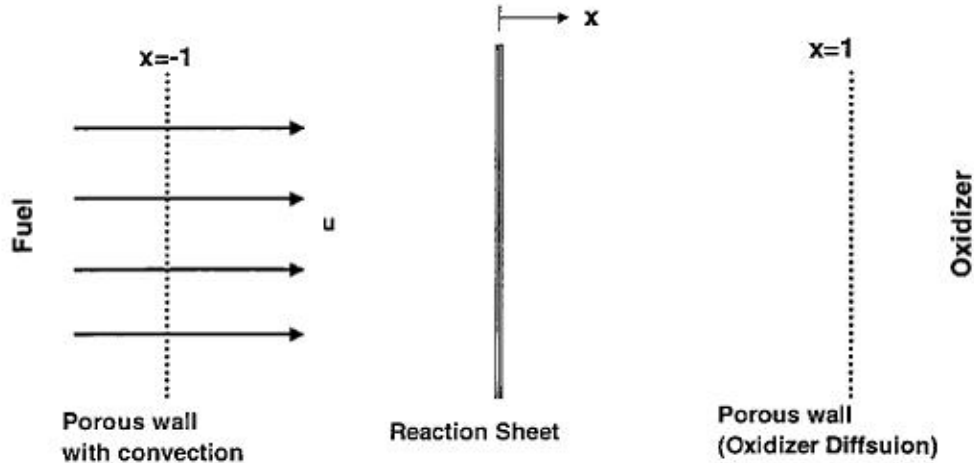


Figure 3.1: Sketch describing the one-dimensional diffusion problem used for code validation [5]

3.1 One-Dimensional Validation

A validation study is undertaken to compare the one-dimensional results obtained from the current solver with those obtained by Vance et al [5] for a diffusion flame between plane parallel porous walls. Vance et al [5], investigate the stability of a one-dimensional problem with flowing fuel and diffusing oxidant ($Le_f = Le_o = 1$) on opposite sides of the reaction sheet. Using perturbation analysis they find that for Lewis numbers less than unity the upper branch of the S response curve is stable and the middle branch is unstable. At Lewis numbers greater than unity there are damped oscillations for $1 < Le < Le_c$ but the entire upper branch is stable. For Lewis numbers greater than a critical value L_c the beginning of the upper branch of the S response curve is unstable.

Figure 3.1 shows a sketch of the problem considered. Here the fuel travels through a porous wall at a finite speed u toward another porous wall with diffusing oxidizer. A flame sheet forms from the interaction of the fuel and the diffused oxidizer. The flow

is assumed to be uniform, radiative heat losses are ignored, and a single step irreversible Arrhenius reaction is assumed [5]. The non-dimensional equations are given by

$$\frac{\partial T}{\partial t} + Pe \frac{\partial T}{\partial x} = \frac{\partial^2 T}{\partial x^2} + \omega, \quad (3.3)$$

$$\frac{\partial y_i}{\partial t} + PeLe \frac{\partial y_i}{\partial x} = \frac{\partial^2 y_i}{\partial x^2} - \omega, \quad (3.4)$$

where $i = O, F$. The boundary conditions are

$$T = T_o \quad y_F = 1 \quad y_O = 0 \quad \text{at } x = -1,$$

$$T = T_o \quad y_F = 0 \quad y_O = 1 \quad \text{at } x = +1.$$

Figure 3.2 shows the two leading eigenvalues for this problem for a Lewis number of 2.0, where the two eigenvalues form a complex conjugate pair beyond point B' . Between points B' and C' the real parts of the eigenvalues are positive thus implying that the flame is unstable for this range of Damköhler numbers and so small perturbations would lead to oscillations which grow in time and eventually result in extinction. Beyond C' , however, perturbations would cause damped oscillations resulting in a non-oscillatory steady state. This behavior is also illustrated by solving equations 3.3-3.4 using a second-order correct finite difference method and the results from this are shown in Figure 3.3, where the unstable solution is for a Damköhler number lower than C' and the stable solution is for a Damköhler number greater than that at C' .

For the purposes of code validation the above system is solved using the finite difference solver used in the current study. The steady state solution of the system given in equations

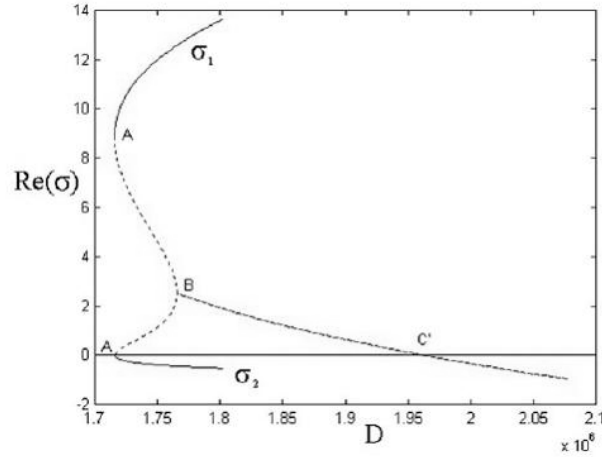


Figure 3.2: Leading two eigenvalues for one-dimensional code validation problem for $Le = 2.0$, $T_a = 4.0$, $Pe = 0.0$, $T_0 = 0.05$ [5]

3.3 and 3.4 are computed using COLSYS [30] and used as initial conditions for the solver. Figures 3.4 a and b show the steady state solutions at Damköhler numbers of $1.955e6$ and $2.050e6$ respectively.

Figures 3.5 and 3.6 shows transient results obtained for $Le = 2.0$, $Pe = 0.0$, $T_a = 4.0$, $T_0 = 0.05$. As seen from this plot, the results are similar to the ones obtained by Vance

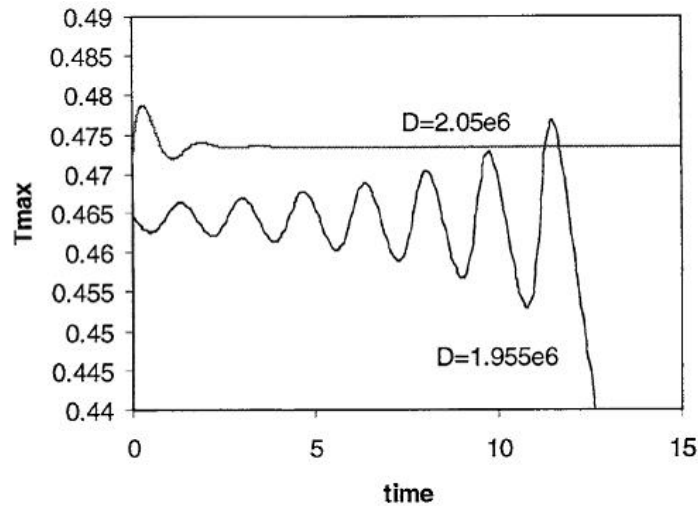
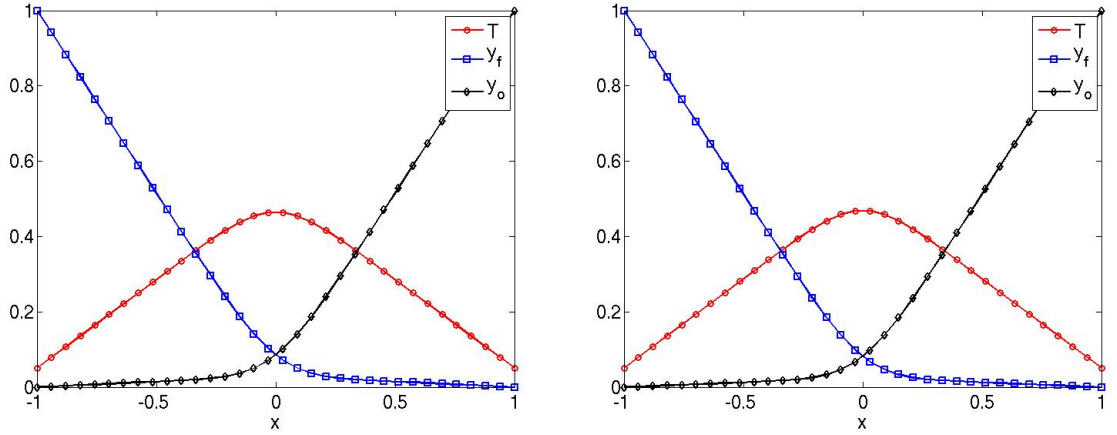


Figure 3.3: Transient solution for one-dimensional code validation problem $Le = 2.0$, $Pe = 0.0$, $T_a = 4.0$, $T_0 = 0.05$ [5]



a.

b.

Figure 3.4: Steady state solutions for $Le = 2.0$, $Pe = 0.0$, $T_a = 4.0$, $T_0 = 0.05$, a. $D = 1.955e6$, b. $D = 2.050e6$

et al. Small perturbations at $D = 2.050e6$ cause damped oscillations which eventually die down and lead to a non-oscillatory steady state. At $D = 1.955e6$ the system is unstable and the amplitude of the oscillations increase with time and eventually the flame is extinguished. These results show that the finite difference solver is able to capture both the steady state and the transient characteristics of the simplified problem considered by Vance et. al. [5]. These results validate the finite different solver in one dimension, and the same finite difference scheme is used in all three spatial dimensions.

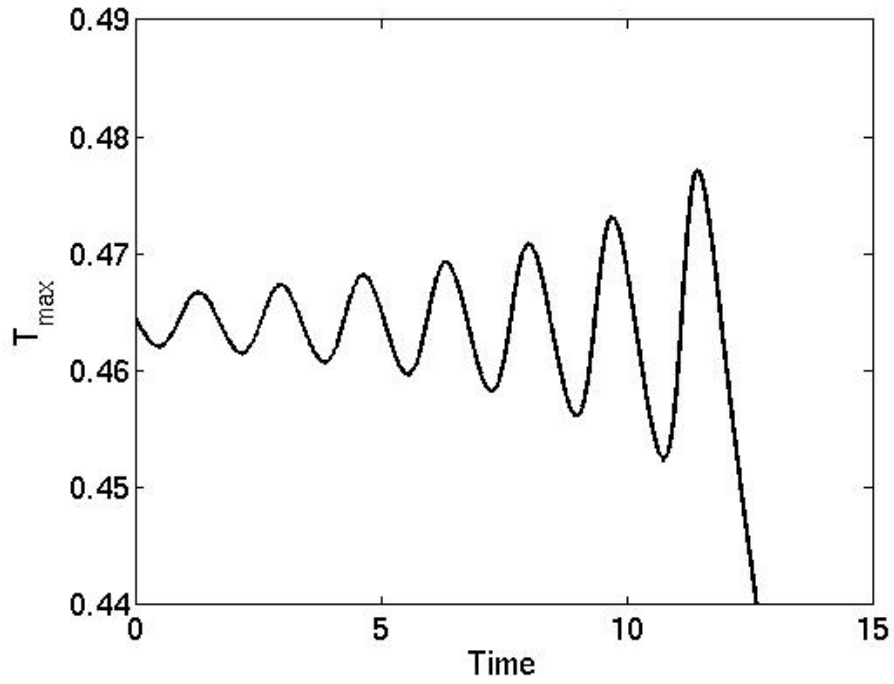


Figure 3.5: Transient solution for $Le = 2.0$, $Pe = 0.0$, $T_a = 4.0$, $T_0 = 0.05$, $D = 1.955e6$

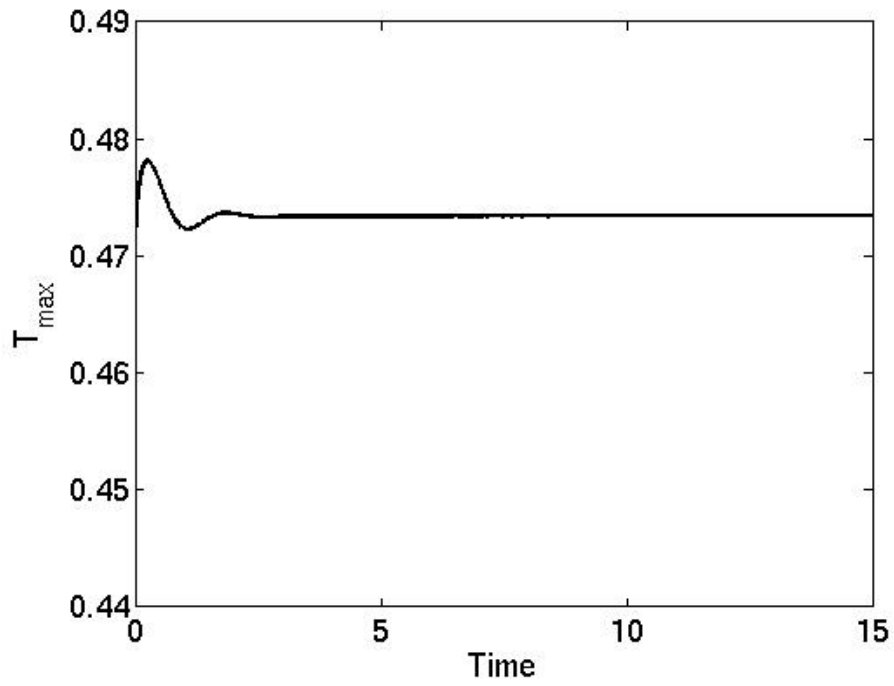


Figure 3.6: Transient solution for $Le = 2.0$, $Pe = 0.0$, $T_a = 4.0$, $T_0 = 0.05$, $D = 2.050e6$

3.2 Parallel Implementation

The solver is adapted for parallel processing using the Message Passing Interface (MPI). In the parallel implementation each processor is assigned a portion of the three-dimensional domain. A processor completes each step of the Runge-Kutta iterations for its domain and then communicates with its neighbor to exchange the necessary boundary values. Results of a performance study for the parallel implementation are given in figures 3.7 and 3.8. Here the problem size, n , is given by,

$n = 16$: 16 X 16 X 16 in (r, θ, z) ,

$n = 32$: 32 X 32 X 32,

$n = 64$: 64 X 64 X 64,

$n = 128$: 128 X 128 X 128,

and p is the number of processors. The speedup (S_p) [32] is defined as,

$$S_p = \frac{\text{serial time}}{\text{parallel time}} = \frac{t_1}{t_p}, \quad (3.5)$$

and the efficiency (E_p) [32], is defined as,

$$E_p = \frac{\text{serial cost}}{\text{parallel cost}} = \frac{t_1}{pt_p}. \quad (3.6)$$

Here, the serial time, t_1 , is the time taken for one processor to complete an assigned task, and the parallel time, t_p , is the time taken for p processors to complete the same task in parallel.

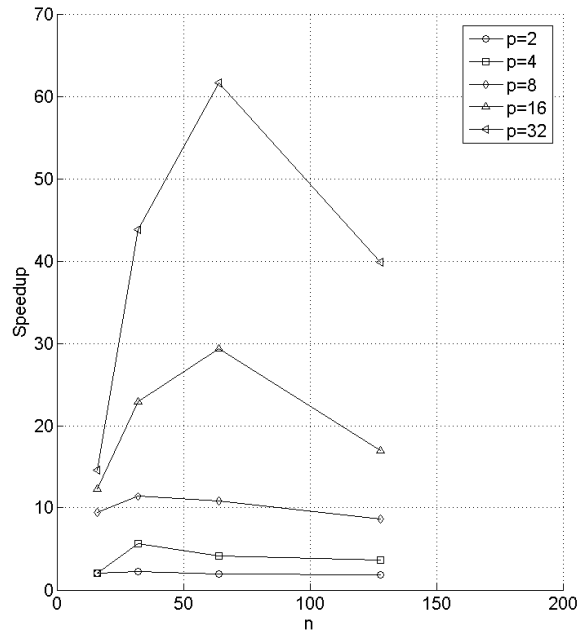


Figure 3.7: Speedup as a function of the problem size

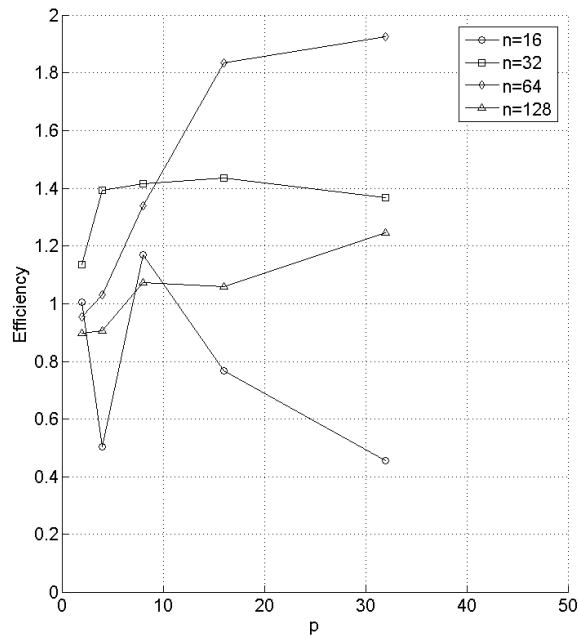


Figure 3.8: Efficiency as a function of the number of processors

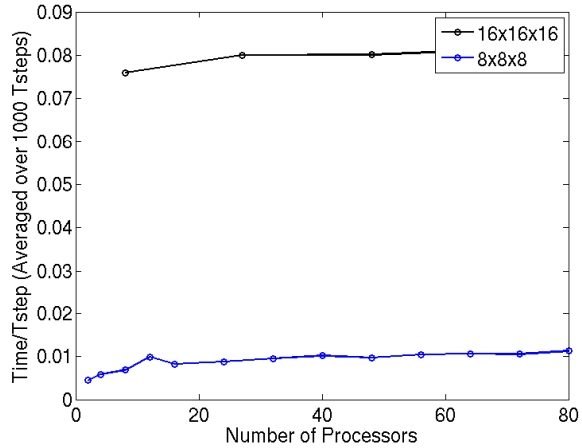


Figure 3.9: Scalability of the parallel code

Figure 3.7 shows the speedup as a function of the problem size for different number of processors. It is evident that an increase in the number of processors results in an increase in the speedup. As the problem size is increased, at first the speedup increases but it reaches a peak value and then decreases until it asymptotes to a particular value. Figure 3.8 shows that the efficiency is higher than 1 for most of the problem size/number of processor combinations. The solver is inefficient when the problem size is too small relative to the number of processors used. In these cases the communication time between the processors is higher than the time necessary for the computations and so additional processors actually result in longer run times.

Figure 3.9 demonstrates the scalability of the parallel code with increasing number of processors. Here, each processor is assigned either 8^3 or 16^3 grid points. As seen from the figure, the time taken remains fairly constant with increasing number of processors, and the consequent increase in the total problem size.

3.3 Solution Methodology

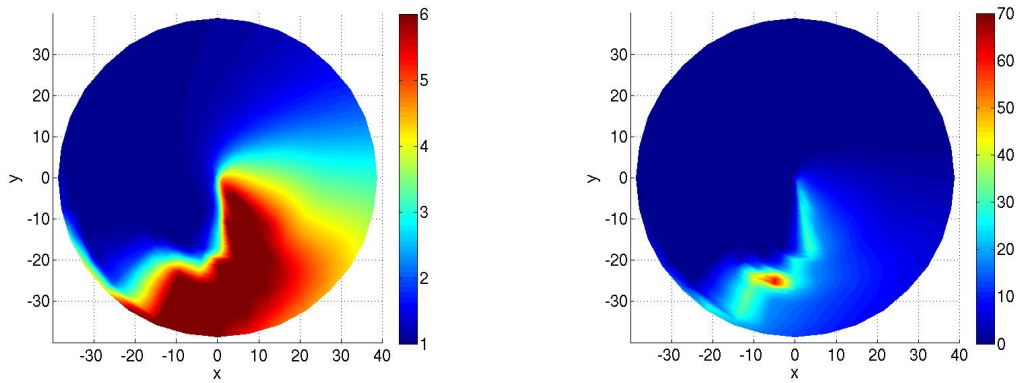
In order to solve the three-dimensional unsteady energy and species equations, the one-dimensional Burke-Schumann type flame sheet solution is used as the initial condition. This solution is computed using COLSYS [30]. This is a reasonable approach since the simulations commence at large Damköhler numbers where the fast chemistry limit is valid, and so the response is one-dimensional. Radial and angular perturbations are introduced into the system once the steady state solution is reached for a given Damköhler number. If the small perturbations do not grow and the flat flame persists, the simulations are restarted at a lower Damköhler number using the three-dimensional unperturbed solution from the previous Damköhler number as the initial condition. This process is repeated till the system becomes unstable to the perturbations and non-uniform flames appear.

3.4 Grid Convergence

Figures 3.10-3.13 show contour plots for the temperature and reaction rate for four different grids. The parameters used for these simulations are $D = 0.14$, $\phi = 2$, $H_0 = 0.1$, $T_s = 1.0$, $\beta = 20$, and $Z_e = 15$. As seen from figure 3.10 the flame is not fully resolved when a 32^3 grid is used, however, it is evident from 3.11-3.13 that the contours vary little as the grid densities in r and θ are increased from 64^3 - $128 \times 128 \times 64$. The flame rotates counter-clockwise and the oscillations at the trailing edge of the flame are seen in all three cases. These oscillations are difficult to resolve due to the dynamic nature of the flame. Although there are some differences in the size of the spiral between the grids, the general shape of the spiral is grid independent. Comparison of the integral value of the reaction rates over the entire spatial domain, between the 64^3 , 96^3 and the $128 \times 128 \times 64$ grids, given in table 3.2, shows differences within 5% between the 64^3 and the two finer grids. Thus, for the results shown in the following sections a 64^3 grid is used.

Grid	\int Reaction Rate	Difference (%)
64^3	1.27×10^3	
96^3	1.22×10^3	3.94
$128 \times 128 \times 64$	1.21×10^3	4.72

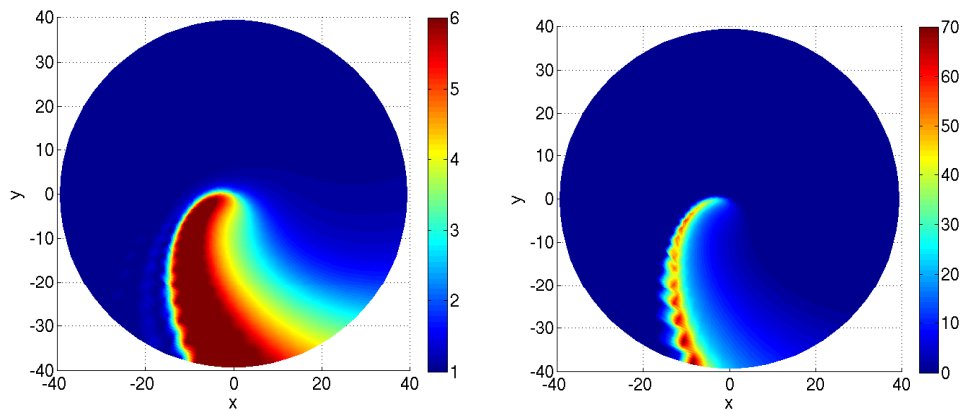
Table 3.2: Comparison of the sum of reaction rates



a. Temperature

b. Reaction Rate

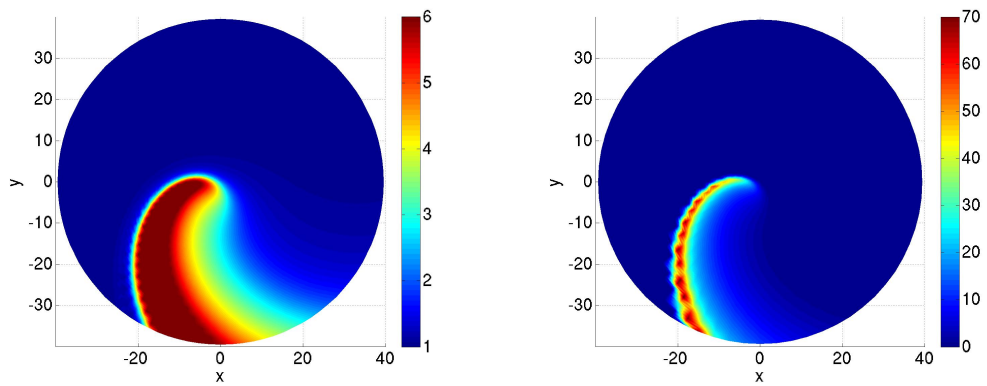
Figure 3.10: Temperature and reaction rate contours for a 32 x 32 x 32 grid



a. Temperature

b. Reaction Rate

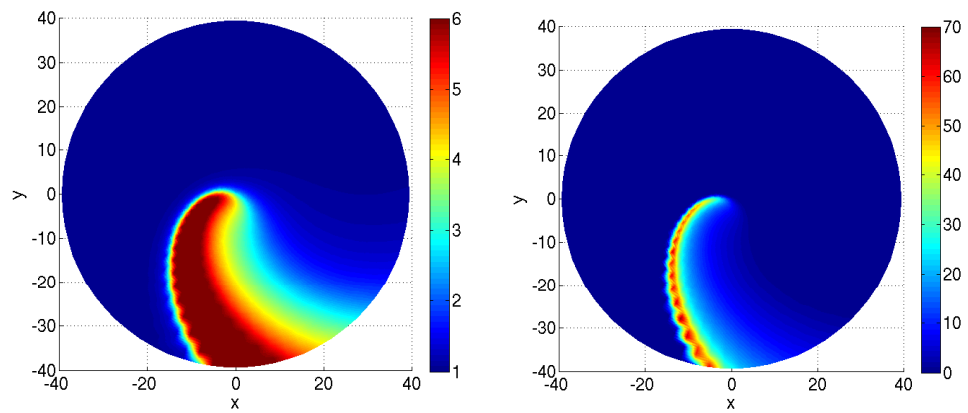
Figure 3.11: Temperature and reaction rate contours for a 64 x 64 x 64 grid



a. Temperature

b. Reaction Rate

Figure 3.12: Temperature and reaction rate contours for a 96 x 96 x 96 grid



a. Temperature

b. Reaction Rate

Figure 3.13: Temperature and reaction rate contours for a 128 x 128 x 64 grid

Chapter 4

Results

4.1 The Burke-Schumann Flame Sheet

The Burke-Schumann limit is important to consider in order to gain a fundamental understanding of the diffusion flame, and to establish initial conditions for numerical solutions. This limit arises as $D \rightarrow \infty$ resulting in an infinite reaction rate that can be balanced by taking the flame sheet to be very thin such that $Y_f Y_0 \rightarrow 0$. This thin flat flame sheet forms at a distance z^* from the burner surface and separates the fuel and the oxidizer. At this limit the combustion field is expected to be a function of z and t only. The energy and species equations then become

$$\mathbb{L}(T) = -\beta\alpha_i^{-1}\mathbb{L}(Y_i) = \Omega, \quad (4.1)$$

where

$$\mathbb{L} = \frac{\partial}{\partial t} - H \frac{\partial}{\partial z} - \frac{\partial^2}{\partial z^2} \quad (4.2)$$

however it should be noted that only the steady state is considered in order to solve for the Burke-Schumann flame sheet. The boundary conditions are

$$\text{at } z = 0, \quad T = T_s, \quad \frac{\partial Y_f}{\partial z} = H_0(Y_f - 1), \quad Y_o = 0, \quad (4.3)$$

$$\text{at } z \rightarrow \infty, \quad T = T_\infty, \quad Y_f = 0, \quad Y_o = \phi^{-1}. \quad (4.4)$$

The Schvab-Zeldovich variables are

$$Z_+ = T + \beta\alpha_f^{-1}Y_f \quad \text{and} \quad Z_- = T + \beta\alpha_o^{-1}Y_o. \quad (4.5)$$

As $D \rightarrow \infty$,

$$\mathbb{L}(Z_+) = \mathbb{L}(Z_-) = 0 \quad (4.6)$$

and the boundary conditions are

$$\text{at } z = 0, \quad \frac{\partial Z_+}{\partial z} = \frac{\partial Z_-}{\partial z} + H_0(Z_+ - T_s - \beta\alpha_f^{-1}), \quad Z_- = T_s,$$

and

$$\text{at } z \rightarrow \infty, \quad Z_+ = T_\infty, \quad Z_- = T_\infty - \beta\phi^{-1}$$

Thus, the temperature and species profiles are given by,

$$0 < z < z^* : \quad T = Z_+, \quad Y_f = \beta^{-1}\alpha_f(Z_- - Z_+), \quad Y_o = 0,$$

and

$$z^* < z < z_\infty : \quad T = Z_-, \quad Y_f = 0, \quad Y_o = \beta^{-1}\alpha_o(Z_+ - Z_-).$$

The matching condition

$$Z_+(z^*) = Z_-(z^*) \quad (4.7)$$

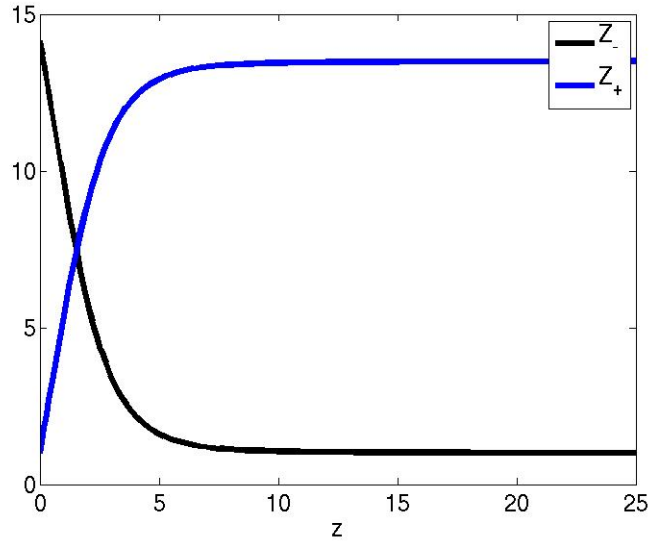


Figure 4.1: Burke-Schumann solution, Schwab-Zeldovich variables

is used to determine z^* . The steady state solutions for Z_+ and Z_- are obtained using COLSYS and are shown in figure 4.1 while the temperature and species profiles are shown in figure 4.2. As seen from this figure, for $H_0 = 0.1$, $T_s = 1.0$ and $\beta = 25.0$, the baseline parameters for this study, the Burke-Schumann flame temperature, $T^* = 7.43$, and the flame location, $z^* = 1.54$. These of the flame temperature and flame location are used in section 2.3 in the scaling factor for the Damköhler number.

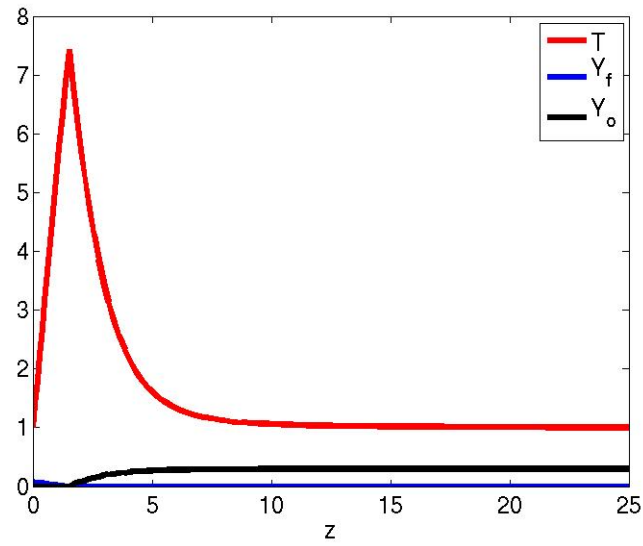


Figure 4.2: Burke-Schumann solution, temperature and species profiles

4.2 Non-uniform Flames at a Mixture Strength Value of 2.0

The stability of the three-dimensional spinning burner configuration is investigated using small pure mode perturbations. It is found that at appropriate Damköhler numbers these perturbations result in non-uniform flame patterns such as holes and spirals. This phenomenon is first investigated for parameter values of $\phi = 2.0$, $Y_{o\infty} = 0.2$, $H_0 = 0.1$, $T_s = 1.0$, $\beta = 25$, and $Z_e = 40$. Figures 4.3 and 4.4 show the velocity profiles and the S-shaped response curve for this set of parameters. The extinction point, D_E , is approximately 1.48 as seen from figure 4.4. $D^* = 1.96$ represents the highest Damköhler number at which sustainable non-uniform flames appear. The non-uniform flames observed in this study include flame holes, single spirals and double spirals as shown in figures 4.6-4.10.

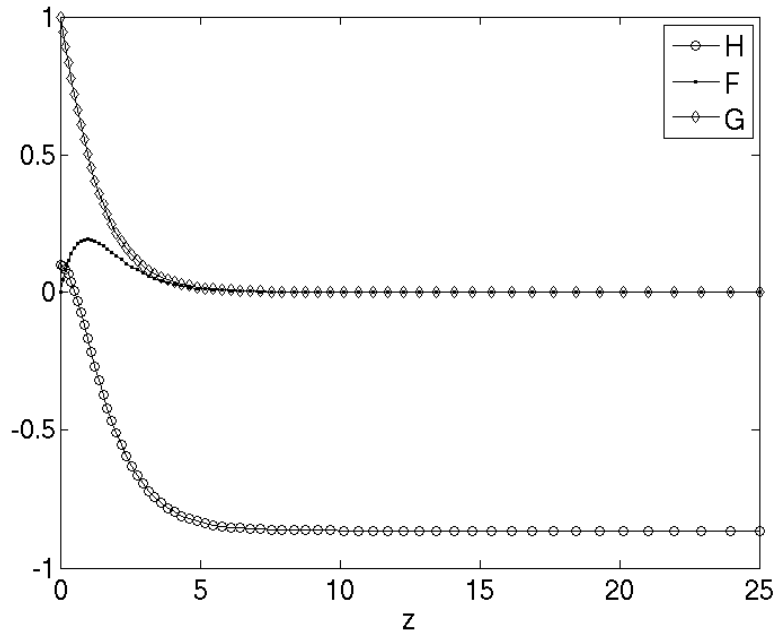


Figure 4.3: Non-dimensional velocities

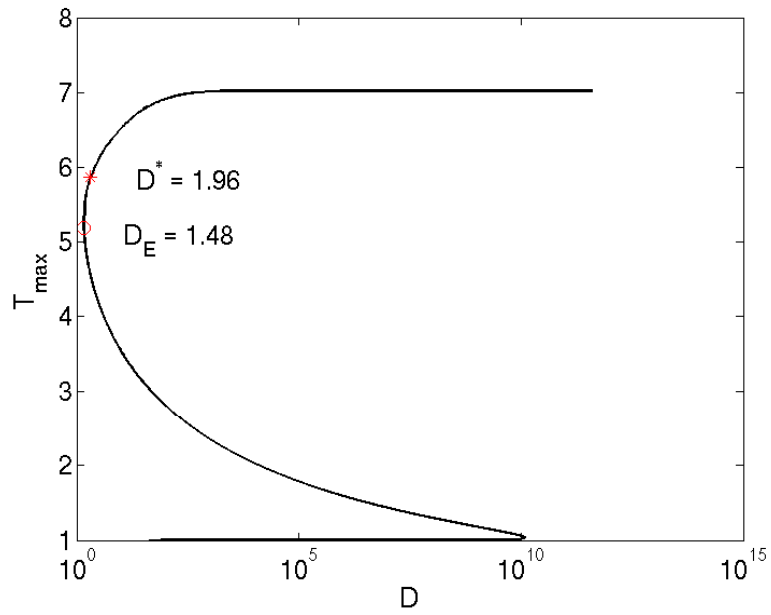


Figure 4.4: S-shaped response

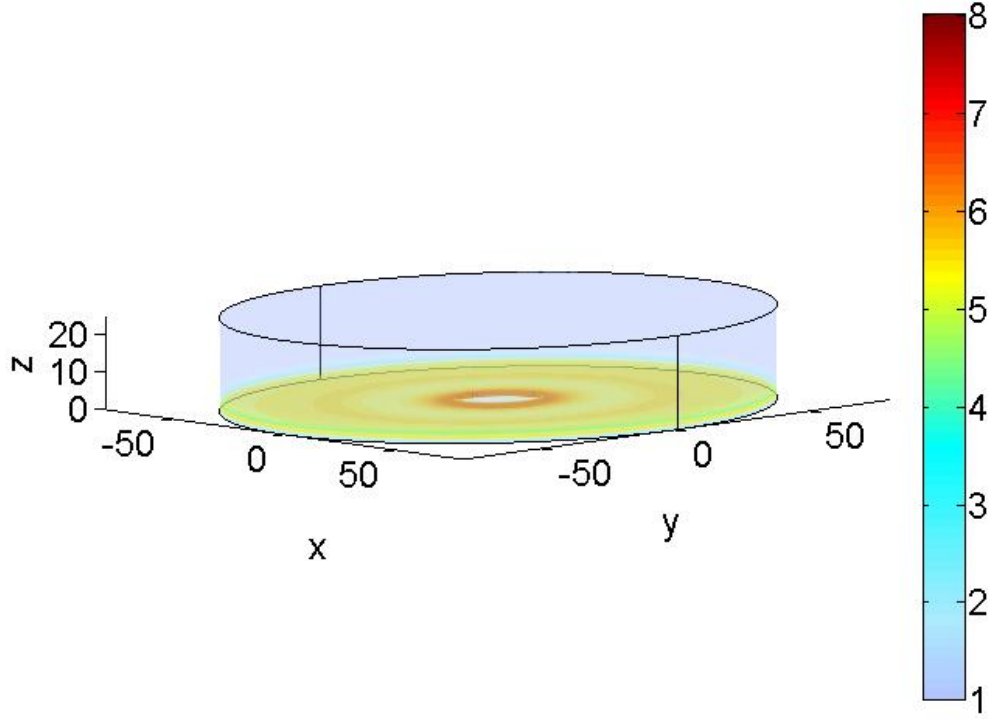


Figure 4.5: Temperature contour of a flame hole for $\phi = 2.0$, $Y_{o\infty} = 0.2$, $H_0 = 0.1$, $T_s = 1.0$, $\beta = 25$, $Z_e = 40$ and $D = 1.96$

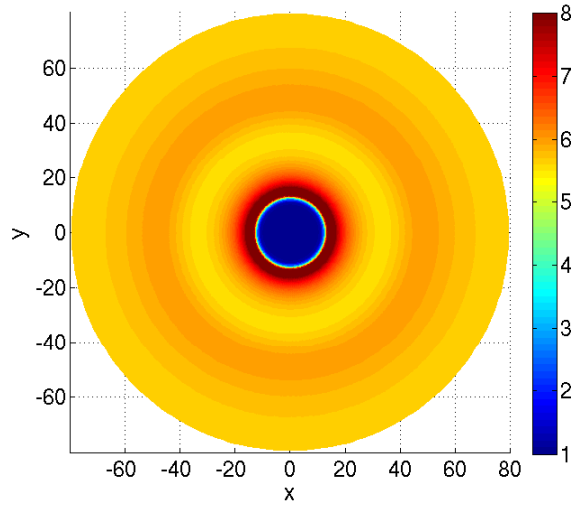


Figure 4.6: Temperature contour of a flame hole for $\phi = 2.0$, $Y_{o\infty} = 0.2$, $H_0 = 0.1$, $T_s = 1.0$, $\beta = 25$, $Z_e = 40$ and $D = 1.96$

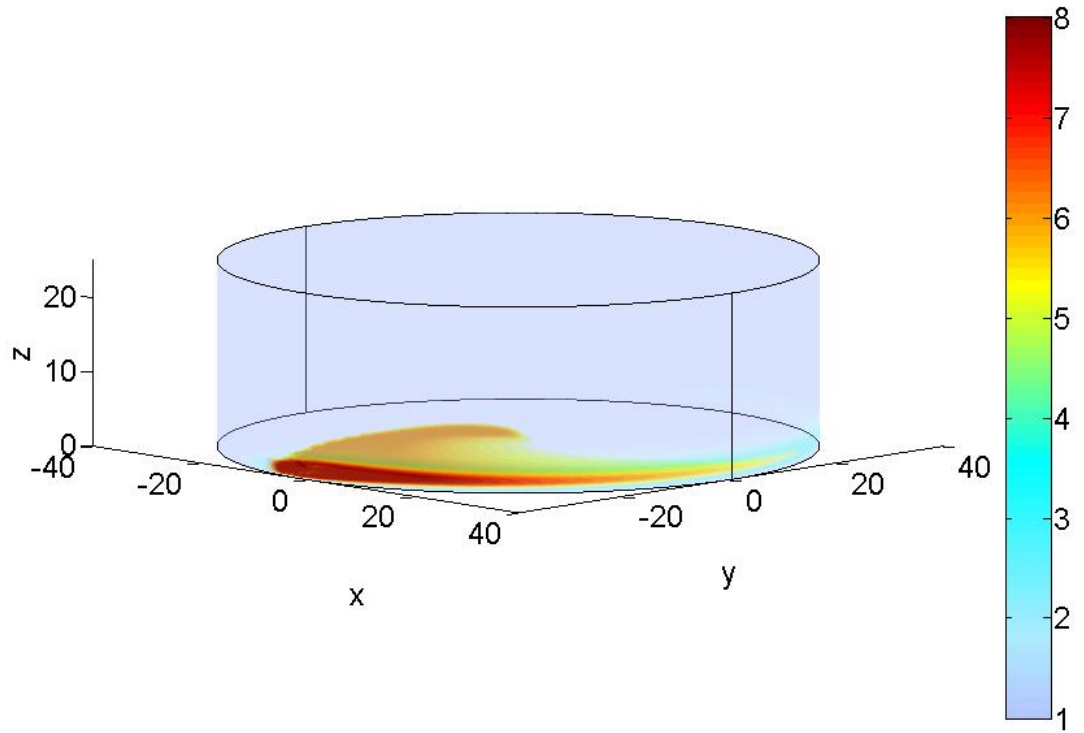


Figure 4.7: Temperature contour of a single spiral for $\phi = 2.0$, $Y_{o\infty} = 0.2$, $H_0 = 0.1$, $T_s = 1.0$, $\beta = 25$, $Z_e = 40$ and $D = 1.91$

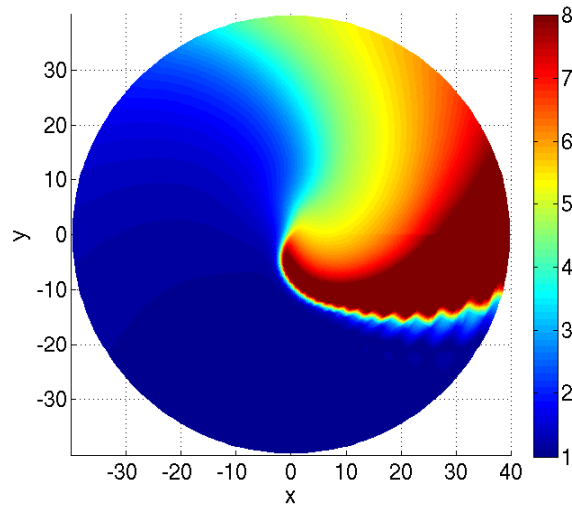


Figure 4.8: Temperature contour of a single spiral for $\phi = 2.0$, $Y_{o\infty} = 0.2$, $H_0 = 0.1$, $T_s = 1.0$, $\beta = 25$, $Z_e = 5.43$ and $D = 1.91$

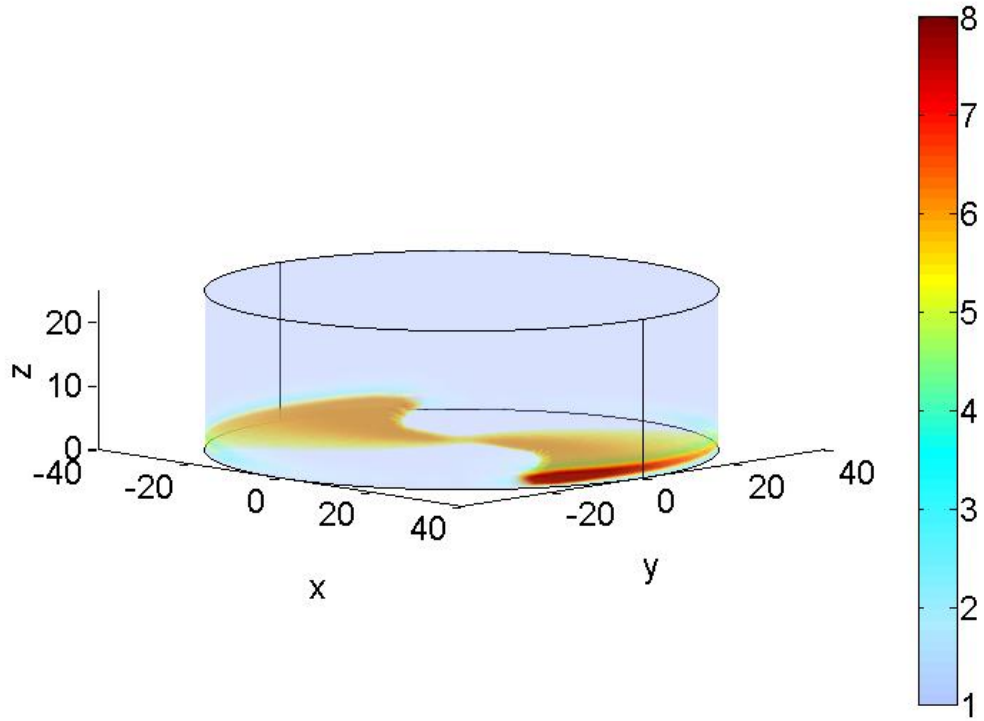


Figure 4.9: Temperature contour of a double spiral for $\phi = 2.0$, $Y_{\infty} = 0.2$, $H_0 = 0.1$, $T_s = 1.0$, $\beta = 25$, $Z_e = 40$ and $D = 1.85$

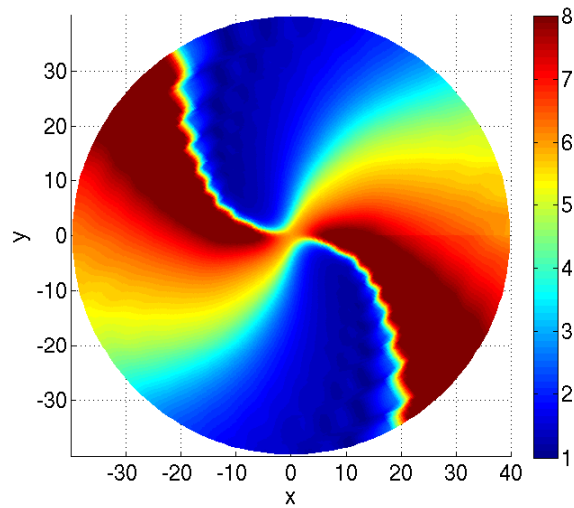


Figure 4.10: Temperature contour of a double spiral for $\phi = 2.0$, $Y_{\infty} = 0.2$, $H_0 = 0.1$, $T_s = 1.0$, $\beta = 25$, $Z_e = 5.43$ and $D = 1.85$

As seen from figure 4.4 the range of Damköhler numbers within which these non-uniform flames appear is small. However, this range can be further divided into smaller groups where different modes are viable. For example, for the set of parameters listed above, the flame hole appears for $D = 1.96$ to $D = 1.92$, while single spirals appear for $D = 1.91$ to $D = 1.85$ and so on. It is expected that as the Damköhler number is lowered further the ranges within which higher modes are sustained can also be determined. However, for this section the discussion is limited up to double spirals, primarily due to the fact that for the higher modes the ranges become smaller and so it is difficult to identify distinct regions corresponding to each mode. The progression of the flames from the flame hole to the single armed and then the multiarmed spirals with decreasing Damköhler number is reminiscent of the observations of Nayagam and Williams [3] where the flames transition from flame holes to spirals with increasing angular velocity. It should be noted here that in the current formulation the Damköhler number is inversely proportional to the angular velocity. Thus the trends observed in the simulations are similar to those found in the experimental studies. The flame patterns are analyzed further in the following sections.

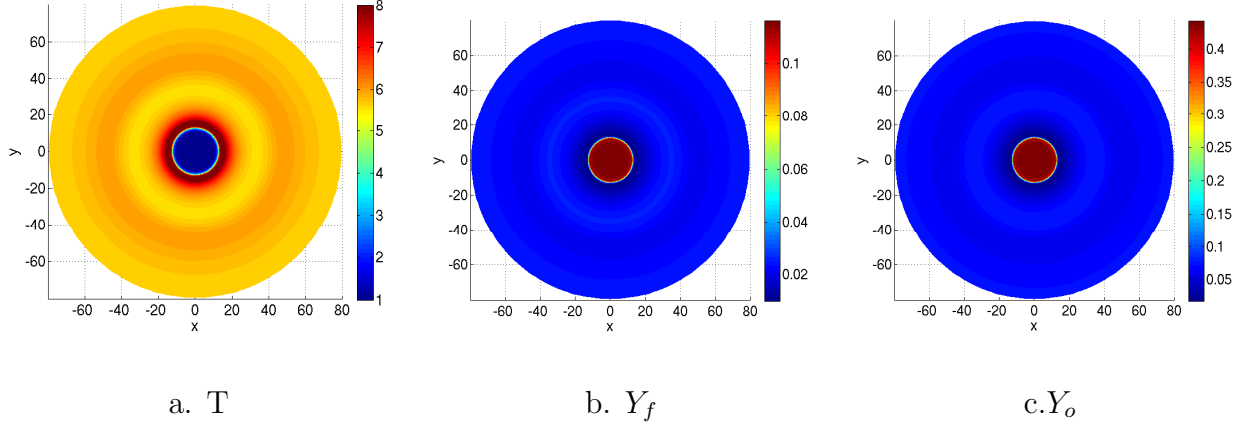
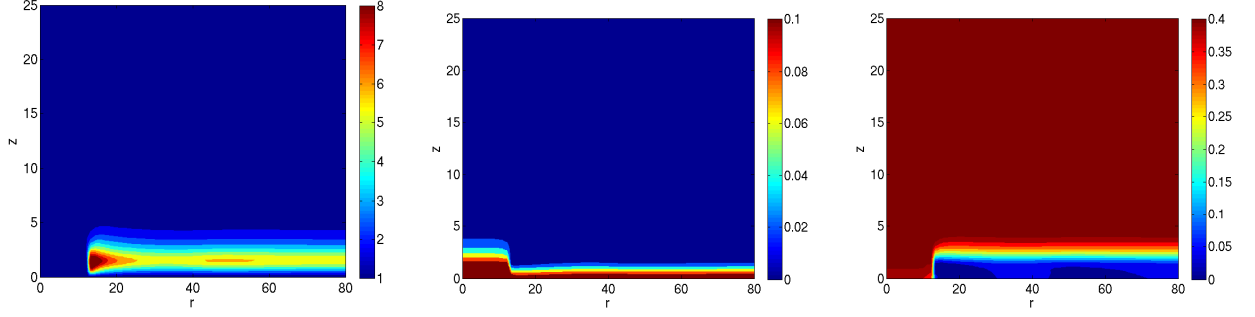


Figure 4.11: Temperature and species contours of a flame hole for $\phi = 2.0$, $Y_{o\infty} = 0.2$, $H_0 = 0.1$, $T_s = 1.0$, $\beta = 25$, $Z_e = 5.43$ and $D = 1.96$

4.3 Flame Hole

Figures 4.11a-c show the temperature and species contours in the xy -plane of a flame hole at $D = 1.96$. Here, a central cold region is surrounded by an axisymmetric, annular flame sheet. A region of high temperature appears immediately adjacent to the boundary of the flame hole and then the temperature gradually decreases and oscillates along the radius. The geometry of the flame hole is better illustrated in the temperature and species contours in the rz plane given in figures 4.12a-c. Here, the edge of the flame is at a radial location of approximately $r = 13.4$. The temperature is high in the triangular region near the edge of the flame as compared to the tail of the flame. The fuel and oxidizer contours suggest that there is some mixing near the edge of the hole. However, beyond the edge, the fuel and oxidizer seem separated suggesting that beyond the boundary region of the hole, where some premixing may occur, there exists purely a diffusion flame. The characteristics of the edge of the flame hole is further analyzed in terms of the cross scalar dissipation parameter in a following section.

The radial oscillations in the trailing diffusion flame beyond the hole region are visible in



a. T

b. Y_f

c. Y_o

Figure 4.12: Temperature and species contours of a flame hole for $\phi = 2.0$, $Y_{o\infty} = 0.2$, $H_0 = 0.1$, $T_s = 1.0$, $\beta = 25$, $Z_e = 5.43$ and $D = 1.96$

the rz contours as well. These oscillations can be explained by considering small perturbations in the large z field. As $z \rightarrow \infty$ the angular and radial velocities become negligible while the axial velocity asymptotes to H_∞ . Here, the solution of the homogeneous heat equation is given by

$$T = \exp(-1/2[H_\infty + \sqrt{H_\infty^2 + 4\mu^2}]z)J_0(\mu r). \quad (4.8)$$

It is found that the wavelength of the radial oscillations shown in figure 4.13 correspond to $\mu \approx 0.14$ which implies

$$T = \exp(H_\infty z)J_0(\mu r) \quad (4.9)$$

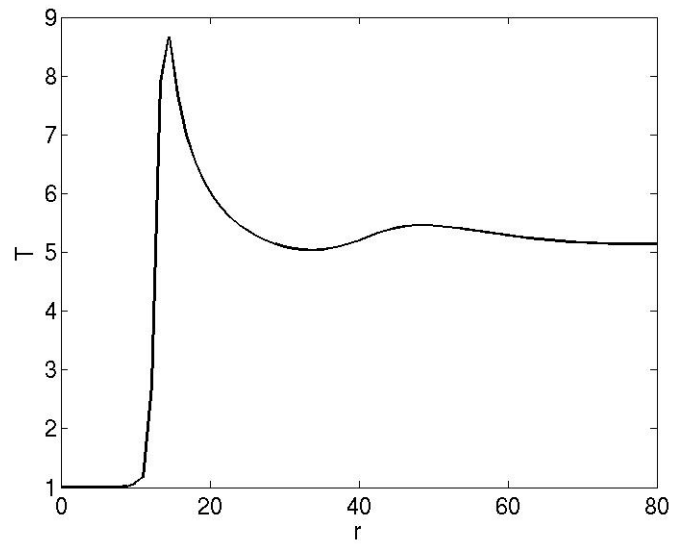


Figure 4.13: Radial temperature profile at $\theta = 0 \text{ rad}$.

4.3.1 Effect of Damköhler Number on Flame Hole Radius

As discussed in section 4.3 the flame hole is the first non-uniform flame observed as the value of the Damköhler number nears D_E . The flame hole forms at a Damköhler number of 1.96 while a single spiral forms at $D = 1.9$. It is found that at Damköhler numbers between these two values the flame hole expands with decreasing Damköhler number. Flame holes are simulated for $1.940 \leq D \leq 1.960$ and the flame hole radius, defined as the distance from the axis to the point where the temperature rises above 5 in the stoichiometric plane, are tabulated in table 4.1. Figure 4.14 shows the Damköhler number as a function of the flame hole radius while figures 4.15-4.19 show temperature contours of flame holes at different Damköhler numbers in the xy and rz planes.

D	Flame Hole Radius	Temp (r=80)	1-D Flame Temp
1.960	13.37	5.54	5.857
1.955	20.35	5.61	5.857
1.950	22.73	5.40	5.857
1.945	31.24	5.87	5.857
1.940	34.97	5.76	5.848

Table 4.1: Damköhler number and flame hole radii

It is evident from 4.1 that there is a significant increase in the flame hole radius within the range of Damköhler numbers considered. The expansion of the flame holes suggests that either there is an increase in the radial dissipation away from the axis and as the Damköhler

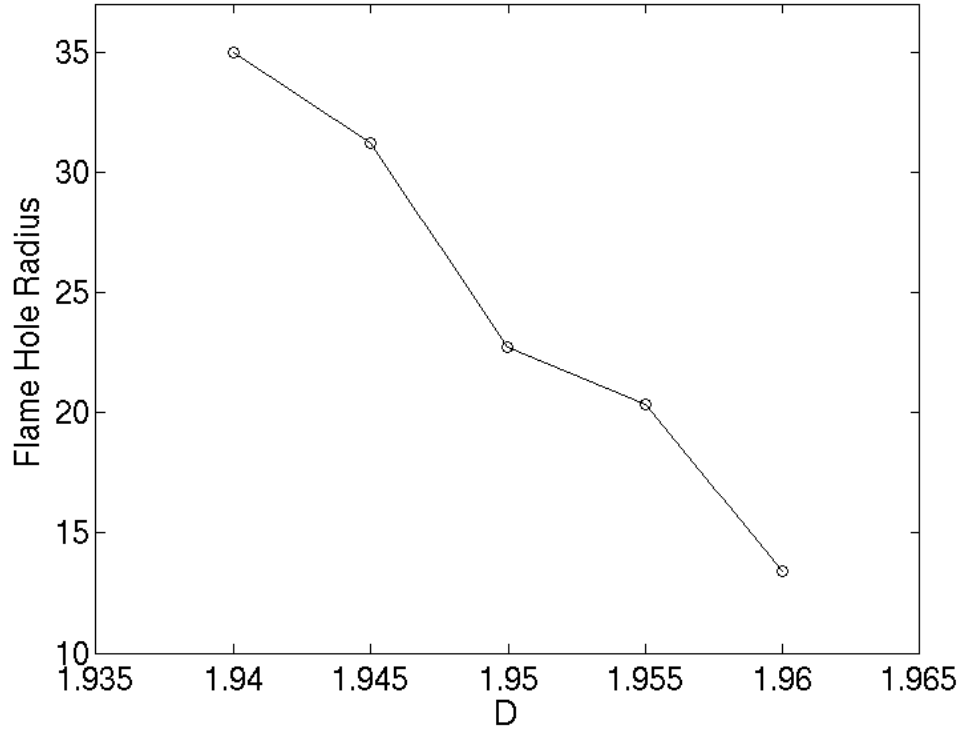


Figure 4.14: Flame hole radius as a function of Damköhler number

number decreases the reaction is not fast enough to sustain a flame so the hole expands, or that there is increased dissipation out of the plane in the quenched region as compared to the region where the flame prevails. The temperature contours in the rz plane suggest that the tail of the flame is purely a diffusion flame and from table 4.1 it is seen that the temperatures at $r = 80$ are generally close to the flame sheet temperatures. These contours also demonstrate that as the hole expands the hot triangular region adjacent to the flame hole also expands. Figures 4.20-4.24 show the reaction rate contours of the flame holes corresponding to Damköhler numbers from 1.96 to 1.94. These contours clearly demonstrate that the flame is tribrachial. As the Damköhler number is decreased and the hole radius increases the reaction rate in the rich premixed arm increases. Also, the height of the premixed arms increase as the Damköhler number decreases. Figure 4.25 demonstrates the

relationship between the curvature (κ) in the rz plane at the stoichiometric height, with the radial velocity. Here, κ is defined as,

$$\kappa = \frac{d^2y}{dr^2} / [1 + \left(\frac{dy}{dr}\right)^2]^{3/2}, \quad (4.10)$$

[33], where $y = f(r)$ is the curve representing the reaction rate contour. As seen here, the curvature in the rz plane changes considerably with the hole radius.

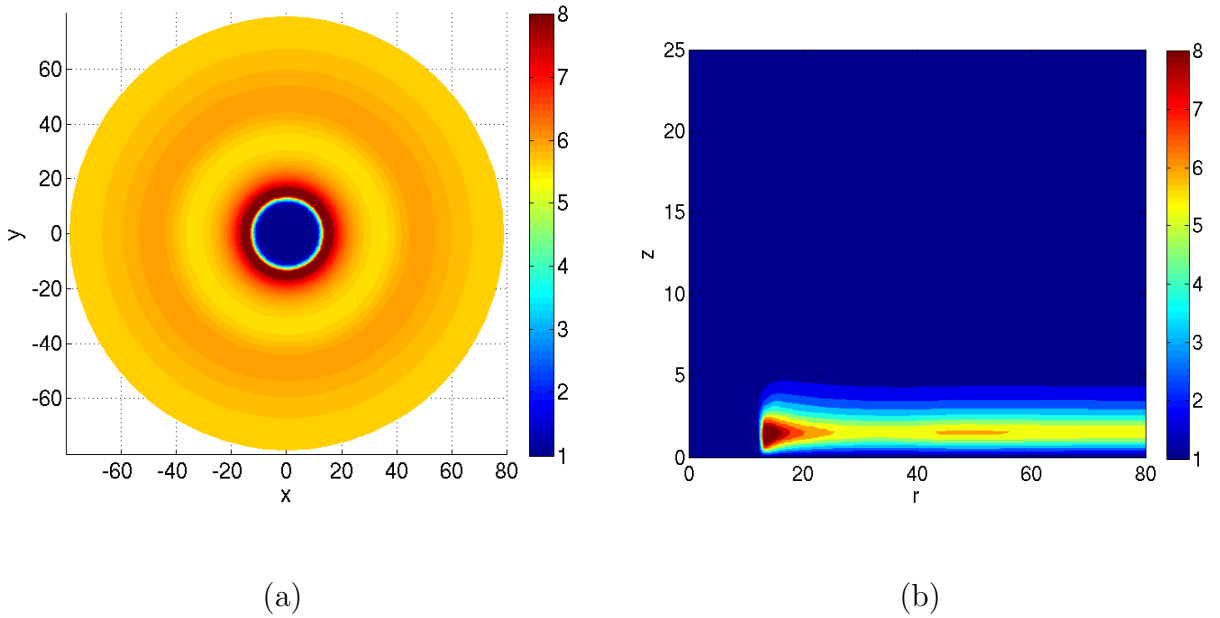
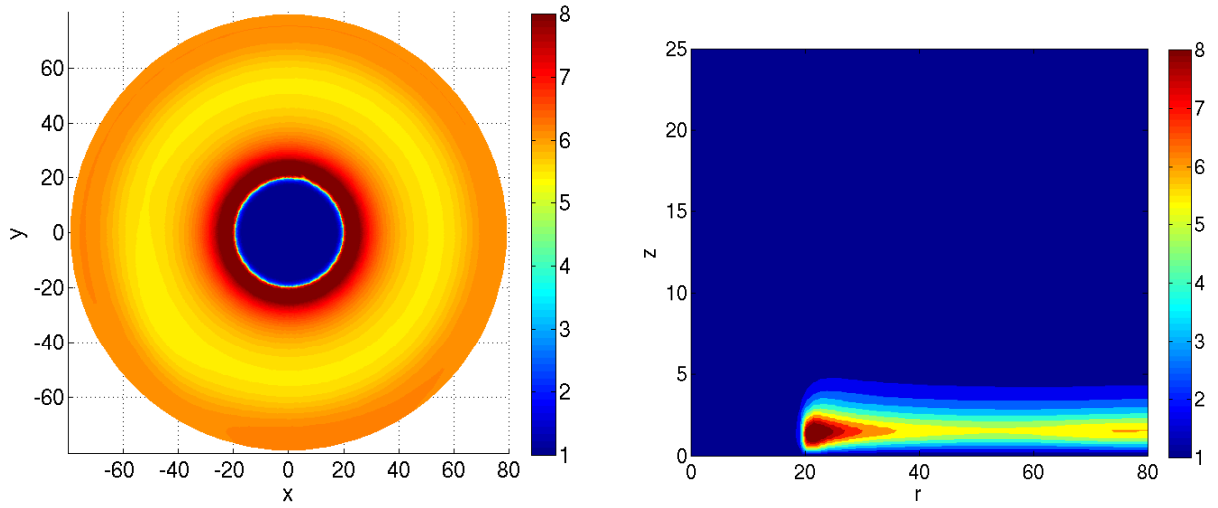


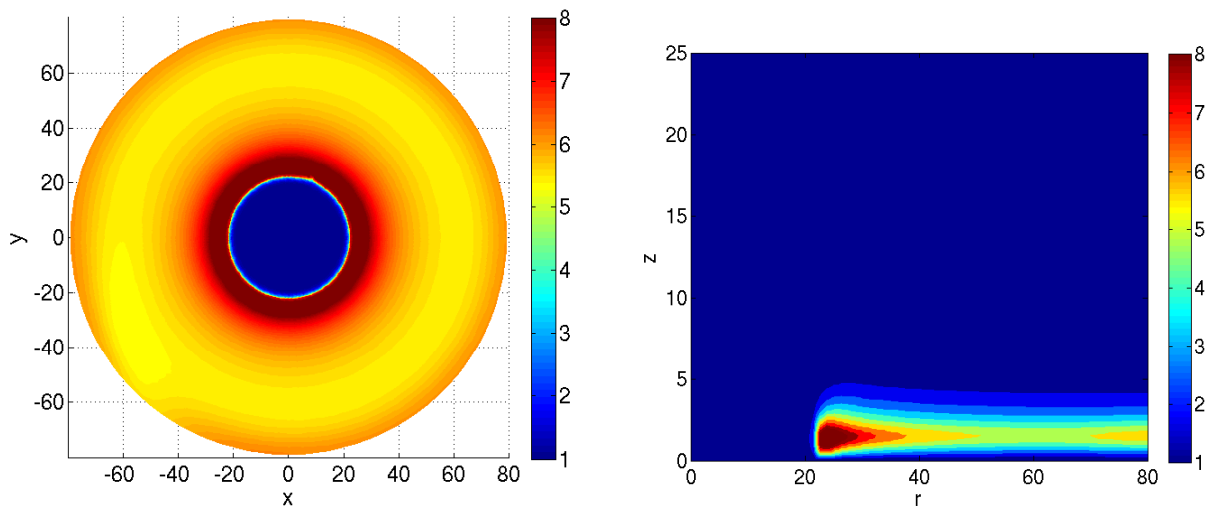
Figure 4.15: Temperature contours of the flame hole in the xy and the rz planes at $D = 1.96$



(a)

(b)

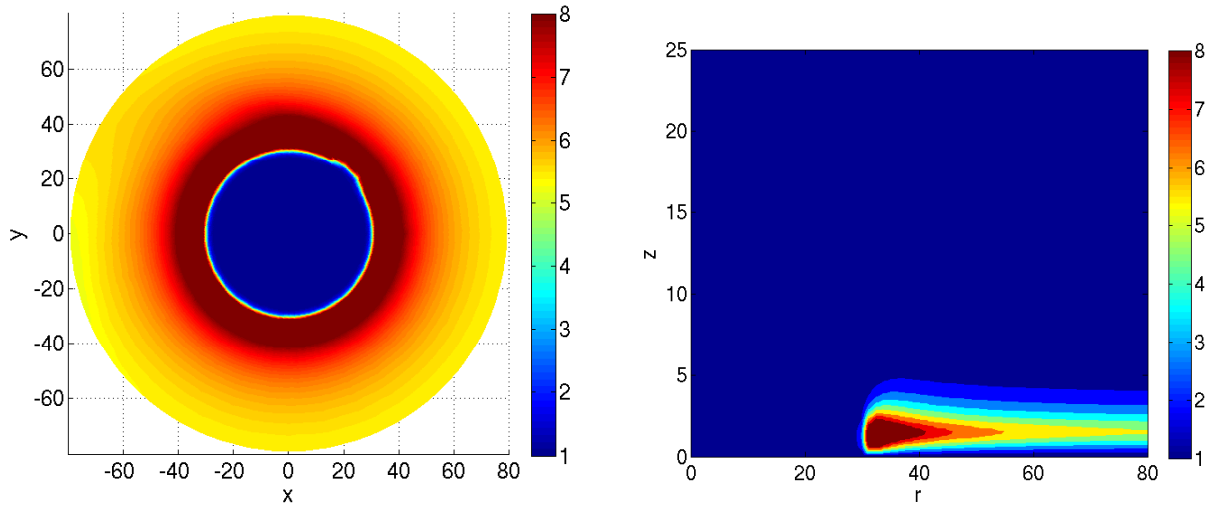
Figure 4.16: Temperature contours of the flame hole in the xy and the rz planes at $D = 1.955$



(a)

(b)

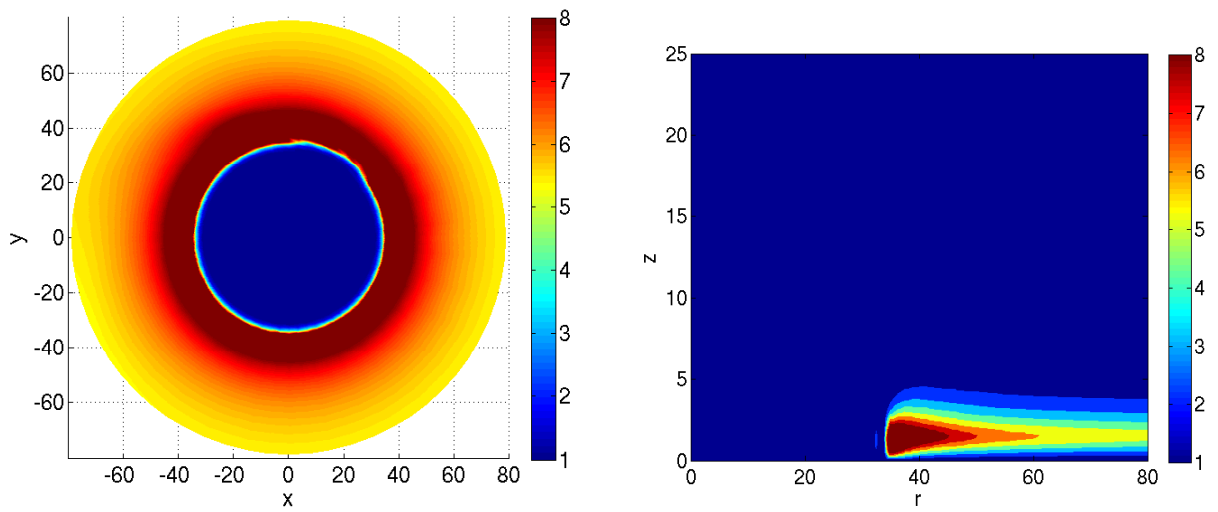
Figure 4.17: Temperature contours of the flame hole in the xy and the rz planes at $D = 1.95$



(a)

(b)

Figure 4.18: Temperature contours of the flame hole in the xy and the rz planes at $D = 1.945$



(a)

(b)

Figure 4.19: Temperature contours of the flame hole in the xy and the rz planes at $D = 1.94$

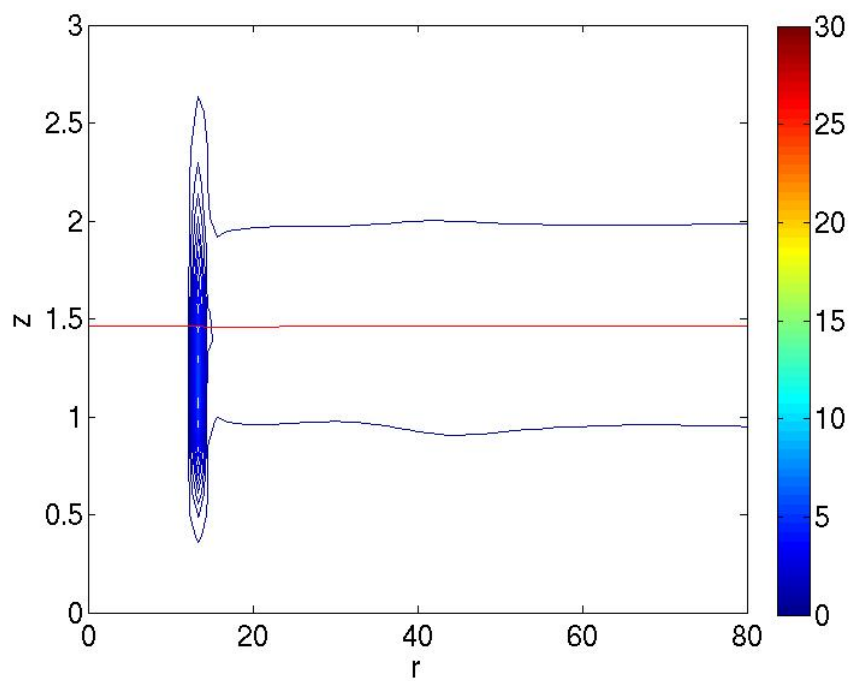


Figure 4.20: Reaction rate contours at $D=1.96$

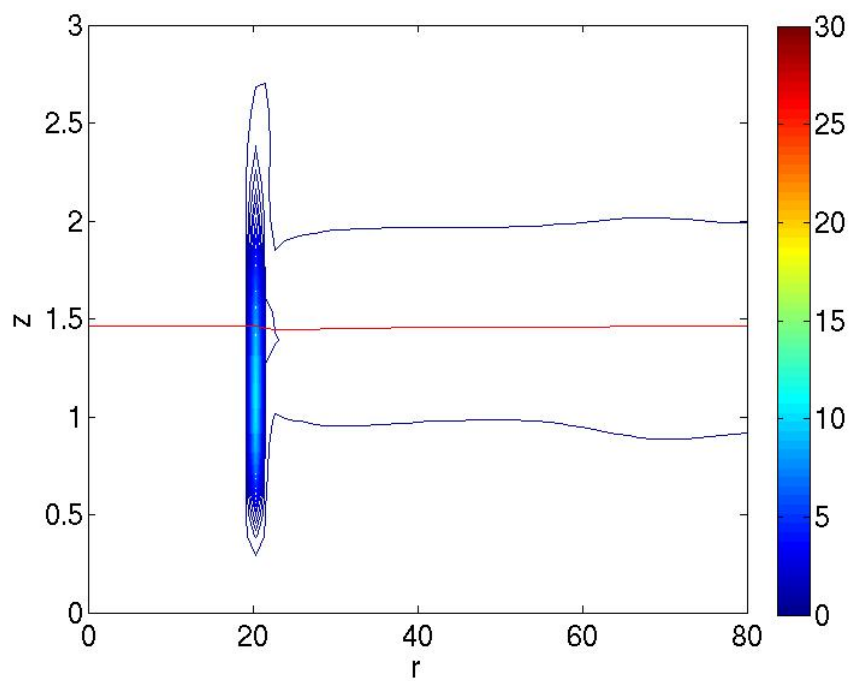


Figure 4.21: Reaction rate contours at $D=1.955$

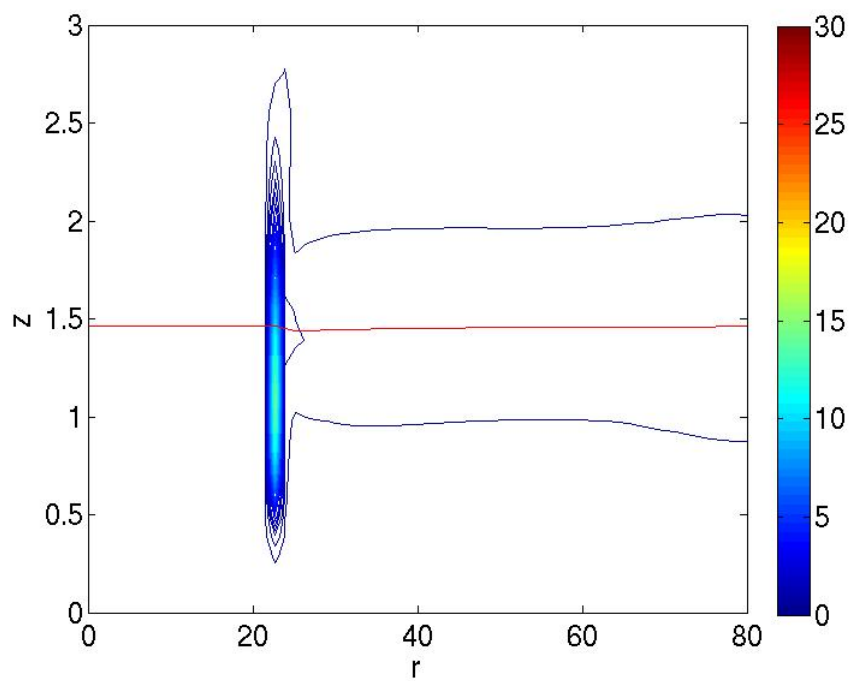


Figure 4.22: Reaction rate contours at $D=1.95$

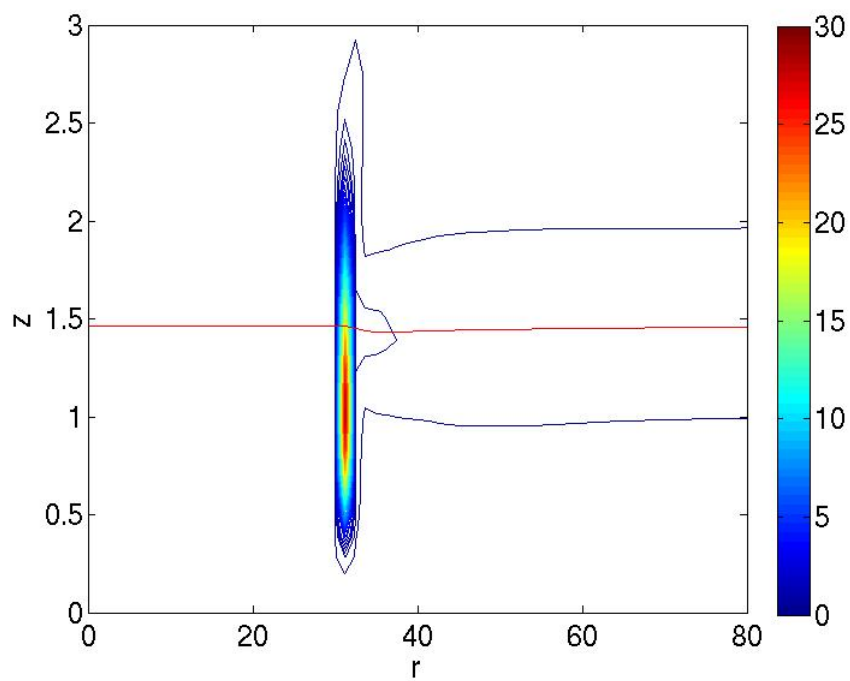


Figure 4.23: Reaction rate contours at $D=1.945$

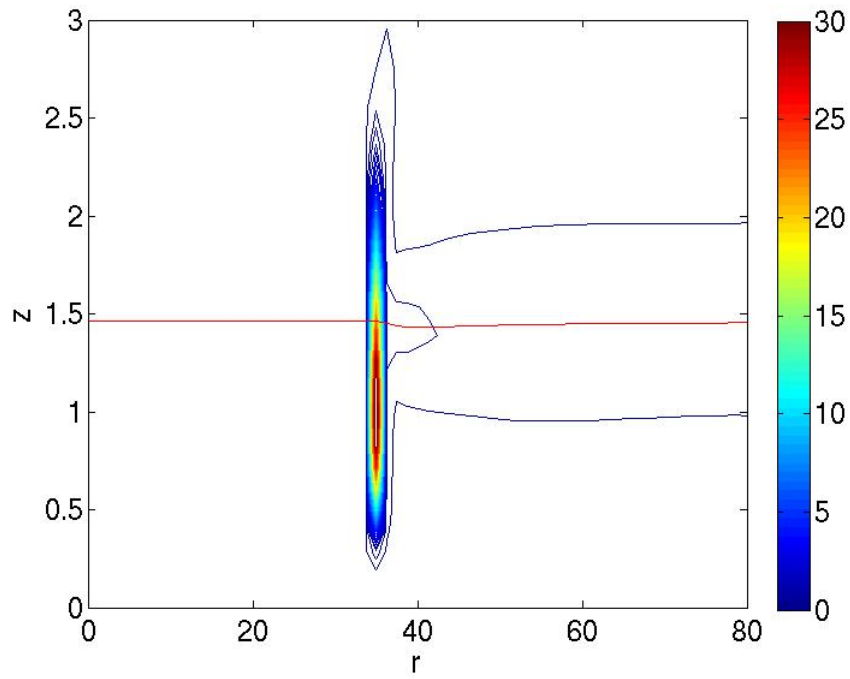


Figure 4.24: Reaction rate contours at $D=1.94$

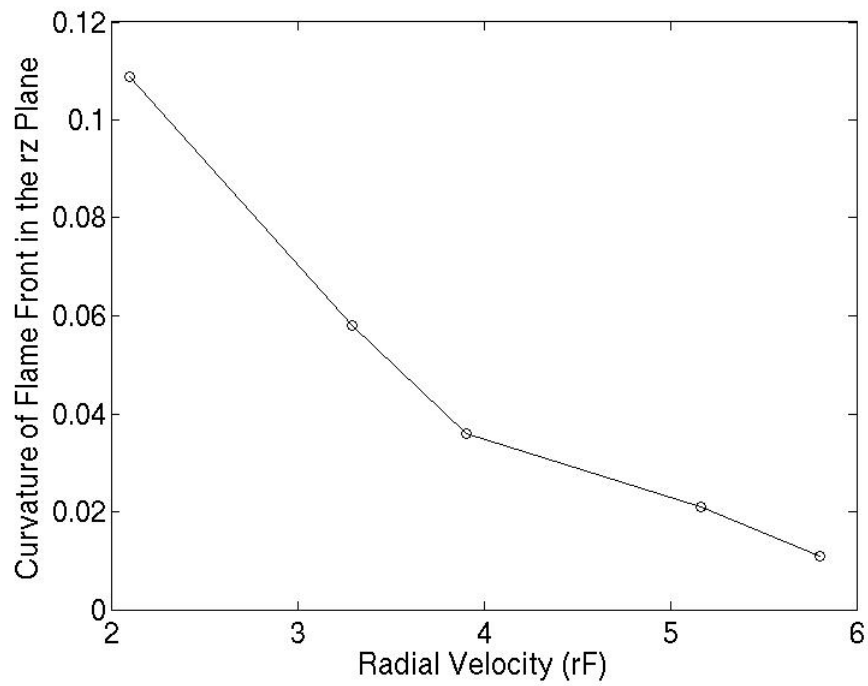


Figure 4.25: Curvature of flame front in the rz plane at stoichiometric vs the radial velocity

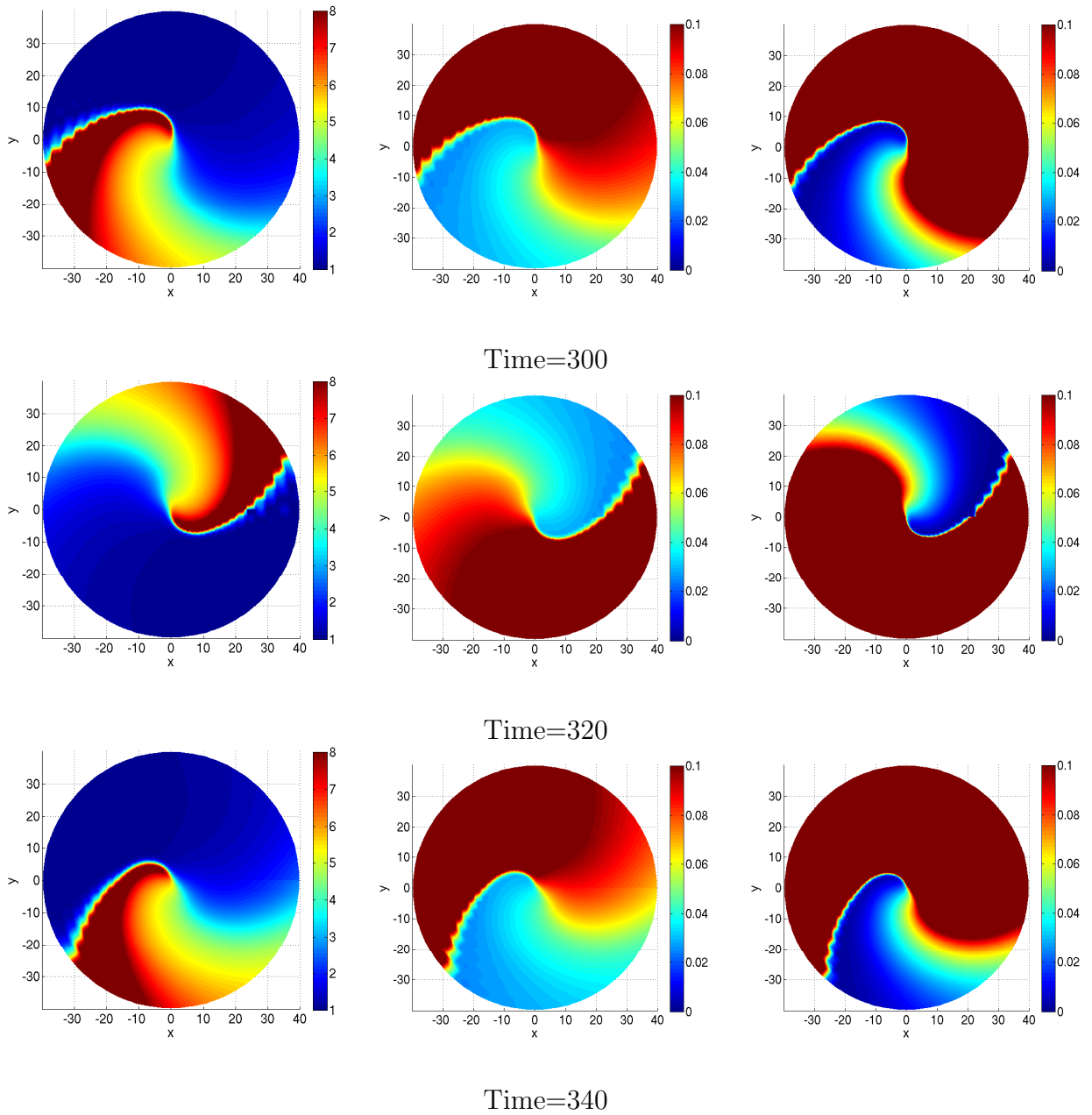
4.4 Single Spiral

Figure 4.26 shows the temperature and species contours for a single spiral for $D = 1.91$, at three different times. The spiral rotates as a rigid body at a rate of -0.14 rad/time , while the burner rotates at $b_0 = 1 \text{ rad/time}$ and at the stoichiometric height the angular velocity is $b = 0.36 \text{ rad/time}$. This high relative angular velocity is believed to be one of the main factors contributing to the differences in the characteristics of the leading edge as compared to the trailing one. As seen from figure 4.8 the temperature gradient is steep at the leading edge while there is a more gradual variation at the tail. This trend is similar to the one seen in the case of the flame hole where the stationary “leading edge” displays a high temperature gradient. Another point of note are the wiggles that are present at the leading edge of the spiral. These oscillations arise due to difficulties in fully resolving the dynamic edge of the flame. It is found that increasing the grid density reduces the prominence of these oscillations, however, due to time constraints, the finer grid is not used.

The shape of the spiral is affected by the velocity field as well. In the $r\theta$ plane the temperature profile can be described as a wave that is advected in θ . The line connecting the peak temperatures of these waves at each r location is at an angle that can be approximated by the resultant of the radial and angular velocities. This is demonstrated in figure 4.28 where the velocity field is superimposed on the temperature contours. As seen here the velocity vectors are almost tangent to the temperature contours. This is further demonstrated in figure 4.29 where the slope of the leading edge in the $r\theta$ plane is plotted against r . As seen here, the slope is linearly proportional to r , other than toward the radial boundary.

As in the case of the flame holes, both the fuel and oxidizer seem to be consumed only at

the regions of high temperature, i.e. the flame region. It is also apparent from the contours in the $z\theta$ plane given in figure 4.27 that there is very little mixing in the flame region suggesting that the flame is primarily a diffusion flame. In the simulations, the geometry of the flames do not change once the spiral shape is assumed. Simulations have been run for about four revolutions without any significant changes in the flame geometry.



T
 Y_f
 Y_o

Figure 4.26: Temperature and species contours of a single spiral for $\phi = 2.0$, $Y_{o\infty} = 0.2$, $H_0 = 0.1$, $T_s = 1.0$, $\beta = 25$, $Z_e = 5.43$ and $D = 1.91$ at $time = 300, 320, 340$

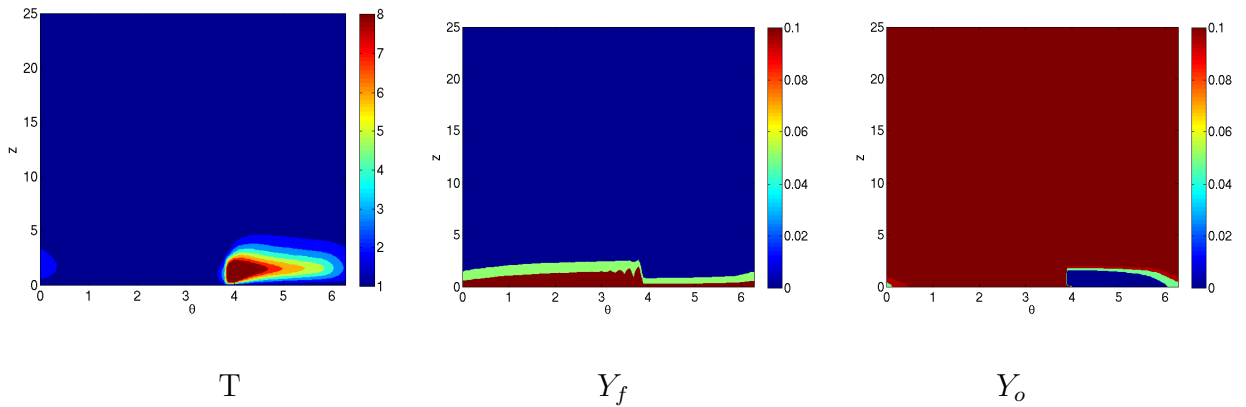


Figure 4.27: Temperature and species contours in the $z\theta$ plane of a single spiral for $\phi = 2.0$, $Y_{o\infty} = 0.2$, $H_0 = 0.1$, $T_s = 1.0$, $\beta = 25$, $Z_e = 5.43$ and $D = 1.91$ at *time* = 340

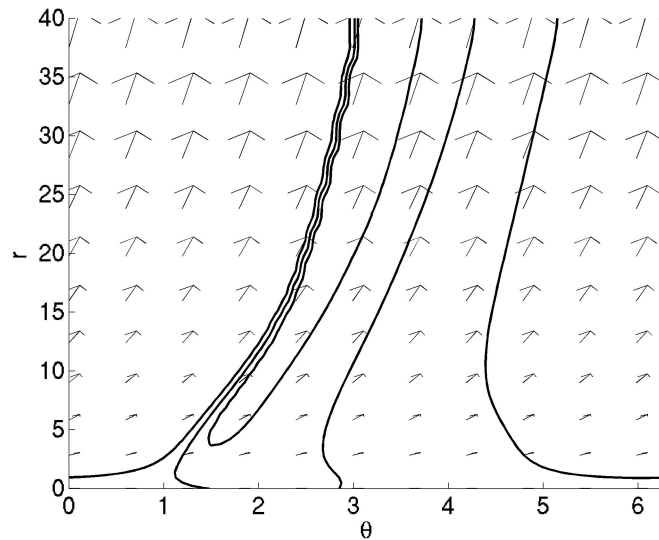


Figure 4.28: Single spiral contours and relative velocity vectors for case 1, $D = 1.91$. Contour Values: 4, 6, 8.

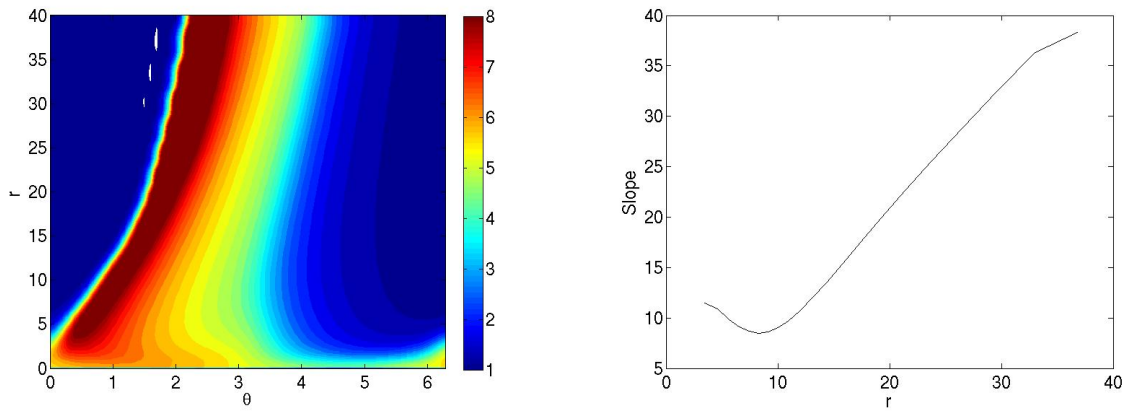


Figure 4.29: Slope of leading edge as function of r



Figure 4.30: Single spiral observed in the experiments of Nayagam and Williams (Printed with permission).

4.4.1 Comparison with Experiment

The single spirals simulated in this study are qualitatively similar to the one observed in the experiments. A snapshot of one such spiral is shown in figure 4.30 (obtained in a private communication with Vedha Nayagam and printed with permission). This spiral rotates clockwise and the temperature gradients at the leading edge are steeper than those in the trailing one. One primary difference between the experimental results and the simulated ones is the absence of tip meandering in the simulated spirals. This difference could be attributed to hydrodynamics effects which are ignored in the current study. However, the qualitative similarities between the experimental and numerical spirals suggest that the inception of these non-uniform flames is a result of thermo-diffusional instabilities although their propagation may be affected by changes in the flow field.

4.4.2 Effect of Damköhler Number on the Single Spiral

Figure 4.31 shows single spirals simulated for the parameter values of section 4.2 at Damköhler numbers of 1.90, 1.88 and 1.86 while figure 4.32 shows an overlay plot. As seen here, the shape of the spirals are similar but the area between the leading and trailing edges of the spirals decreases slightly as the Damköhler number decreases. The angular velocity of all three spirals is approximately 0.14 rad/time . Therefore, the Damköhler number does not have a discernable effect on the angular velocity of the single spiral. It appears that if the Damköhler number is in the range within which single spirals can be sustained, the spirals may form due to the appropriate perturbations and, the dynamics and geometry of the single spiral are primarily functions of the velocity field as represented by the similarity variables.

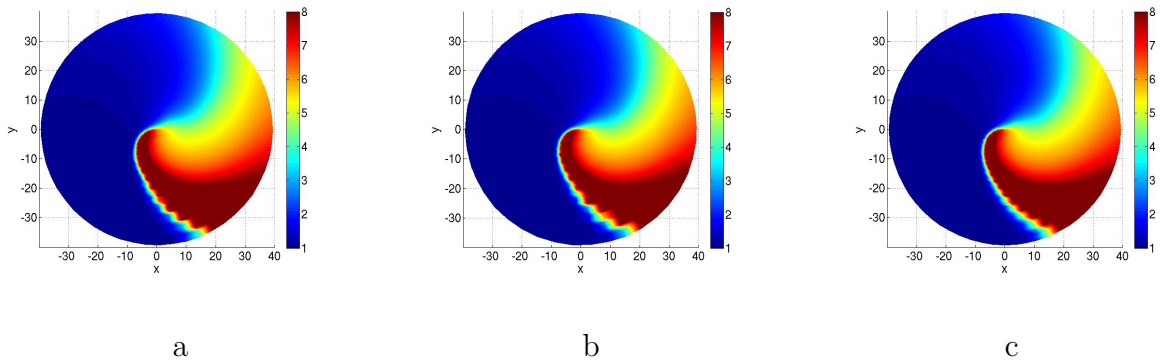


Figure 4.31: Temperature contours of single spirals for $\phi = 2.0$, $Y_{o\infty} = 0.2$, $H_0 = 0.1$, $T_s = 1.0$, $\beta = 25$, $Z_e = 40$ at a. $D = 1.91$, b. $D = 1.88$ and c. $D = 1.86$

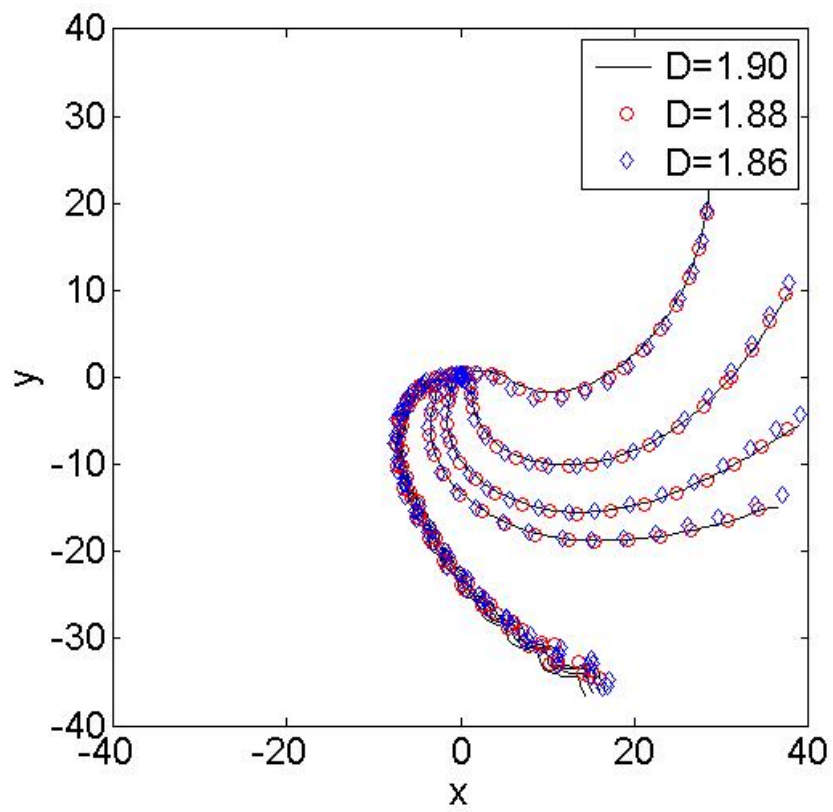
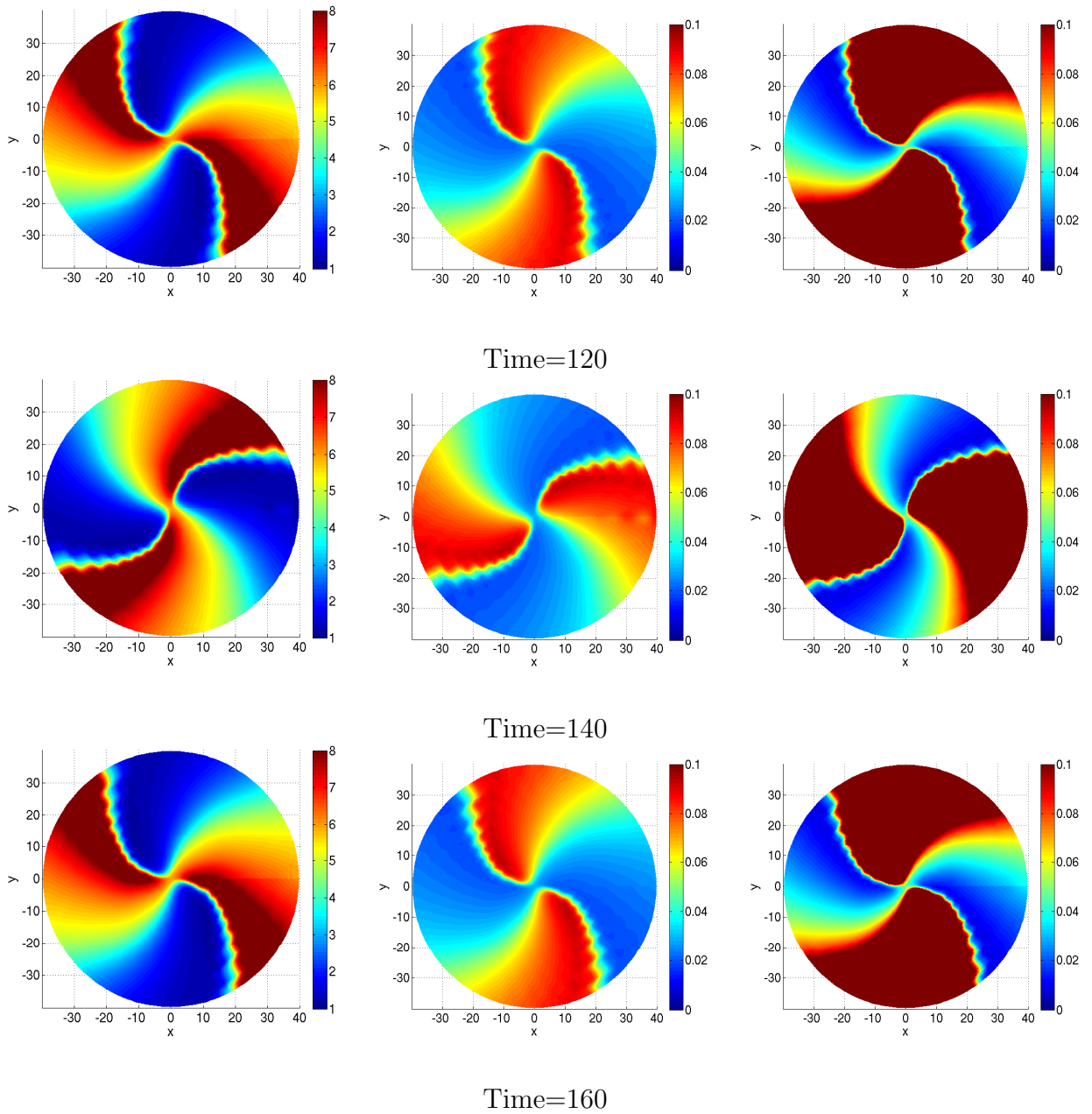


Figure 4.32: Overlay of spirals for $D = 1.90$, $D = 1.88$ and $D = 1.86$

4.5 Double Spiral

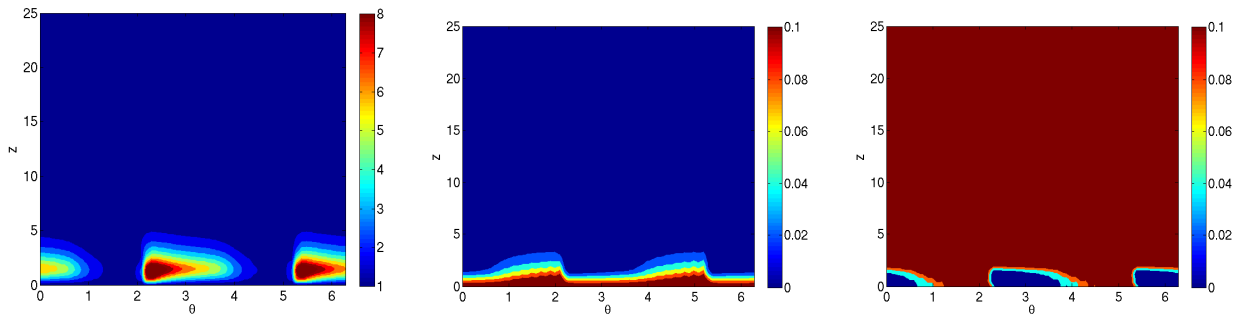
The double spirals in figure 4.33 are for $D = 1.85$ at times 120, 140 and 160. As in the case of the single spiral, the leading edge of the flame relative to the flow, is the one with the steeper temperature gradients and the temperature contours in the $z\theta$ plane, as shown in figures 4.34. Also, each arm of the double spiral is similar in shape to the single spiral discussed in the previous section. However, in contrast to the single spiral, the double spiral rotates in the same direction as the burner, and the curvature of the leading edge is concave. These differences in the dynamics and the shape of the spirals in the xy plane is attributed to interactions between the two arms of the spiral as depicted in the temperature contours shown in figure 4.34, where some tip interaction is apparent. Thus, along with the Damköhler number and the velocity profile, interactions between the spirals also affect the shape and dynamics of these flames.

It should also be mentioned that it appears from the flame contours in figures 4.34 and 4.12 that the shape of the flame bars in the $z\theta$ plane are equivalent although there is a curvature difference in the flame shape in the xy plane. This suggests that the mode of the instability only affects the lateral dynamics of the flame.



T
 Y_f
 Y_o

Figure 4.33: Temperature and species contours of a double spiral for $\phi = 2.0$, $Y_{o\infty} = 0.2$, $H_0 = 0.1$, $T_s = 1.0$, $\beta = 25$, $Z_e = 5.43$ and $D = 1.85$ at $time = 120, 140, 160$



T

Y_f

Y_o

Figure 4.34: Temperature and species contours in the $z\theta$ plane of a double spiral for $\phi = 2.0$, $Y_{\infty} = 0.2$, $H_0 = 0.1$, $T_s = 1.0$, $\beta = 25$, $Z_e = 5.43$ and $D = 1.85$ at *time* = 160

4.6 Non-uniform Flames at a Mixture Strength Value of 5.0

Non-uniform flames are also simulated for a pure methane burner. The parameter values for the results in this section are, $\phi = 5.0$, $Y_{o\infty} = 0.2$, $H_0 = 0.05$, $T_s = 1.0$, $\beta = 50$, and $Z_e = 5.43$. Figures 4.35 and 4.36 show the velocity profiles and the S-shaped response curve for this set of parameters. The extinction point, D_E , is approximately 5.56 and $D^* = 6.70$. As in the previous section, the non-uniform flames observed in this section include flame holes, single spirals and double spirals as shown in figures 4.37, 4.38 and 4.39 respectively. The geometry of these flames is very similar to the ones in the previous section but the dynamics are different. The single spiral rotates clockwise at an angular velocity of 0.07 rad/time while the double spiral rotates counterclockwise at an angular velocity of 0.75 rad/time . Also, the range of Damköhler numbers within which the instabilities occur is larger. This suggests that the injection velocity and the mixture strength affect the range of Damköhler numbers within which the non-uniform flames appear.

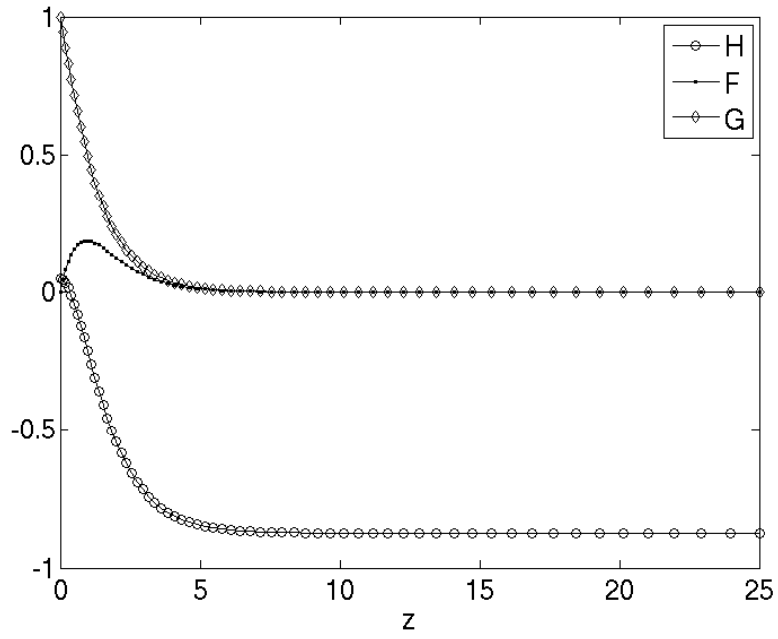


Figure 4.35: Non-dimensional Velocities

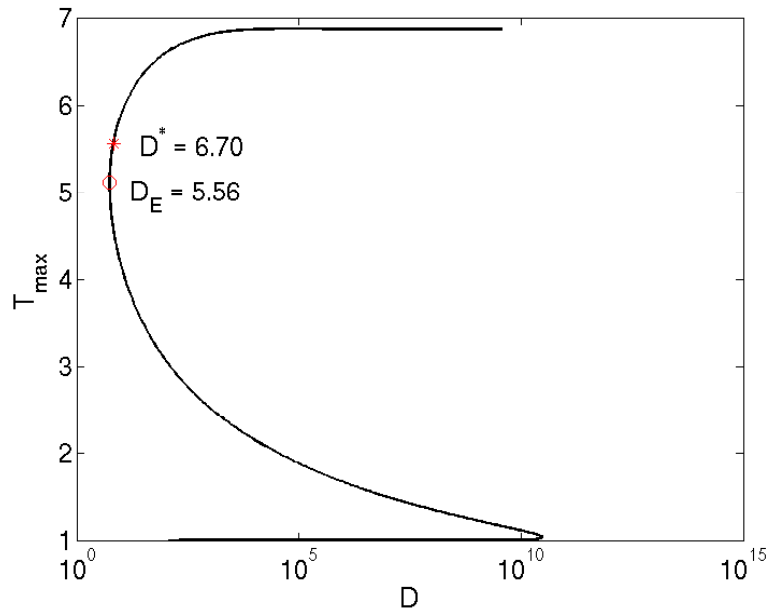


Figure 4.36: S-shaped Response

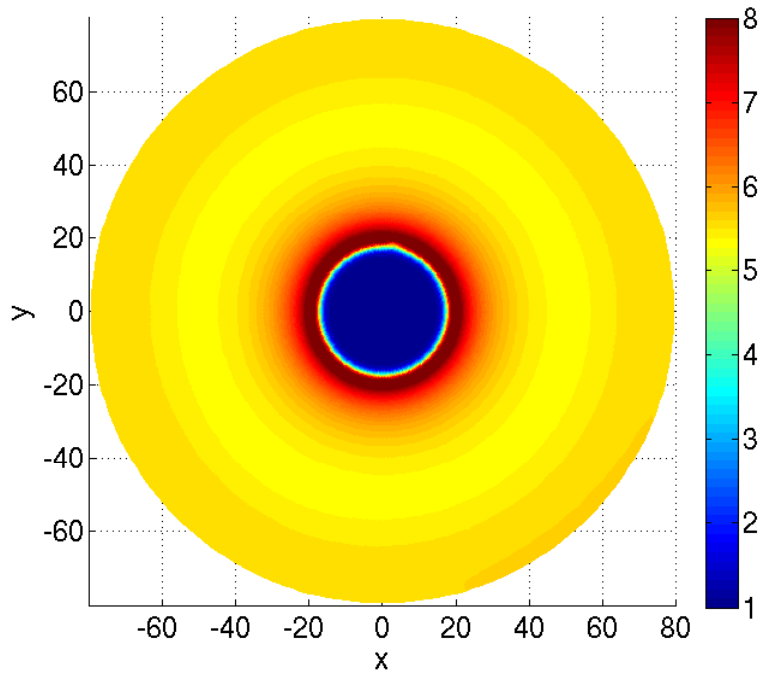


Figure 4.37: Temperature contour of a flame hole for $\phi = 5.0$, $Y_{\infty} = 0.2$, $H_0 = 0.1$, $T_s = 1.0$, $f\beta = 50$, $Z_e = 5.43$ and $D = 6.7$

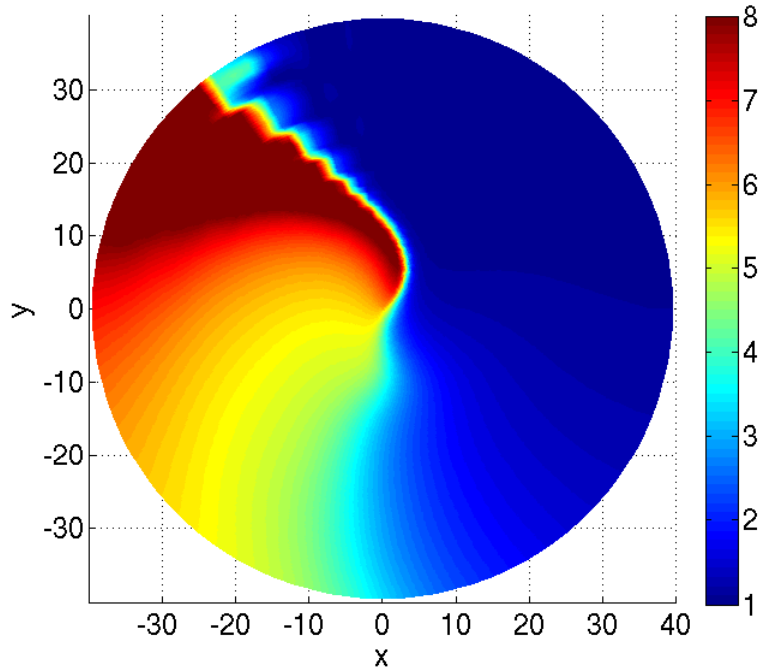


Figure 4.38: Temperature contour of a single spiral for $\phi = 5.0$, $Y_{\infty} = 0.2$, $H_0 = 0.1$, $T_s = 1.0$, $f\beta = 50$, $Z_e = 5.43$ and $D = 6.6$

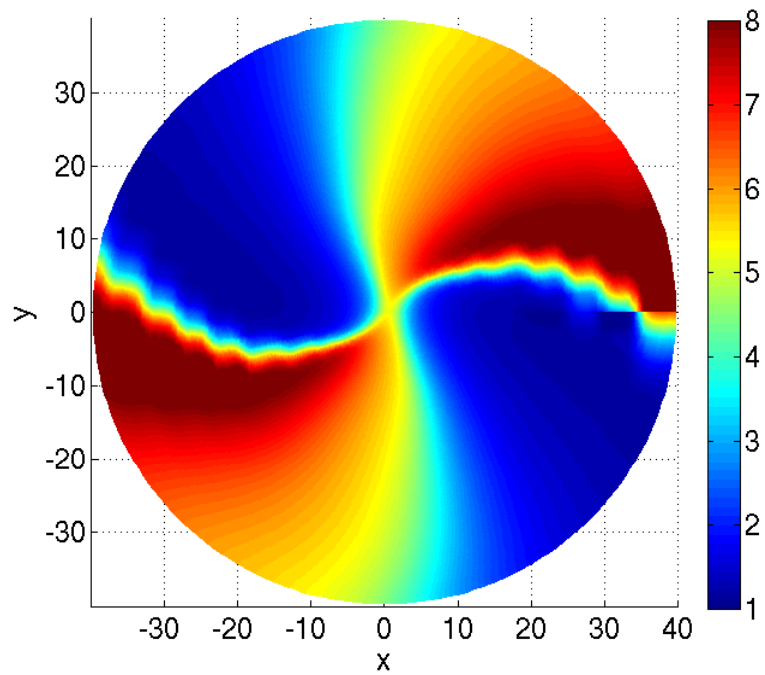


Figure 4.39: Temperature contour of a double spiral for $\phi = 5.0$, $Y_{\infty} = 0.2$, $H_0 = 0.1$, $T_s = 1.0$, $\beta = 50$, $Z_e = 5.43$ and $D = 6.2$

4.7 Effect of Parameters of Study on the Stability of the System

In the previous sections it has been shown that the Damköhler number is the crucial parameter affecting the stability of the system. However, other factors such as boundary conditions are also expected to have an effect, especially in terms of the range of Damköhler numbers within which non-uniform flames can be sustained. This is demonstrated in table 4.2 where the extinction Damköhler numbers are reported for four different parameter combinations. Here the heat release parameter is adjusted to fix the Burke-Schumann flame temperature. These values suggest that the injection velocity and the mixture strength have a considerable effect on the stability of the system while the effect of the temperature at the burner exit is small in comparison. Increasing the mixture strength leads to a shrinkage of the range whereas an increase in the injection velocity leads to an expansion. The trend in terms of the mixture strength is opposite to that observed by Kukuck and Matalon [18] for planar oscillations in diffusion flames. In the case of the spinning burner, an increase in the mixture strength leads to a shifting of the height of stoichiometry away from the burner surface to a region where the radial and angular velocities are lower in magnitude since the velocity profile remains unchanged. This reduction in the velocities in the vicinity of the flame sheet may have a stabilizing effect and so the Damköhler number range for instability is significantly reduced. An increase in the injection velocity, on the other hand, results in both a shift in the stoichiometric height and velocity profile. This dual change may be the cause of the expansion of the range.

Case	H_0	ϕ	T_s	D_E	D^*	D_E/D^*
1	0.10	2.0	1.0	1.48	1.96	0.76
2	0.10	2.0	1.4	1.46	1.95	0.75
3	0.10	5.0	1.0	1.78	1.87	0.95
4	0.05	5.0	1.0	5.25	6.32	0.83

Table 4.2: Effect of Parameters of Study on D^* .

4.8 Scalar and Cross Scalar Dissipation Rates of the Non-uniform Flames

The formation of flame patterns in the Von Karman boundary layer may have important implications for modeling turbulent flames, especially in terms of non-premixed and partially premixed turbulent combustion. Currently, turbulence models do not explicitly account for local vortices within a turbulent mixing layer. Flames in the vicinity of localized vortices may exhibit behavior similar to the flames in the boundary layer of a spinning burner. Thus it may be necessary to incorporate such behavior into existing turbulence models.

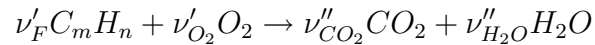
In turbulence modeling it is necessary to derive relationships between parameters such as a conserved scalar, that is not depleted by chemical reactions, and the reaction rate. The dissipation of the conserved scalar is a popular choice. In turbulent flames the conditional expectation of the dissipation of a conserved scalar, conditioned upon the value of the scalar, is proportional to the mean reaction rates [34]. Bilger [35] gives a relationship between the dissipation of a conserved scalar and the reaction rate valid in the fast chemistry limit,

$$w_i = \frac{1}{2} \rho \chi \frac{\partial^2 Y_i^e}{\partial Z^2}. \quad (4.11)$$

Although this model is only valid in the fast chemistry limit, dependencies like these are important and it is pertinent to derive similar relationships beyond the fast chemistry limit. Investigating the scalar dissipation profiles of the non-uniform flames which are typically a consequence of finite rate chemistry may provide some insight into expanding the scope of turbulence models. Thus, in this section, correlations between the dissipation of a conserved scalar and the flame patterns in the Von Karman boundary layer is explored.

The conserved scalars mentioned above are typically derived either from linear combinations of the species equations by elimination of the reaction rate term, or from elemental conservation. Linear relationships exist between all such conserved scalars if all the diffusivities are equal and there are two uniform reactant feeding streams [34],[36]. However, when the scalars are not linearly related the choice of the conserved scalar is dependent upon the particular problem.

The mixture fraction, a conserved scalar, is often utilized in the description of non-premixed combustion to determine the flame surface [37]. The expression for the mixture fraction is derived from the species governing equations by eliminating the reaction terms. For a reaction given by,



the mixture fraction is

$$Z = \frac{\nu Y_F - Y_{O_2} + Y_{O_{2,2}}}{\nu Y_{F,1} + Y_{O_{2,2}}}, \quad (4.12)$$

where, $\nu = \nu'_{O_2} W_{O_2} / \nu_F W_F$, the W_i s are the molecular weights and the subscripts 1 and 2 represent values at the fuel supply and oxidizer boundaries respectively. The species mass fractions at the boundaries serve to normalize the mixture fraction so that it has a value of 1 at the fuel boundary and 0 at the oxidizer boundary. The stoichiometric mixture fraction is given by,

$$Z_{st} = \left[1 + \frac{\nu Y_{F,1}}{Y_{O_{2,2}}} \right]^{-1}. \quad (4.13)$$

In non-premixed combustion

$$Z(\vec{x}, t) = Z_{st} \quad (4.14)$$

is used to define the flame surface [37]. Steady combustion is achieved when a balance exists between the chemical heat release and the heat dissipated away from the stoichiometric surface by diffusion and convection. The effects of finite rate chemistry become evident when such a balance does not exist [38]. Hence it is helpful to define a diffusive time

$$\tau_\chi \approx \chi_s^{-1} \quad (4.15)$$

where χ_s is the scalar dissipation rate at the stoichiometric surface. The scalar dissipation rate represents a diffusion time scale imposed by the mixing field and is given by

$$\chi = 2D\nabla Z \cdot \nabla Z, \quad (4.16)$$

where Z is the conserved scalar. Flame quenching occurs when the value of the instantaneous scalar dissipation rate exceeds a threshold, χ_q . The value of χ_q is obtained from the solution of one-dimensional steady strained diffusion flames and is used as a reference point for quenching in turbulent combustion modeling [38]. It is important to note that simulation results of Favier and Vervisch [38] indicate that the scalar dissipation rate needed to initiate quenching is higher than that necessary to maintain or propagate a quenched zone.

Another important factor that needs to be considered is the increase in the product of the reactant mass fractions in the regions bordering the quenched zones [38]. Under stoichiometric conditions this suggests that the flame itself may be a combination of partially premixed and non-premixed regions. Thus, it is useful to identify premixed regions so as to fully understand the structure of the flame and the quenching mechanism. The cross scalar dissipation rate is a parameter that may be used to distinguish between premixed and diffusion flames [38],[39]. The cross scalar dissipation rate

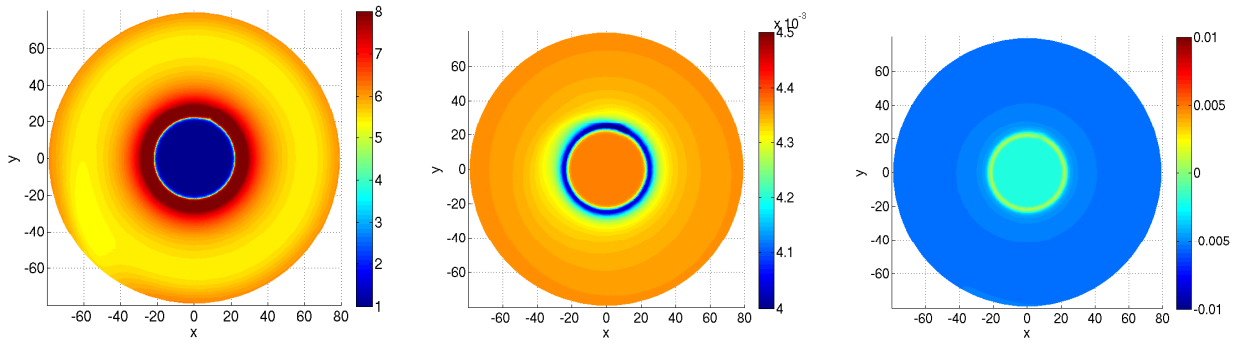
$$\chi_c = 2D\nabla Y_f \cdot \nabla Y_o \quad (4.17)$$

is positive for a premixed flame and negative for a diffusion flame [38].

Figures 4.40-4.42 show the contours of the instantaneous scalar dissipation rates, and the cross scalar dissipation rates for a flame hole, a single spiral and a double spiral, in the xy plane. These contours are at the plane where the mass fractions are in stoichiometric proportions. It is evident from these figures that the instantaneous scalar dissipation rate is generally higher in the regions where quenching has occurred. In comparison to the temperature contours, in the quenched regions, the scalar dissipation rate has a value higher than 0.00435 for all three flames. Another interesting characteristic that is common among the flames is that regions of premixing, as indicated by positive values of χ_c are thin and are limited to regions bordering those with low scalar dissipation rates. With respect to the temperature contours these premixed regions are in areas where the temperature transitions rapidly from hot to cold values.

The curvatures of the contours of both the scalar dissipation and the cross scalar dissipation rates are similar to those of the temperature. It is also important to note that the maximum positive value of the cross scalar dissipation rate is higher in the case of the single spiral than that for the flame hole or the double spiral. This may be attributed to the higher angular velocity with which the single spiral rotates about the axis of the burner.

The contours of the scalar dissipation and the cross-scalar dissipation provide insight in terms of the structure of the flame and their relationship to the dissipation away from the stoichiometric surface. In other words, the chemical reaction in the quenched regions is not sufficient to balance the dissipation away from the stoichiometric plane. This leads to flame extinction because the Damköhler number at which these flame patterns are observed are

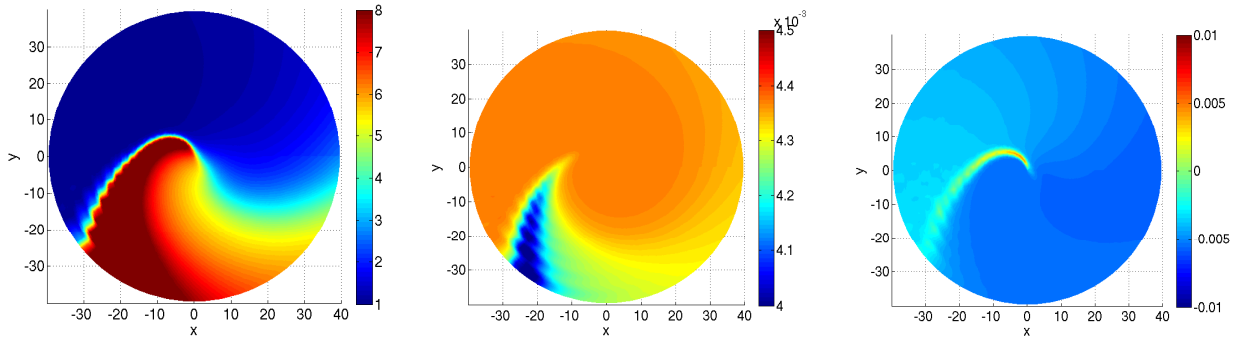


a. T

b. χ

c. χ_c

Figure 4.40: Temperature, scalar and cross scalar contours in the xy plane of a flame hole for $\phi = 2.0$, $Y_{\infty} = 0.2$, $H_0 = 0.1$, $T_s = 1.0$, $\beta = 25$, $Z_e = 5.43$ and $D = 1.95$

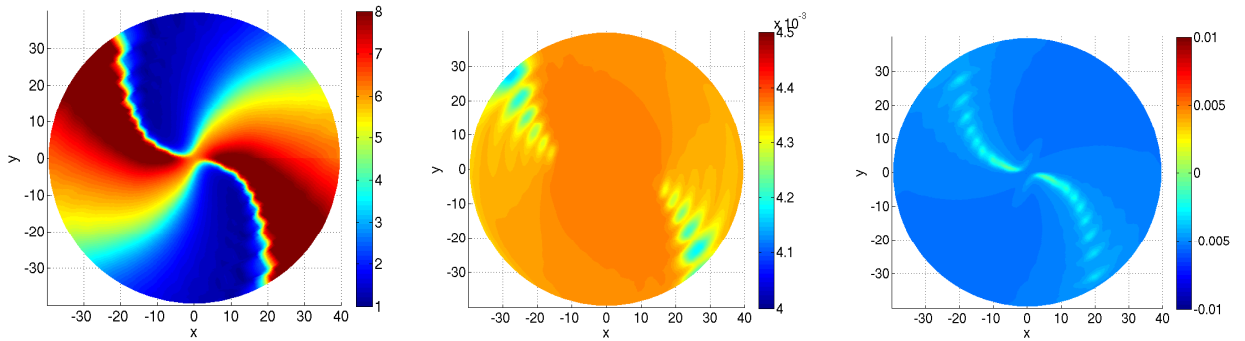


a. T

b. χ

c. χ_c

Figure 4.41: Temperature, scalar and cross scalar contours in the xy plane of a single spiral for $\phi = 2.0$, $Y_{\infty} = 0.2$, $H_0 = 0.1$, $T_s = 1.0$, $\beta = 25$, $Z_e = 5.43$ and $D = 1.9$



a. T

b. χ

c. χ_c

Figure 4.42: Temperature, scalar and cross scalar contours in the xy plane of a double spiral for $\phi = 2.0$, $Y_{\infty} = 0.2$, $H_0 = 0.1$, $T_s = 1.0$, $\beta = 25$, $Z_e = 5.43$ and $D = 1.85$

low enough such that finite rate chemistry can be expected. The largest Damköhler number at which a flame pattern can be sustained could thus be considered as the transition point where the chemistry is no longer infinitely fast.

Within the range of finite chemistry, however, several distinct flame patterns have been observed. These flame patterns are both functions of the nature of the perturbation and the Damköhler number. The scalar and cross scalar dissipation, however, do not provide much information about the dynamics of these flames. Therefore, it may be necessary to include other pertinent parameters in models for representing the effect of localized vortices in turbulent combustion. So further analysis is necessary to ascertain the driving factor for the dynamics of the flame patterns observed in this study.

4.9 Conclusion

In this study a simple model is utilized to gain some insights into the stability of diffusion flames supported by a spinning porous plug methane burner. The evolution of the flame holes and spirals indicate that diffusion flames supported by the rotating porous plug burner become unstable at near extinction Damköhler numbers on the upper branch of the S-response curve. It is shown that these multidimensional instabilities are thermo-diffusional in nature. The flames have three-dimensional characteristics and the spirals are dynamic in nature. They rotate about the axis of the burner and the single-armed spiral rotates clockwise while the double-armed spiral rotates counter clockwise. The primary factors affecting the shape and dynamics of the spirals are identified as the velocity field and the interaction between spiral flames. It is also found that the mixture strength and the injection velocity have a significant effect on the range of Damköhler numbers within which the system is prone to instability.

Appendix A

Nondimensionalizing the Governing Equations

Continuity

$$\frac{\partial \rho}{\partial t} + \frac{1}{r^*} \frac{\partial(\rho r^* u)}{\partial r^*} + \frac{1}{r^*} \frac{\partial(\rho v)}{\partial \theta} + \frac{\partial(\rho w)}{\partial z^*} = 0 \quad (\text{A.1})$$

For steady flow with radial symmetry,

$$\frac{1}{r^*} \frac{\partial(\rho r^* u)}{\partial r^*} + \frac{\partial(\rho w)}{\partial z^*} = 0 \quad (\text{A.2})$$

For constant density,

$$\frac{1}{r^*} \frac{\partial(r^* u)}{\partial r^*} + \frac{\partial(w)}{\partial z^*} = 0 \quad (\text{A.3})$$

Using nondimensional variables:

$$r = \sqrt{\frac{b^*}{\nu_\infty}} r^*, \quad z = \sqrt{\frac{b^*}{\nu_\infty}} z^*, \quad \bar{T} = \frac{T}{T_\infty}, \quad \bar{Y}_i = \frac{Y_i}{Y_{f0}}$$

where, b^* is the angular velocity of the burner.

We seek a similarity solution of the form:

$$u = b^* r^* F, \quad v = b^* r^* G, \quad w = \sqrt{b^* \nu_\infty} H, \quad p = \rho b^* \nu_\infty P$$

where F, G, H and P are functions of z .

Non-dimensionalizing the equation we get,

$$\begin{aligned} \frac{1}{r} b^* r F + b^* F + b^* r \frac{\partial F}{\partial r} + \frac{\partial}{\partial z} \sqrt{b^* \nu_\infty} \sqrt{\frac{b^*}{\nu_\infty}} H &= 0 \\ \rightarrow 2F + H' &= 0 \end{aligned}$$

(A.5)

Momentum

r-Momentum:

Incompressible flow with constant transport properties,

$$\begin{aligned} & \rho \left(\frac{\partial u}{\partial t} + u \frac{\partial u}{\partial r^*} + \frac{v}{r^*} \frac{\partial u}{\partial \theta} - \frac{v^2}{r^*} + w \frac{\partial u}{\partial z^*} \right) \\ &= -\frac{\partial p}{\partial r^*} + \mu \left[\frac{\partial}{\partial r^*} \left(\frac{1}{r^*} \frac{\partial(r^*u)}{\partial r^*} \right) + \frac{1}{r^{*2}} \frac{\partial^2 u}{\partial \theta^2} - \frac{2}{r^{*2}} \frac{\partial v}{\partial \theta} + \frac{\partial^2 u}{\partial z^{*2}} \right] \end{aligned} \quad (\text{A.6})$$

Using the steady equation with radial symmetry,

$$u \frac{\partial u}{\partial r^*} - \frac{v^2}{r^*} + w \frac{\partial u}{\partial z^*} = -\frac{\partial p}{\partial r^*} + \nu_\infty \left[\frac{\partial}{\partial r^*} \left(\frac{1}{r^*} \frac{\partial r^* u}{\partial r^*} \right) + \frac{\partial^2 u}{\partial z^{*2}} \right] \quad (\text{A.7})$$

Using the similarity variables defined in Equation A:

$$\begin{aligned} & b^{*2} r^* F^2 + b^{*2} r^* H F' - b^{*2} r^* G^2 + \frac{b^* F}{r^*} - \frac{b^* F}{r^*} = \nu_\infty \frac{b^{*2} r^* F''}{\nu_\infty} \\ & \therefore F'' = F^2 + F' H - G^2 \end{aligned} \quad (\text{A.8})$$

θ -Momentum: Steady equation with radial symmetry,

$$\rho \left(u \frac{\partial v}{\partial r^*} - w \frac{\partial v}{\partial z^*} + \frac{1}{r^*} u v \right) = \mu \left[\frac{\partial^2}{\partial r^{*2}} \left(\frac{1}{r^*} \frac{\partial r^* u}{\partial r^*} \right) + \frac{\partial^2 u}{\partial z^{*2}} \right] \quad (\text{A.9})$$

Using similarity variables defined in Equation A:

$$\begin{aligned} & r^* b^* F G + b^* r^* H G' + b^* r^* F G = \nu_\infty \left(\frac{b^* G}{r^*} - \frac{b^* G}{r^*} + \frac{b^* r^*}{\nu_\infty} G'' \right) \\ & \therefore G'' = 2FG + HG' \end{aligned} \quad (\text{A.10})$$

z-Momentum: Steady equation with radial symmetry,

$$\rho \left(u \frac{\partial w}{\partial r^*} - w \frac{\partial w}{\partial z^*} \right) = -\frac{\partial p}{\partial z^*} + \mu \left[\frac{1}{r^*} \frac{\partial}{\partial r^*} \left(r^* \frac{\partial w}{\partial r^*} \right) + \frac{\partial^2 w}{\partial z^{*2}} \right] \quad (\text{A.11})$$

Using similarity variables defined in Equation A:

$$b^* \sqrt{b^* \nu_\infty} H H' = \frac{1}{\rho} \left[-\rho b^* \sqrt{b^* \nu_\infty} P' + b^* \sqrt{b^* \nu_\infty} H'' \right]$$

$$\rightarrow H'' - H H' - P' = 0$$

$$\therefore 2HF - 2F' = P'$$

(A.12)

Energy Equation

$$\begin{aligned}
& \rho C_p \left(\frac{\partial T}{\partial t} + u \frac{\partial T}{\partial r^*} + \frac{v}{r^*} \frac{\partial T}{\partial \theta} + w \frac{\partial T}{\partial z^*} \right) - \left(\frac{\partial P}{\partial t} + u \frac{\partial P}{\partial r^*} + \frac{v}{r^*} \frac{\partial P}{\partial \theta} + w \frac{\partial P}{\partial z^*} \right) \\
& - \lambda \left[\frac{1}{r^*} \frac{\partial}{\partial r^*} \left(r^* \frac{\partial T}{\partial r^*} \right) + \frac{1}{r^{*2}} \frac{\partial^2 T}{\partial \theta^2} + \frac{\partial^2 T}{\partial z^{*2}} \right] = - \sum \omega_i \Delta h_i \\
& - \frac{1}{r^*} \left[\frac{\partial}{\partial r^*} \left(r^* \rho T \sum C_{pi} Y_i V_i r^* \right) + \frac{\partial}{\partial \theta} \left(\rho T \sum C_{pi} Y_i V_i \theta \right) + \frac{\partial}{\partial z^*} \left(\rho T \sum C_{pi} Y_i V_i z^* \right) \right] \\
& + 2 \left[\left(\frac{\partial u}{\partial r^*} \right)^2 + \left(\frac{1}{r^*} \frac{\partial v}{\partial \theta} + \frac{u}{r^*} \right)^2 + \left(\frac{\partial w}{\partial z^*} \right)^2 \right] + \left[r^* \frac{\partial}{\partial r^*} \left(\frac{v}{r^*} \right) + \frac{1}{r^*} \frac{\partial u}{\partial \theta} \right]^2 \\
& + \left[\frac{1}{r^*} \frac{\partial w}{\partial \theta} + \frac{\partial v}{\partial z^*} \right] + \left[\frac{\partial u}{\partial z^*} + \frac{\partial w}{\partial r^*} \right]^2 - \frac{2}{3} \left[\frac{1}{r^*} \frac{\partial}{\partial r^*} (r^* u) + \frac{1}{r^*} \frac{\partial v}{\partial \theta} + \frac{\partial w}{\partial z^*} \right]^2
\end{aligned} \tag{A.13}$$

For low mach number flows:

$$\rho C_p \left(\frac{\partial T}{\partial t} + u \frac{\partial T}{\partial r^*} + \frac{v}{r^*} \frac{\partial T}{\partial \theta} + w \frac{\partial T}{\partial z^*} \right) - \lambda \left(\frac{1}{r^*} \frac{\partial T}{\partial r^*} + \frac{\partial^2 T}{\partial r^{*2}} + \frac{1}{r^{*2}} \frac{\partial^2 T}{\partial \theta^2} + \frac{\partial^2 T}{\partial z^{*2}} \right) = Q \Omega \tag{A.14}$$

Nondimensionalizing,

$$\frac{\partial \bar{T}}{\partial \tau} + r F \frac{\partial \bar{T}}{\partial r} + G \frac{\partial \bar{T}}{\partial \theta} + H \frac{\partial \bar{T}}{\partial z} - \frac{1}{Pr} \left(\frac{1}{r} \frac{\partial \bar{T}}{\partial r} + \frac{\partial^2 \bar{T}}{\partial r^2} + \frac{1}{r^2} \frac{\partial^2 \bar{T}}{\partial \theta^2} + \frac{\partial^2 \bar{T}}{\partial z^2} \right) = \bar{\Omega} \tag{A.15}$$

Species Equation

$$\rho \left(\frac{\partial Y_i}{\partial t} + u \frac{\partial Y_i}{\partial r^*} + \frac{v}{r^*} \frac{\partial Y_i}{\partial \theta} + w \frac{\partial Y_i}{\partial z^*} \right) + \frac{1}{r^*} \frac{\partial}{\partial r^*} (r^* \rho Y_i V_{ir}) + \frac{1}{r^*} \frac{\partial}{\partial \theta} (\rho Y_i V_{i\theta}) + \frac{\partial}{\partial z^*} (\rho Y_i V_{iz^*}) = -\alpha_i \Omega \quad (\text{A.16})$$

where,

$$V_{ir^*} = -\frac{D}{Y_i} \frac{\partial Y_i}{\partial r^*}, \quad V_{i\theta} = -\frac{D}{Y_i r} \frac{\partial Y_i}{\partial \theta}, \quad V_{iz^*} = -\frac{D}{Y_i} \frac{\partial Y_i}{\partial z^*}$$

Simplifying,

$$\rightarrow \rho \left(\frac{\partial Y_i}{\partial t} + u \frac{\partial Y_i}{\partial r^*} + \frac{v}{r^*} \frac{\partial Y_i}{\partial \theta} + w \frac{\partial Y_i}{\partial z^*} \right) - \rho D \left(\frac{\partial^2 Y_i}{\partial r^{*2}} + \frac{1}{r^*} \frac{\partial Y_i}{\partial r^*} + \frac{1}{r^{*2}} \frac{\partial^2 Y_i}{\partial \theta^2} + \frac{\partial^2 Y_i}{\partial z^{*2}} \right) = -\alpha_i \Omega \quad (\text{A.18})$$

Nondimensionalizing,

$$\frac{\partial \bar{Y}_i}{\partial \tau} + rF \frac{\partial \bar{Y}_i}{\partial r} + G \frac{\partial \bar{Y}_i}{\partial \theta} + H \frac{\partial \bar{Y}_i}{\partial z} - \frac{1}{Sc_i} \left(\frac{1}{r} \frac{\partial \bar{Y}_i}{\partial r} + \frac{\partial^2 \bar{Y}_i}{\partial r^2} + \frac{1}{r^2} \frac{\partial^2 \bar{Y}_i}{\partial \theta^2} + \frac{\partial^2 \bar{Y}_i}{\partial z^2} \right) = -\alpha_i \bar{\Omega} \quad (\text{A.19})$$

Appendix B

Code Verification

B.0.1 Grid Refinement Study

This section summarizes the results from the grid refinement study conducted to verify that the centered difference derivative routines being used in this study are fourth order accurate. For this grid refinement study, derivatives of some common functions are computed using the fourth order scheme. An average error is then calculated over all grid points according to

$$L2 = \frac{1}{n} \sum \sqrt{(f_{exact} - f_{numerical})^2}, \quad (\text{B.1})$$

where n is the total number of grid points. This error is computed for a grid with grid refinement ratio of 2 between successive grids. The order of grid convergence is then computed

$$E = L2 = Ch^p + \text{Higher order terms}, \quad (\text{B.2})$$

where h is the grid spacing, C a constant and p is the order of convergence. If the higher order terms are neglected, and a logarithm is taken,

$$\text{Ln}(E) = \text{Ln}(C) + p\text{Ln}(h), \quad (\text{B.3})$$

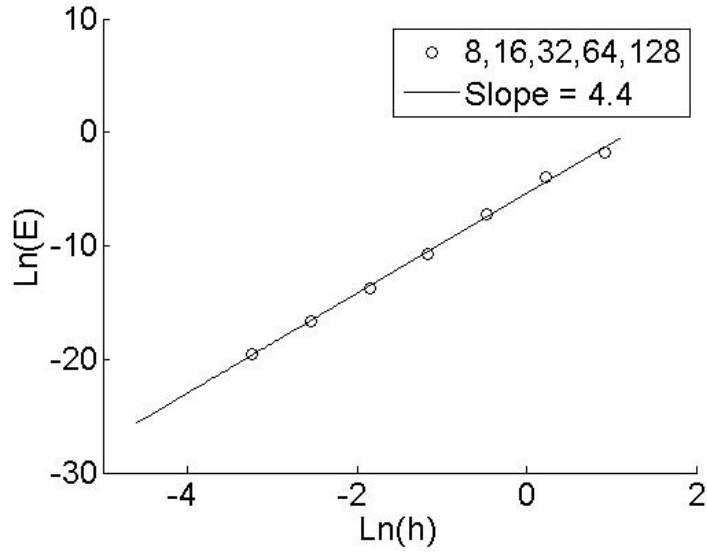


Figure B.1: Order of Grid Convergence

then the order of convergence is the slope of the plot of $\text{Ln}(E)$ versus $\text{Ln}(h)$. Figure B.1 is a plot of equation B.3 for several grids. The grids used for the study are listed in the legend. The solid line is a trend line derived using a least squares method. The slope of the trendline is also listed in the legend. As seen from the figure, the slope of the least squares fit curve is 4.4. Also, the average value of p obtained considering,

$$E_1 = Ch_1^p \quad (\text{B.4})$$

$$E_2 = Ch_2^p \quad (\text{B.5})$$

$$\text{where, } h_2 = h_1/2 \quad (\text{B.6})$$

$$\rightarrow \frac{E_1}{E_2} = \left(\frac{h_1}{h_1/2} \right)^p = 2^p \quad (\text{B.7})$$

$$\rightarrow p = \frac{\ln(E_1/E_2)}{\ln 2} \quad (\text{B.8})$$

is $p = 4.52$. Thus, the derivative routines being used are fourth order accurate.

B.0.2 Benchmark Studies

In this section the solutions to some simple problems are summarized in order to validate the solver. In all these problems the initial and boundary conditions are stated and the steady state solutions are obtained using the solver developed for the current study.

Benchmark Problem 1

The first problem consists of a simple three-dimensional second order partial differential equation. This problem is used to verify that the basic functions of the solver are implemented properly.

$$T' = T_{x_1x_1} + T_{x_2x_2} + T_{x_3x_3} \quad (\text{B.9})$$

This parabolic partial differential equation has the exact solution

$$T = 1 + e^{-3t}(\sin(x_1)\sin(x_2)\sin(x_3)). \quad (\text{B.10})$$

At steady state the temperature converges to a value of 1.0 as the exponential term decays to 0. This partial differential equation is solved in the domain

$$0 < x_1 < 2\pi \quad 0 < x_2 < 2\pi \quad 0 < x_3 < 2\pi.$$

and the initial conditions are calculated using equation B.10 with $t=0$,

$$T(0, x_1, x_2, x_3) = 1 + \sin(x_1)\sin(x_2)\sin(x_3), \quad (\text{B.11})$$

while the six boundaries are set to unity.

$$\begin{aligned} T(t, 0, x_2, x_3) &= 1.0 & T(t, 2\pi, x_2, x_3) &= 1.0 \\ T(t, x_1, 0, x_3) &= 1.0 & T(t, x_1, 2\pi, x_3) &= 1.0 \\ T(t, x_1, x_2, 0) &= 1.0 & T(t, x_1, x_2, 2\pi) &= 1.0 \end{aligned} \quad (\text{B.12})$$

Figures B.2 and B.3 show the relative percentage error for the solution for a 16 cubed and a 32 cubed grid. As seen from this figure, the relative error is very small at steady state. This indicates that the code is capable of solving the above three dimensional system with a relative error of 0.003% for a 32 cubed grid.

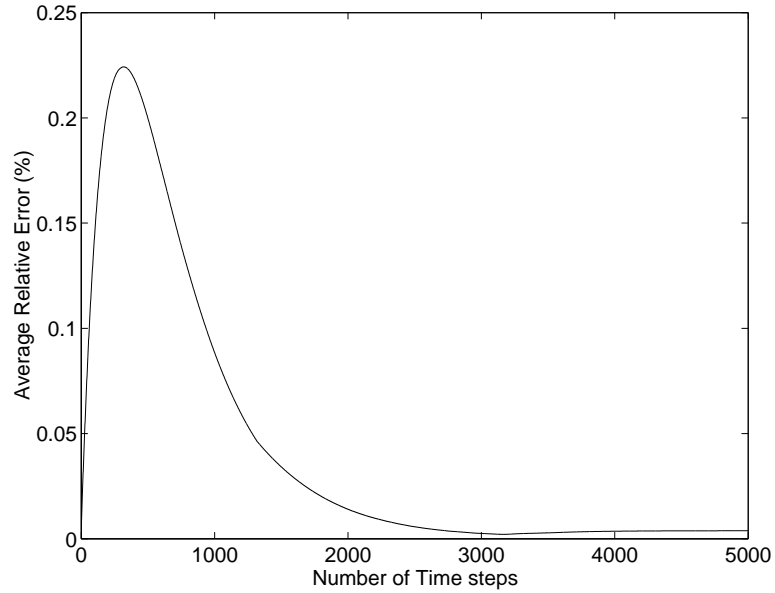


Figure B.2: Benchmark Problem 1, Grid=16 cubed

Benchmark Problem 2

This problem is considered to ensure that the boundary conditions are applied appropriately for a problem in cylindrical coordinates, where the reciprocal of r appears as a coefficient to one of the derivative terms. This, if not dealt with appropriately, causes a singularity at $r = 0$. Here, the variables in the runge kutta iteration are computed from $r = 0$ to $r = n - 1$ and the boundary condition is applied at these points. The problem is given by

$$T_t = \frac{1}{4} \left[\frac{1}{r} \frac{\partial T}{\partial r} + \frac{\partial^2 T}{\partial r^2} \right] + Q, \quad (\text{B.13})$$

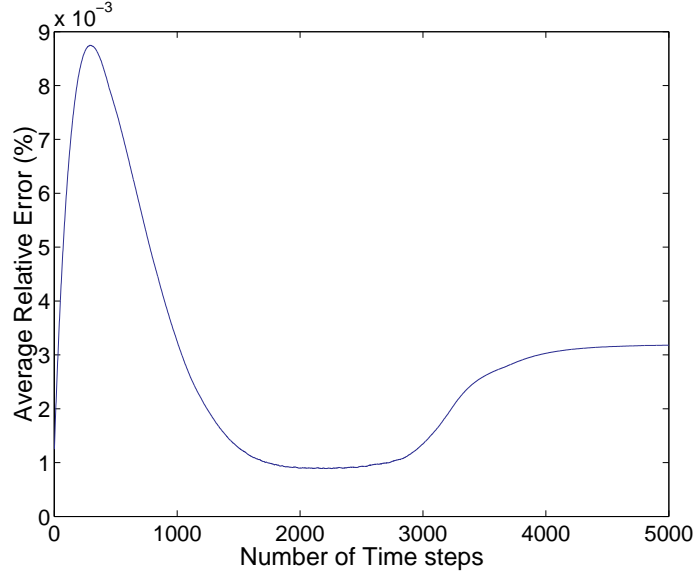


Figure B.3: Benchmark Problem 1, Grid = 32 cubed

where the source term is

$$Q = -0.0001r^2 e^{-0.01r^2} e^{-0.01t}. \quad (\text{B.14})$$

The boundary conditions are

$$\frac{\partial T}{\partial r}(t, 0) = 0.0 \quad \text{and} \quad \frac{\partial T}{\partial r}(t, 40) = 0. \quad (\text{B.15})$$

For this equation, the exact solution of T is

$$T = e^{-0.01r^2} e^{-0.01t}. \quad (\text{B.16})$$

Figure B.4 shows the temperature profile after 5000 time steps from the numerical and exact solutions. Figure B.5 shows the absolute error at each r location, and as seen here the errors are very small. These plots show that the boundary conditions are applied appropriately and that the code is able to solve problems in cylindrical coordinates.

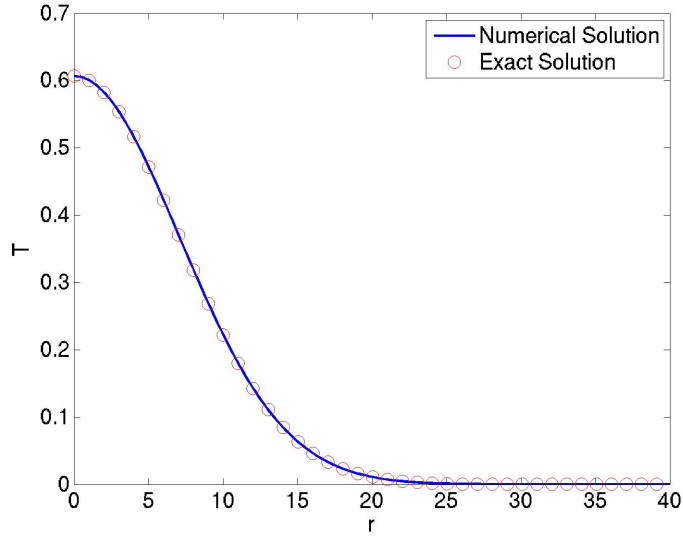


Figure B.4: Temperature Profile for Benchmark Problem 2

Benchmark Problem 3

The third problem involves solving simultaneously, partial differential equations for the species and the temperature. The governing equations are

$$T_t = \lambda_1(uT_{x_1x_1} + vT_{x_2x_2} + wT_{x_3x_3}) - \beta(T_{x_1} + T_{x_2} + T_{x_3}) + Q_1, \quad (\text{B.17})$$

$$Y_t = \lambda_2(Y_{x_1x_1} + Y_{x_2x_2} + Y_{x_3x_3}) - Q_1T + Q_2. \quad (\text{B.18})$$

The boundary conditions are

$$T(t, 0, x_2, x_3) = 1.0 \quad T(t, 2\pi, x_2, x_3) = 1.0,$$

$$T(t, x_1, 0, x_3) = 1.0 \quad T(t, x_1, 2\pi, x_3) = 1.0,$$

$$T(t, x_1, x_2, 0) = 1.0 \quad T(t, x_1, x_2, 2\pi) = 1.0,$$

$$Y(t, 0, x_2, x_3) = 1.0 \quad Y(t, 2\pi, x_2, x_3) = 1.0,$$

$$Y(t, x_1, 0, x_3) = 1.0 \quad Y(t, x_1, 2\pi, x_3) = 1.0,$$

$$Y(t, x_1, x_2, 0) = 1.0 \quad Y(t, x_1, x_2, 2\pi) = 1.0,$$

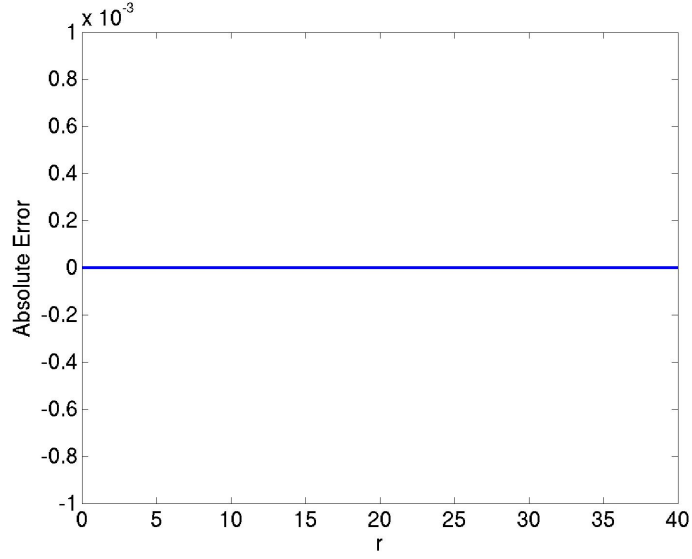


Figure B.5: Error for Benchmark Problem 2

and $u = v = w = 1.0$ for all grid points. If the exact solutions of T and Y are taken as

$$T = 1 + e^{-3t}(\sin(x_1)\sin(x_2)\sin(x_3)), \quad (\text{B.19})$$

$$Y = 1 + e^{-3t}(\sin(x_1)\sin(x_2)\sin(x_3)), \quad (\text{B.20})$$

and if $\lambda_1 = 1$ the value of Q_1 is

$$Q_1 = \beta(T_{x_1} + T_{x_2} + T_{x_3}). \quad (\text{B.21})$$

The value of Q_2 is

$$Q_2 = Q_1 T. \quad (\text{B.22})$$

Figures B.6 and B.7 show the differences between the computed and analytical solutions, for the temperature and species respectively. These results show that after 2000 time steps the difference between the analytical results and the computed results is less than 0.01%.

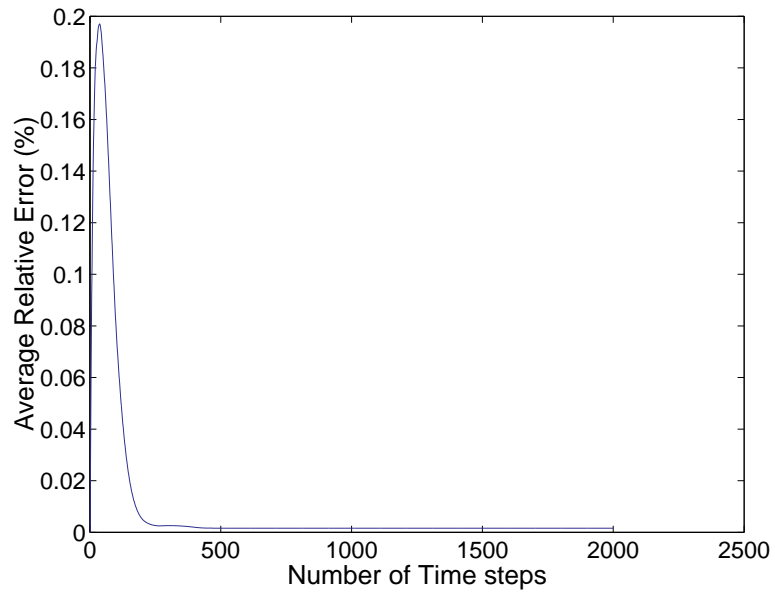


Figure B.6: Benchmark Problem 3, Error in the Temperature, Grid = 16 cubed

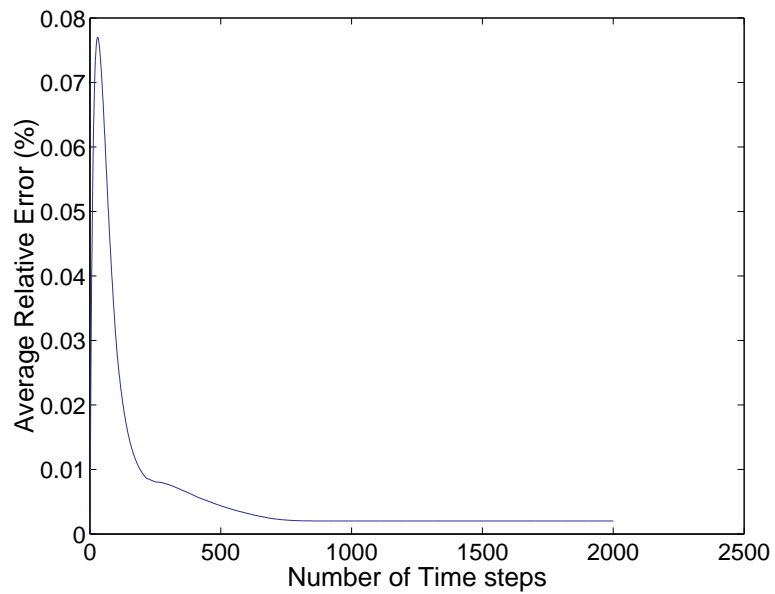


Figure B.7: Benchmark Problem 3, Error in the Species, Grid = 16 cubed

Appendix C

Normal Mode Analysis

The stability of the system is examined using a numerical normal mode analysis. The perturbed solutions are defined as

$$\begin{bmatrix} F(z) \\ G(z) \\ H(z) \\ T(r, \theta, z, t) \\ Y_f(r, \theta, z, t) \\ Y_o(r, \theta, z, t) \end{bmatrix} = \begin{bmatrix} F(z) \\ G(z) \\ H(z) \\ T_{ss}(z) \\ Y_{fss}(z) \\ Y_{oss}(z) \end{bmatrix} + \begin{bmatrix} 0 \\ 0 \\ 0 \\ \hat{T}(z) \\ Y_f \hat{}(z) \\ \hat{Y}_o(z) \end{bmatrix} Ar^k e^{\omega\tau + ik\theta}, \quad (\text{C.1})$$

where, $T_{ss}(z)$, $Y_{fss}(z)$, and $Y_{oss}(z)$ are the 1-dimensional steady state solutions, ω is the growth rate and k is the wavenumber. Detailed derivation of the separated form is included in the appendix. Upon substituting the above perturbed solutions into the field equations

and linearizing, equations for $\hat{T}(z)$, $\hat{Y}_f(z)$, and $\hat{Y}_o(z)$ are obtained

$$\omega\hat{T} + kF\hat{T} + ikG\hat{T} + H\hat{T}' - \hat{T}'' = \beta\hat{\Omega}, \quad (\text{C.2})$$

$$\omega\hat{Y}_f + kF\hat{Y}_f + ikG\hat{Y}_f + H\hat{Y}_f' - \hat{Y}_f''/Le_f = \alpha_f\hat{\Omega}, \quad (\text{C.3})$$

$$\omega\hat{Y}_o + kF\hat{Y}_o + ikG\hat{Y}_o + H\hat{Y}_o' - \hat{Y}_o''/Le_o = \alpha_o\hat{\Omega}, \quad (\text{C.4})$$

where,

$$\hat{\Omega} = D\bar{D}e^{-Ze/T_{ss}}(Y_{oss}\hat{Y}_f + Y_{fss}\hat{Y}_o + Y_{fss}Y_{oss}Ze\hat{T}T_{ss}^{-2}). \quad (\text{C.5})$$

The boundary conditions for the linearized system are

$$\hat{T}(0) = 0, \quad \hat{Y}_o'(0) = PeLe_o\hat{Y}_o(0), \quad \hat{Y}_f'(0) = PeLe_f\hat{Y}_f(0), \quad (\text{C.6})$$

$$\hat{T}(\infty) = 0, \quad \hat{Y}_o(\infty) = 0, \quad \text{and} \quad \hat{Y}_f(\infty) = 0. \quad (\text{C.7})$$

When discretized, equations C.2-C.7 define a matrix eigenvalue problem of the form

$$(\mathbf{A} + \omega\mathbf{B})\vec{X} = 0, \quad (\text{C.8})$$

where \mathbf{A} is

$$\begin{bmatrix}
 1 & 0 & 0 & 0 & 0 & 0 & 0 & 0 & 0 & -0 \\
 0 & \frac{3}{2\Delta z} + PeLe_o & 0 & 0 & -\frac{4}{2\Delta z} & 0 & 0 & \frac{1}{2\Delta z} & 0 & -0 \\
 0 & 0 & \frac{3}{2\Delta z} + PeLe_f & 0 & 0 & -\frac{4}{2\Delta z} & 0 & 0 & \frac{1}{2\Delta z} & -0 \\
 \Pi_1 & 0 & 0 & \Gamma_{1_1} & D\bar{D}e^{-ZeT_{ss1}^{-1}}Y_{f1} & D\bar{D}e^{-ZeT_{ss1}^{-1}}Y_{o1} & \bar{\Pi}_1 & 0 & - & -0 \\
 0 & \Pi_2 & 0 & \Lambda_1 & \Gamma_{2_1} & D\bar{D}e^{-ZeT_{ss1}^{-1}}Y_{o1} & 0 & \bar{\Pi}_2 & 0 & -0 \\
 0 & 0 & \Pi_3 & \Lambda_1 & D\bar{D}e^{-ZeT_{ss1}^{-1}}Y_{f1} & \Gamma_{3_1} & 0 & 0 & \bar{\Pi}_3 & -0 \\
 | & | & | & | & | & | & | & | & | & | \\
 | & | & | & | & | & | & | & | & | & | \\
 | & | & | & | & | & | & | & | & | & | \\
 | & | & | & | & | & | & | & | & 1 & 0 & 0 \\
 | & | & | & | & | & | & | & | & 0 & 1 & 0 \\
 | & | & | & | & | & | & | & | & 0 & 0 & 1
 \end{bmatrix} \tag{C.9}$$

where,

$$\begin{aligned}
 \Pi_1 &= H/2\Delta z + 1/\Delta z^2, & \bar{\Pi}_1 &= -H/2\Delta z + 1/\Delta z^2, \\
 \Pi_2 &= H/2\Delta z + 1/Le_f\Delta z^2, & \bar{\Pi}_2 &= -H/2\Delta z + 1/Le_f\Delta z^2, \\
 \Pi_3 &= H/2\Delta z + 1/Le_o\Delta z^2, & \bar{\Pi}_3 &= -H/2\Delta z + 1/Le_o\Delta z^2, \\
 \Lambda_j &= D\bar{D}Y_{ossj}Y_{fssj}ZeT_{ssj}^{-2}, \\
 \Gamma_{1_j} &= -kF_{ssj} - ikG_{ssj} - 2\Delta z^{-2} + \beta Y_{fssj}Y_{ossj}D\bar{D}e^{-ZeT_{ssj}^{-1}}ZeT_{ssj}^{-2}, \\
 \Gamma_{2_j} &= -kF_{ssj} - ikG_{ssj} - 2\Delta z^{-2} + \alpha_f Y_{ossj}D\bar{D}e^{-ZeT_{ssj}^{-1}}, \\
 \Gamma_{3_j} &= -kF_{ssj} - ikG_{ssj} - 2\Delta z^{-2} + \alpha_o Y_{fssj}D\bar{D}e^{-ZeT_{ssj}^{-1}}.
 \end{aligned} \tag{C.10}$$

\mathbf{B} is given by,

$$\begin{aligned}
 B(i, i) &= 1, \quad \text{for } i = 4, \text{ to } i = 3N - 3, \\
 B(i, i) &= 0, \quad \text{for } i = 1, \quad 3N - 2, \quad 3N - 1, \quad 3N, \\
 B(i, j) &= 0, \quad \text{for } i, \neq j
 \end{aligned}$$

and

$$\vec{X}^T = \left[T_0 \quad Y_{o0} \quad Y_{f0} \quad T_1 \quad Y_{o1} \quad Y_{f1} \quad T_2 \quad Y_{o2} \quad Y_{f2} \quad - \quad - \quad - \quad - \quad T_N \quad Y_{oN} \quad Y_{fN} \right]. \quad (\text{C.11})$$

Here, N , is the total number of grid pts used in the discretization. Figure C.1 shows the progression of the largest eigenvalue from stable (< 0) to unstable (> 0) values, for wavenumbers of 1 to 7, $N = 50$. As seen from this figure, at high Damköhler numbers the largest eigenvalue for all the modes asymptotes to a negative value. As the Damköhler number decreases the eigenvalue transitions from this stable branch to an unstable one. The Damköhler number at which this transition occurs decreases as the wavenumber increases. Table C shows the Damköhler numbers for which the system becomes unstable alongside the Damköhler numbers that are observed in the three-dimensional simulations for a 64^3 grid. The extinction Damköhler number for this problem is $D_E = 1.46$

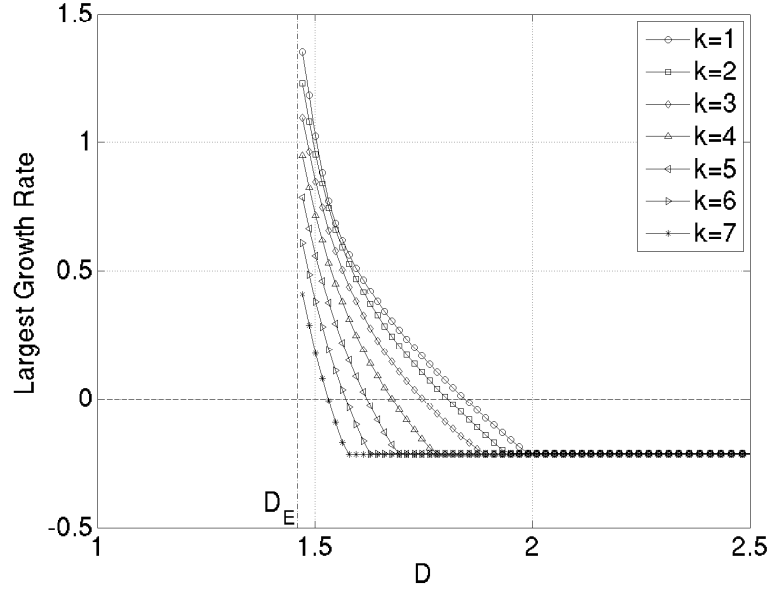


Figure C.1: The first eigenvalue as a function of D for several k 's, $N = 50$

k	$D(N = 50)$	$D(N = 100)$	$D(3\text{-D}, 64^3 \text{ Grid})$
1	1.845	1.82	1.90
2	1.806	1.79	1.85
3	1.748	1.74	-
4	1.678	1.67	-
5	1.620	1.61	-
6	1.572	1.56	-
7	1.531	1.49	-

Table C.1: Transition Damköhler Numbers from the eigenvalue problem and from 3-D simulations for $k = 1$ to $k = 7$

Appendix D

Eigenvalue Problem: Separation of Variables

The non-dimensional system is given by,

$$F = \frac{u}{b_0 r}, \quad G = \frac{v}{b_0 r}, \quad H = \frac{w}{\sqrt{b_0 \nu}}, \quad (\text{D.1})$$

where F , G , H are functions of z . The resulting non-dimensional equations are

$$H' = -2F, \quad (\text{D.2})$$

$$F'' = F^2 + F'H - G^2, \quad (\text{D.3})$$

$$G'' = 2FG + HG', \quad (\text{D.4})$$

$$P' = 2HF - 2F'. \quad (\text{D.5})$$

$$F(0) = 0, \quad G(0) = G_0 = 1, \quad H(0) = H_0, \quad P(0) = 0,$$

$$F(\infty) = 0, \quad G(\infty) = 0. \quad (\text{D.6})$$

$$L[T, Y_i] - M[Pr^{-1}T, Pr^{-1}Le_i Y_i] = \Omega[\beta, -\alpha_i], \quad (\text{D.7})$$

where

$$\mathbf{L} = \frac{\partial}{\partial t} + rF \frac{\partial}{\partial r} + G \frac{\partial}{\partial \theta} + H \frac{\partial}{\partial z},$$

$$\mathbf{M} = \frac{1}{r} \frac{\partial}{\partial r} + \frac{\partial^2}{\partial r^2} + \frac{1}{r^2} \frac{\partial}{\partial \theta^2} + \frac{\partial^2}{\partial z^2}.$$

The boundary conditions are,

$$z = 0 : \quad T_0 = T_s, \quad \frac{\partial Y_f}{\partial z} = H_0 Pr Le_f (Y_f - 1), \quad \frac{\partial Y_o}{\partial z} = H_0 Pr Le_o Y_o,$$

$$z = \infty : \quad T_\infty = 1, \quad Y_f = 0, \quad Y_o = \phi^{-1},$$

$$r = 0 : \quad \frac{\partial T}{\partial r} = 0, \quad \frac{\partial Y_i}{\partial r} = 0, \quad r = \infty : \quad \frac{\partial T}{\partial r} = 0, \quad \frac{\partial Y_i}{\partial r} = 0,$$

$$T|_{\theta=0} = T|_{\theta=2\pi}, \quad Y_i|_{\theta=0} = Y_i|_{\theta=2\pi}, \quad \frac{\partial T}{\partial \theta}|_{\theta=0} = \frac{\partial T}{\partial \theta}|_{\theta=2\pi}, \quad \frac{\partial Y_i}{\partial \theta}|_{\theta=0} = \frac{\partial Y_i}{\partial \theta}|_{\theta=2\pi}.$$

The perturbed solutions are defined as

$$\begin{bmatrix} F(z) \\ G(z) \\ H(z) \\ T(r, \theta, z, t) \\ Y_f(r, \theta, z, t) \\ Y_o(r, \theta, z, t) \end{bmatrix} = \begin{bmatrix} F(z) \\ G(z) \\ H(z) \\ T_{ss}(z) \\ Y_{fss}(z) \\ Y_{oss}(z) \end{bmatrix} + \begin{bmatrix} 0 \\ 0 \\ 0 \\ \tilde{T}(r, \theta, z, t) \\ \tilde{Y}_f(r, \theta, z, t) \\ \tilde{Y}_o(r, \theta, z, t) \end{bmatrix}, \quad (\text{D.9})$$

where, $T_{ss}(z)$, $Y_{fss}(z)$, and $Y_{oss}(z)$ are the 1-dimensional steady state solutions. From these equations it is evident that t and θ are readily separable if the perturbations are taken to be

of the form

$$\begin{bmatrix} \tilde{T}(r, \theta, z, t) \\ \tilde{Y}_f(r, \theta, z, t) \\ \tilde{Y}_o(r, \theta, z, t) \end{bmatrix} = \begin{bmatrix} \tilde{T}(r, z) \\ \tilde{Y}_f(r, z) \\ \tilde{Y}_o(r, z) \end{bmatrix} e^{\omega t + ik\theta}. \quad (\text{D.10})$$

The resulting equations are

$$\omega\check{T} + rF\check{T}_r + ikG\check{T} + H\check{T}_z = (\check{T}_r/r + \check{T}_{rr} - k^2\check{T}/r^2 + \check{T}_{zz}) + \beta\check{\Omega}, \quad (\text{D.11})$$

$$\omega\check{Y}_f + rF\check{Y}_f r + ikG\check{Y}_f + H\check{Y}_f z = 1/Le_f (\check{Y}_f r/r + \check{Y}_{frr} - k^2\check{Y}_f/r^2 + \check{Y}_{fzz}) - \alpha_f\check{\Omega}, \quad (\text{D.12})$$

$$\omega\check{Y}_o + rF\check{Y}_o r + ikG\check{Y}_o + H\check{Y}_o z = 1/Le_o (\check{Y}_o r/r + \check{Y}_{orr} - k^2\check{Y}_o/r^2 + \check{Y}_{ozz}) - \alpha_o\check{\Omega}, \quad (\text{D.13})$$

where, $\check{\Omega} = D\bar{D}e^{-Ze/T_{ss}} (Y_{oss}\check{Y}_f + Y_{fss}\check{Y}_o + Y_{fss}Y_{oss}Ze\check{T}/T_{ss}^2)$. Now, taking the perturbations

as

$$\begin{bmatrix} \check{T}(r, z) \\ \check{Y}_f(r, z) \\ \check{Y}_o(r, z) \end{bmatrix} = \begin{bmatrix} R(r)\hat{T}(z) \\ R(r)\hat{Y}_f(z) \\ R(r)\hat{Y}_o(z) \end{bmatrix}, \quad (\text{D.14})$$

the equation for \check{T} becomes

$$\omega + ikG + H\hat{T}'/\hat{T} - \hat{T}''/\hat{T} + \beta\hat{\Omega} = R''/R + R'/(rR) - rFR'/R - k^2/r^2. \quad (\text{D.15})$$

In order for the above equation to be separable, rR'/R has to be a constant because $F = F(z)$. Thus,

$$rR'/R = \text{const} \quad (\text{D.16})$$

$$\rightarrow R = Ar^\alpha. \quad (\text{D.17})$$

Thus,

$$\omega + ikG + H\hat{T}'/\hat{T} - \hat{T}''/\hat{T} + \alpha F + \beta\hat{\Omega} = \alpha(\alpha - 1)r^{\alpha-2}/r^\alpha + \alpha r^{\alpha-1}/(rr^\alpha) - k^2/r^2. \quad (\text{D.18})$$

The right hand side of the above equation must equal a constant. Thus,

$$\alpha^2/r^2 - k^2/r^2 = \text{const}. \quad (\text{D.19})$$

Since α and k are constants, for equation D.19 to be true for all r , the constant must be zero, and so,

$$\alpha = \pm k \quad (\text{D.20})$$

and the equations for \hat{T} , \hat{Y}_f and \hat{Y}_o are

$$\omega\hat{T} + kF\hat{T} + ikG\hat{T} + H\hat{T}_z + \hat{T}_{zz} - \beta\hat{\Omega} = 0, \quad (\text{D.21})$$

$$\omega\hat{Y}_f + kF\hat{Y}_f + ikG\hat{Y}_f + H\hat{Y}_{fz} + 1/Le_f\hat{Y}_{fzz} + \alpha_f\hat{\Omega} = 0, \quad (\text{D.22})$$

$$\omega\hat{Y}_o + kF\hat{Y}_o + ikG\hat{Y}_o + H\hat{Y}_{oz} + 1/Le_o\hat{Y}_{ozz} + \alpha_o\hat{\Omega} = 0, \quad (\text{D.23})$$

where, $\hat{\Omega} = D\bar{D}e^{-Ze/T_{ss}} \left(Y_{oss}\hat{Y}_f + Y_{fss}\hat{Y}_o + Y_{fss}Y_{oss}Ze\hat{T}/T_{ss}^2 \right)$. Thus,

$$\check{T}(r, \theta, z, t) = \sum_{k=0}^{\infty} A_k r^{+k} \hat{T}(z) e^{\omega t + ik\theta}, \quad (\text{D.24})$$

$$\check{Y}_f(r, \theta, z, t) = \sum_{k=0}^{\infty} A_k r^{+k} \hat{Y}_f(z) e^{\omega t + ik\theta}, \quad (\text{D.25})$$

$$\check{Y}_o(r, \theta, z, t) = \sum_{k=0}^{\infty} A_k r^{+k} \hat{Y}_o(z) e^{\omega t + ik\theta}. \quad (\text{D.26})$$

To satisfy the boundary condition, $\partial[\check{T}, \check{Y}_i]/\partial r = 0$ as $r \rightarrow \infty$,

$$\sum_{k=0}^{\infty} k A_k r^{k-1} [\hat{T}(z), \hat{Y}_i(z)] e^{ik\theta} = 0, \quad (\text{D.27})$$

and so

$$\sum_{k=0}^{\infty} k A_k r^k e^{ik\theta} = 0. \quad (\text{D.28})$$

This condition dictates that the coefficients A_k be such that $r \rightarrow \infty$ be included in the region of convergence for $\sum_{k=0}^{\infty} k A_k r^k e^{ik\theta}$. Now, since $k \geq 0$, it follows that $|A_k r^k e^{ik\theta}| \leq |k A_k r^k e^{ik\theta}|$.

Thus, from the theorems that if $\sum |u_n|$ converges and $|v_n| \leq |u_n|$, then $\sum |v_n|$ converges, and if $\sum |u_n|$ converges, then $\sum u_n$ converges, (where $\sum u_n = \sum_{n=1}^{\infty} u_n = u_1 + u_2 + \dots$),

$\sum_{k=0}^{\infty} A_k r^k e^{ik\theta}$ should converge as $r \rightarrow \infty$.

Upon discretization using following expressions for the first and second derivatives at the interior and boundary points

$$\frac{dX_j}{dz} = (X_{j+1} - X_{j-1})/(2\Delta z), \quad (\text{D.29})$$

$$\frac{d^2X_j}{dz^2} = (X_{j+1} - 2X_j + X_{j-1})/(\Delta z)^2, \quad (\text{D.30})$$

$$\frac{dX_0}{dz} = (-3X_0 + 4X_1 - X_2)/(2\Delta z), \quad (\text{D.31})$$

$$\frac{dX_N}{dz} = (-3X_N + 4X_{N-1} - X_{N-2})/(2\Delta z), \quad (\text{D.32})$$

the temperature equation becomes,

$$\begin{aligned} \omega \hat{T}_j = & \hat{T}_j(-kF - ikG + D\bar{D}e^{-Ze/T_{ss}}Y_{fss}Y_{oss} - 2/(\Delta z)^2) \\ & + \hat{T}_{j-1}\{H/(2\Delta z) + 1/(\Delta z)^2\} \\ & + \hat{T}_{j+1}\{-H/(2\Delta z) + 1/(\Delta z)^2\} \\ & + D\bar{D}e^{-Ze/T_{ss}}(Y_{oss}\hat{Y}_f + Y_{fss}\hat{Y}_o). \end{aligned} \quad (\text{D.33})$$

Similarly, discretized equations for the species and boundary conditions are found and the resulting system is given by equation C.8.

Appendix E

Source Code

Makefile

```
SHELL      = /bin/sh
.SUFFIXES: .o .f90 .f

OSTYPE     = $(shell uname)

EXEC       = vkcf

OBJS       = vk_colsys.o dcolsys.o vkvar.o vkpar.o vk_in.o\
             gen_grid.o der_ord_4_2.o grid_map.o func_def.o\
             vk_cf.o vkcf_driver.o\
                                                    10

MX         = mod
CD         = \cd
LN         = ln -sf
RM         = rm -f
ECHO      = echo

#----- options for Blue Horizon (San Diego)
CXX        = g++
F90C       = mpif90
F77C       = mpif77
F90FLAGS   = -qsuffix=f=f90 -qinitauto -qthreaded -qtune=auto
F77FLAGS   = -O3 -Q -qinitauto -qthreaded -qstrict -qtune=auto -qzerosize
LD         = $(F90C)
LDFLAGS    = -bind_at_load
LDLIBS     = -lpmpich -lpich -lmpe
                                                    20

all :      note run
                                                    30
```

```

note:
    $(ECHO) "Building $(EXEC) on a $(OSTYPE) system. $(F90C)"
    -$(RM) $(EXEC)

$(EXEC):    $(OBJS)
            $(LD) $(LDFLAGS) $(F90FLAGS) -o $(EXEC) $(OBJS) $(LDLIBS)

run :      $(EXEC)                                     40

seq :
    -$(CD) orig_code;$(MAKE)

#----- dependencies
vk_colsys.o: vk_colsys.f dcolsys.o
dcolsys.o: dcolsys.f
vkvar.o: vkvar.f90
vk_in.o: vk_in.f90 vkvar.o
vkpar.o: vkpar.f90 vkvar.o vk_in.o                    50
gen_grid.o: gen_grid.f90 vkvar.o
der_ord_4_2.o: der_ord_4_2.f90 vkvar.o
grid_map.o: grid_map.f90 der_ord_4_2.o
func_def.o: func_def.f90 vkvar.o
vk_cf.o: vk_cf.f90 vkvar.o vkpar.o der_ord_4_2.o
vkcf_driver.o: vkcf_driver.f90 vkvar.o vk_in.o gen_grid.o der_ord_4_2.o grid_map.o func_def.o vk_cf.o vkpar.o

#----- implicit rules
%.o: %.f90
    $(F90C) -c $(F90FLAGS) $<                          60
%.o: %.f
    $(F77C) -c $(F77FLAGS) $<
.C.o :
    $(CXX) -c $(OFLAGS) $<
###%.o: %.f90
###  $(F90C) -c $(F90FLAGS) $< -o $@
###%.o: %.f
###  $(F77) -c $(FFLAGS) $< -o $@
#----- clean
clean                                     70

new : clean note run

clean: runclean
    -$(RM) -f *~ *.o *.mod *.s $(EXEC)
runclean:
    -$(RM) -f core fort.* $(EXEC)
#-----

```

Driver

```

PROGRAM vk
!
```

```

=====
! This is the top level driver for the parallel version
! of the three-dimensional fourth order Runge Kutta
! code used for solving the Spinning Disk Flame Sheet
! Problem
!
! Date : April 2005
=====
!
!
! USE vkvar
! USE vk_in
! USE gen_grid
! USE der_ord_4
! USE grid_map
! USE func_def
! USE vk_cf
! USE vkpar
!
!
! IMPLICIT NONE
!
! INTEGER :: var,nn,npts,k,j,i
! REAL*8 :: tt1, tt2, mod1,tout,time1,time2,total_time
!
! Initiate MPI
=====
!
! call MPI_INIT(ierr)
! call MPI_COMM_RANK(MPI_COMM_WORLD, id, ierr)
! call MPI_COMM_SIZE(MPI_COMM_WORLD, nprocs, ierr)
! CALL MPI_BARRIER(MPI_COMM_WORLD,ierr)
!
!
! Read Inputs
=====
!
! CALL input
! CALL grid_assign
! CALL MPI_BARRIER(MPI_COMM_WORLD,ierr)
!
! Allocate arrays, set up grid and initial conditions and
! communicate with adjacent processors
=====
!
! CALL allocate
! CALL grid
! if (irestart==0) CALL initial_conditions(nvar)
! if (irestart==1.or.irestart==2) CALL restart
! if (irestart==3) CALL initial_colsys
!
! CALL MPI_BARRIER(MPI_COMM_WORLD,ierr)
! CALL vk_buffer_comm(1,fsize)
! CALL init_runge

```

10

20

30

40

50

```

CALL MPI_BARRIER(MPI_COMM_WORLD,ierr)
!
  if (id==0) then
    print 1, 'D=',Damk, 'Le_F=', Le1, 'Pr=', Pr,'Pe=',Pe
  end if
! format(a6,f24.4,a6,f4.2,a6,f4.2,a6,f4.2)
! If there is a stretch map the derivaties
!=====
!
  CALL der_map
!
! Print pertinent parameters to screen
!=====
!
!
!
! Integrate until tstop is reached
!=====
!
  if (irestart==0) then
    if (id==0) open(UNIT=222,file='vkout.dat',status='replace')
    t = 0.0
  end if
!
  if (irestart==3) then
    if (id==0) open(UNIT=222,file='vkout.dat',status='replace')
    t = 0.0
  end if
!
  if (irestart==1) then
    if (id==0) open(UNIT=222,file='vkout.dat',status='old',position='append')
    t = tlast
  end if
!
  if (irestart==2) then
    if (id==0) open(UNIT=222,file='vkout.dat',status='replace')
    t = 0.0
  end if
!
  time1 = MPI_WTIME()
  DO nn=1,n_tstep
!
    tout = t + dt
    CALL rk54(t,tout)
    CALL MPI_BARRIER(MPI_COMM_WORLD,ierr)
!
    if (mod(nn,err_out_freq)==0) CALL track_error(t)
    if (nn==51000.and.pert.ne.0.0) CALL perturb
    if (mod(nn,cont_out_freq)==0.and.nn.ne.n_tstep) then
      CALL vk_communication(1,fsize)
      CALL output(t,nn)
    end if
!

```



```

END DO
!
time2 = MPI_WTIME()
nn = nn-1
CALL vk_communication(1,fsize)
CALL output(t,nn)
!
CLOSE(222)
!
!
! Gather the temperature and species values from all the processors
! and write them to the output file
!=====
!
if (id ==0) print *, 'Wrote output'
!
total_time = time2-time1
!
if (id == 0) print 22, 'Time taken: ', total_time
!
22 format(2x,a12,1f36.20)
!
print *, id, 'RUN COMPLETED'
!
! Deallocate all arrays and call for a stop
!=====
!
deallocate(f,ferr,cc,cc1,Q1,fprime,VEL)
!
call MPI_FINALIZE(ierr)
!
STOP
!
END PROGRAM vk

```

Global Variables

```

MODULE vkvar
  IMPLICIT NONE
!
  SAVE
!
  INCLUDE "mpif.h"
!
  INTEGER, PARAMETER :: nx1max=100
  INTEGER, PARAMETER :: nx2max=100
  INTEGER, PARAMETER :: nx3max=100
  INTEGER, PARAMETER :: nmax=nx1max
  INTEGER, PARAMETER :: neqmax=6
  INTEGER :: n_tstep, nvar, n1, n2, n3, irestart, twrite
  REAL*8 :: t, tlast, pert, wnum, RHO, CP, U, V, W, LAMBDA, Q, OMEGA, STRETCH1, STRETCH2, STRETCH3
  REAL*8 :: T0, TINF, tprev, H0, b0
  REAL*8 :: dx1, dx2, dx3, rmt, rm, kny

```

```

REAL*8, DIMENSION(:), TARGET, ALLOCATABLE :: ibnd,jbnd,kbnd
INTEGER :: iord,err_out_freq,cont_out_freq
INTEGER :: neqn,nx1,nx2,nx3
REAL*8 :: x1min,x2min,x3min,x1max,x2max,x3max,dt,dt1
REAL*8 :: tend,cfl,tmax
REAL*8 :: dx1min,dx2min,dx3min,x1lrnx,x2lrnx,x3lrnx,x1knx1,x2knx2
REAL*8, DIMENSION(:), TARGET, ALLOCATABLE :: ack,bck,cck
INTEGER :: ikutta,nstage,ikk,n2x,noutput2,noutput1,grd1,grd2,grd3
REAL*8, DIMENSION(:), POINTER :: wf
REAL*8, DIMENSION(:,:,:), TARGET, ALLOCATABLE :: cc1
REAL*8, DIMENSION(:,:,:), TARGET, ALLOCATABLE :: cc
REAL*8, DIMENSION(:,:,:), TARGET, ALLOCATABLE :: rkj
REAL*8, DIMENSION(:,:,:), TARGET, ALLOCATABLE :: fprime
REAL*8, DIMENSION(:,:,:), TARGET, ALLOCATABLE:: dfdx1,dfdx2,dfdx3
REAL*8, DIMENSION(:,:,:), TARGET, ALLOCATABLE :: df2dx1,df2dx2,df2dx3
REAL*8, DIMENSION(:,:,:), TARGET, ALLOCATABLE :: df2dx1dx2,df2dx1dx3,df2dx2dx3
REAL*8, DIMENSION(:), POINTER :: b,d,rl,u1,a
REAL*8 :: alp1st,a1st,b1st,alp2st,a2st,b2st
!
REAL*8, DIMENSION(:,:), TARGET, ALLOCATABLE :: Q1
REAL*8, DIMENSION(:,:), TARGET, ALLOCATABLE :: Q2
REAL*8, DIMENSION(:,:,:), TARGET, ALLOCATABLE :: f
REAL*8, DIMENSION(:,:,:), TARGET, ALLOCATABLE :: ferr
REAL*8, DIMENSION(:,:,:), TARGET, ALLOCATABLE :: fx1
REAL*8, DIMENSION(:,:,:), TARGET, ALLOCATABLE :: fx2
REAL*8, DIMENSION(:,:,:), TARGET, ALLOCATABLE :: fx3
REAL*8, DIMENSION(:,:,:), TARGET, ALLOCATABLE :: ff1
REAL*8, DIMENSION(:,:,:), TARGET, ALLOCATABLE :: ff2
REAL*8, DIMENSION(:,:,:), TARGET, ALLOCATABLE :: ff3
REAL*8, DIMENSION(:), TARGET, ALLOCATABLE :: x1
REAL*8, DIMENSION(:), TARGET, ALLOCATABLE :: x2
REAL*8, DIMENSION(:), TARGET, ALLOCATABLE :: x3
REAL*8, DIMENSION(:), TARGET, ALLOCATABLE :: xx1
REAL*8, DIMENSION(:), TARGET, ALLOCATABLE :: xx2
REAL*8, DIMENSION(:), TARGET, ALLOCATABLE :: xx3
REAL*8, DIMENSION(:), TARGET, ALLOCATABLE :: dxidx
REAL*8, DIMENSION(:), TARGET, ALLOCATABLE :: dxi2dx2
REAL*8, dimension(:,:,:), target, allocatable :: f_prime
REAL*8, dimension(:,:,:), target, allocatable :: f_prime_periodic
REAL*8, dimension(:,:,:), target, allocatable :: f_pprime_per
REAL*8, dimension(:,:,:), target, allocatable :: f_periodic
REAL*8, dimension(:,:,:), target, allocatable :: f_pprime
REAL*8, dimension(:,:,:), target, allocatable :: f_cpprime
REAL*8, dimension(:,:), target, allocatable :: VEL
INTEGER :: fsize
REAL*8 :: Pr, Damk, beta, eq1, eps, Le1, Le2, alpha1, alpha2, bcval, Pe
REAL*8 :: tstar, zstar
!
! MPI related variables
INTEGER :: nprocs, id, cart_comm, ierr,ierror, ghostlayer, mpilayer
INTEGER :: x1size, x2size, x3size, tosize, velsize
INTEGER :: sbx1_size,sbx2_size,sbx3_size
INTEGER, dimension(:), TARGET, ALLOCATABLE :: allsize, disp, allrange

```

```

INTEGER, dimension(2) :: loci, locj, lock
INTEGER, dimension(3) :: comm, rid, rsize, coords, free, dims,periodic
INTEGER, dimension(6) :: idnbr
INTEGER :: err_chk
INTEGER, dimension(3,2) :: dom_bound,sndim
REAL*8,dimension(3) :: sndx
REAL*8, dimension(:, :, :), target, allocatable :: out_f
REAL*8, dimension(:), target, allocatable :: out_x1
REAL*8, dimension(:), target, allocatable :: out_x2
REAL*8, dimension(:), target, allocatable :: out_x3
REAL*8, dimension(:), target, allocatable :: myres
REAL*8, dimension(:), target, allocatable :: allres
REAL*8, dimension(:), target, allocatable :: send_buffx1_r
REAL*8, dimension(:), target, allocatable :: send_buffx1_l
REAL*8, dimension(:), target, allocatable :: send_buffx2_r
REAL*8, dimension(:), target, allocatable :: send_buffx2_l
REAL*8, dimension(:), target, allocatable :: send_buffx3_r
REAL*8, dimension(:), target, allocatable :: send_buffx3_l
REAL*8, dimension(:), target, allocatable :: recv_buffx1_l
REAL*8, dimension(:), target, allocatable :: recv_buffx1_r
REAL*8, dimension(:), target, allocatable :: recv_buffx2_l
REAL*8, dimension(:), target, allocatable :: recv_buffx2_r
REAL*8, dimension(:), target, allocatable :: recv_buffx3_l
REAL*8, dimension(:), target, allocatable :: recv_buffx3_r
!
END MODULE vkvar

```

IO and Perturbations

```

MODULE vk_in
!
CONTAINS
SUBROUTINE input
!
! This SUBROUTINE reads input parameters from file vk.dat
!=====
!
!
! USE vkvar
!
! IMPLICIT NONE
!
! INTEGER :: d1
! REAL*8 :: dummy
!
! open(Unit=14,file="vkcf.dat")
!
! read(14,'(a40)')
! read(14,*) nvar,n_tstep,dt
! read(14,'(a40)')
! read(14,*) ikutta,iord
! read(14,'(a40)')

```

```

read(14,*) H0,b0, eq1
read(14,'(a40)')
read(14,*) x1min,x2min,x3min
read(14,'(a10)')
read(14,*) x1max,x2max,x3max
read(14,'(a40)')
read(14,*) nx1,nx2,nx3
read(14,'(a60)')
read(14,*) STRETCH1, STRETCH2, STRETCH3
read(14,'(a60)')
read(14,*) Pr, Le1, Le2, Damk, alpha1, alpha2, beta, eps, bcval
read(14,'(a60)')
read(14,*) T0, TINF
read(14,'(a80)')
read(14,*) irestart, pert, wnum, err_out_freq, cont_out_freq
read(14,'(a80)')
read(14,*) grd1,grd2,grd3
read(14,'(a80)')
read(14,*) tstar, zstar
close(14)
!
! Check for input errors
!=====
!
err_chk = 0
if (nx1.le.4.or.nx2.le.4.or.nx3.le.4) err_chk = 1
if (n_tstep.le.0) err_chk = 2
if (ikutta.le.0) err_chk = 3
if (Pr.lt.0.or.Le1.lt.0.or.Le2.lt.0.or.Damk.lt.0) err_chk = 4
if (alpha1.lt.0.or.alpha2.lt.0.or.eps.lt.0.or.bcval.lt.0) err_chk = 4
if (irestart.lt.0.or.irestart.gt.3) err_chk = 5
!
CALL ERROR
!
! Run vkcolsys in order to calculate the flowfield
! The velocities are stored in 'vel.dat'
!=====
!
if (id ==0) call vkcolsys(nx3,STRETCH3,x3min,x3max,H0,b0)
CALL MPI_BARRIER(MPI_COMM_WORLD,ierr)
!
open(Unit=15,file="vel.dat")
!
!
! Correct some variables
!=====
!
fsize = nvar+3
!
END SUBROUTINE input
!
!=====
!=====

```

```

!
Subroutine restart
!
USE vkvar
!
IMPLICIT NONE
!
INTEGER :: i,j,k,proc
INTEGER,dimension(2) :: indi,indj,indk
REAL*8, dimension(:,:,:),allocatable :: fres
!
allocate(fres(3,0:sndim(3,1)-1,0:sndim(2,1)-1,0:sndim(1,1)-1))
do i = 1,2
    indi(i) = loci(i)-dom_bound(1,i)
    indj(i) = locj(i)-dom_bound(2,i)
    indk(i) = lock(i)-dom_bound(3,i)
end do
!
if (id==0) then
    open(UNIT=301,file='res.dmp',status='old')
    do k = 0,sndim(3,1)-1
        do j = 0,sndim(2,1)-1
            do i = 0,sndim(1,1)-1
                read(301,*) fres(1,k,j,i), fres(2,k,j,i), fres(3,k,j,i)
            end do
        end do
    end do
    read(301,*) tlast
    close(301)
end if
call MPI_BARRIER(MPI_COMM_WORLD,ierr)
do k = indk(1),indk(2)
    do j = indj(1),indj(2)
        do i = indi(1),indi(2)
            f(1,k,j,i) = fres(1,k,j,i)
            f(2,k,j,i) = fres(2,k,j,i)
            f(3,k,j,i) = fres(3,k,j,i)
            ferr(1,k,j,i) = f(1,k,j,i)
        end do
    end do
end do
deallocate(fres)
end Subroutine restart
!
=====
!
=====
!

```

```

Subroutine allocate
!
  USE vkvar
!
  IMPLICIT NONE
!
  INTEGER :: k
  REAL*8 :: aplace_holder
!
  ALLOCATE(f(1:fsize,lock(1):lock(2),locj(1):locj(2),loci(1):loci(2)))
  ALLOCATE(ferr(1:1,lock(1):lock(2),locj(1):locj(2),loci(1):loci(2)))
  ALLOCATE(fprime(1:fsize,lock(1):lock(2),locj(1):locj(2),loci(1):loci(2)))
  ALLOCATE(rkj(1:nvar,lock(1):lock(2),locj(1):locj(2),loci(1):loci(2)))
  ALLOCATE(cc(1:2*nvar,1:3,lock(1):lock(2),locj(1):locj(2),loci(1):loci(2)))
  ALLOCATE(cc1(1:2,1:3,lock(1):lock(2),locj(1):locj(2),loci(1):loci(2)))
  ALLOCATE(Q1(lock(1):lock(2),locj(1):locj(2),loci(1):loci(2)))
!
  ! Obtain velocity information
!=====
!
  allocate(VEL(1:3,0:nx3-1))
  ALLOCATE(x3(0:nx3-1))
!
  do k = 0,nx3-1
!
    read(15,*) x3(k),&
      &VEL(3,k),VEL(1,k),VEL(2,k)
!
!
  end do
  close(15)
!
! Assign value to Peclet Number
!=====
  Pe = VEL(3,0)*Pr
!
  End Subroutine allocate
!
!=====
!=====
!
Subroutine output(tt,step)
!
  USE vkvar
!
  IMPLICIT NONE
!
  INTEGER, target :: i,j,k
  INTEGER :: ind,proc,iout,tinteger
  INTEGER, pointer :: ii,jj,kk
  INTEGER, dimension(2) :: indi,indj,indk
  INTEGER, INTENT(IN) :: step
  REAL*8, INTENT(IN) :: tt

```

140

150

160

170

180

```

character*20 :: oname,iname
!
ind = 1
if (id == 0) then
  oname = 'vkout_cont'
  iout = 122
  write(iname,23)trim(oname),tt/100
  print *, iname
23  format(a,f6.4,'.dat')
!
  open(UNIT=100,file=trim(iname),status='replace')
!
  do i = 0,nx1-1
    do j = 0,nx2-1
      do k = 0,nx3-1
!
        if (sndim(1,2) == 1) ii => i
        if (sndim(2,2) == 1) jj => j
        if (sndim(3,2) == 1) kk => k
        if (sndim(1,2) == 2) ii => j
        if (sndim(2,2) == 2) jj => j
        if (sndim(3,2) == 2) kk => j
        if (sndim(1,2) == 3) ii => k
        if (sndim(2,2) == 3) jj => k
        if (sndim(3,2) == 3) kk => k
!
        write(100,200) out_f(nvar+1,kk,jj,ii) ,out_f(nvar+2,kk,jj,ii), out_f(nvar+3,kk,jj,ii) ,&
          & out_f(1,kk,jj,ii), out_f(2,kk,jj,ii), out_f(3,kk,jj,ii)
!
        ind = ind+1
!
      end do
    end do
  end do
!
  close(100)
end if
!
!
!
if (id==0) then
  if (mod(step,50000)==0.or.step==n_tstep) then
    oname = 'res'
    write(iname,24)trim(oname),tt/100
    print *, iname
24  format(a,f6.4,'.dmp')
    open(UNIT=101,file=trim(iname),status='replace')
    open(UNIT=102,file='res.dmp',status='replace')
!
    do k = 0,sndim(3,1)-1
      do j = 0,sndim(2,1)-1
        do i = 0,sndim(1,1)-1
!
          write(101,201) out_f(1,k,j,i), out_f(2,k,j,i), out_f(3,k,j,i)

```

```

                write(102,201) out_f(1,k,j,i), out_f(2,k,j,i), out_f(3,k,j,i)
!
                end do
                end do
                end do
                write(101,*) t
                write(102,*) t
                close(101)
                close(102)
            end if
        end if
        deallocate(out_f)
!
        call MPI_BARRIER(MPI_COMM_WORLD,ierr)
!
200 format(2x,3f10.6,3f12.8)
201 format(2x,3f22.18)
!
        End Subroutine output
!
!=====
!=====
!
        Subroutine track_error(curr_time)
!
        USE vkvar
!
        IMPLICIT NONE
!
        INTEGER :: i,j,k
        INTEGER,dimension(nvar) :: indz
        REAL*8, INTENT(IN) :: curr_time
        REAL*8,dimension(2) :: max_temp,max_temp_all,mtempavg,mtempavg_all
        REAL*8 :: err,err_all,qmax,qmaxall,fmax,fmaxall
        REAL*8,dimension(nprocs) :: maxtemp_zval, mtempvalall, mtempavg_zval, mtempavgvalall
        INTEGER :: mind,mind2
        REAL*8, dimension(:,,:), allocatable :: favg
!
        max_temp(1) = 0.0d0
        maxtemp_zval = 0.0d0
        mtempavg(1) = 0.0d0
        mtempavg_zval = 0.0d0
        qmax = 0.d0
        fmax = 0.d0
        err = 0.0d0
        do i = 1,nvar
            indz(i) = 0
            if (sndim(i,2)-3==0) indz(i) = 1
        end do
!
        allocate(favg(lock(1):lock(2),locj(1):locj(2),loci(1):loci(2)))
!
        DO k=lock(1)-dom_bound(3,1)+1,lock(2)-dom_bound(3,2)

```

240

250

260

270

280


```

DO j = locj(1)-dom_bound(2,1)+1,locj(2)-dom_bound(2,2)
  DO i = loci(1)-dom_bound(1,1)+1,loci(2)-dom_bound(1,2)
!
    favg(k,j,i) = (f(1,k,j,i)+f(1,k-1,j,i)+f(1,k,j-1,i)+f(1,k,j,i-1)&
      &+f(1,k-1,j-1,i)+f(1,k-1,j,i-1)+f(1,k,j-1,i-1)+f(1,k-1,j-1,i-1))/dfloat(8)
!
    end DO
  end DO
end DO
!
DO k=lock(1)-dom_bound(3,1),lock(2)-dom_bound(3,2)
  DO j = locj(1)-dom_bound(2,1),locj(2)-dom_bound(2,2)
    DO i = loci(1)-dom_bound(1,1),loci(2)-dom_bound(1,2)
!
      err = err+sqrt(((f(1,k,j,i) - ferr(1,k,j,i))**2))/TINF
      if (f(1,k,j,i).gt.max_temp(1)) then
        max_temp(1) = f(1,k,j,i)
        maxtemp_zval = f(nvar+3,k,j,i)
      end if
!
      if (favg(k,j,i).gt.mtempavg(1)) then
        mtempavg(1) = favg(k,j,i)
        mtempavg_zval = (f(nvar+3,k,j,i)+&
          &f(nvar+3,k-indz(3),j-indz(2),i-indz(1)))/dfloat(2)
      end if
!
      if (Q1(k,j,i).gt.qmax) qmax=Q1(k,j,i)
      if (f(2,k,j,i).gt.fmax) fmax=f(2,k,j,i)
      ferr(1,k,j,i) = f(1,k,j,i)
!
    END DO
  END DO
END DO
mtempavg(2) = id
max_temp(2) = id
!
CALL MPI_REDUCE(err,err_all,1,MPI_DOUBLE_PRECISION,&
  &MPI_SUM,0,MPI_COMM_WORLD,ierr)
CALL MPI_REDUCE(max_temp,max_temp_all,1,MPI_2DOUBLE_PRECISION,&
  &MPI_MAXLOC,0,MPI_COMM_WORLD,ierr)
CALL MPI_REDUCE(mtempavg,mtempavg_all,1,MPI_2DOUBLE_PRECISION,&
  &MPI_MAXLOC,0,MPI_COMM_WORLD,ierr)
CALL MPI_REDUCE(qmax,qmaxall,1,MPI_DOUBLE_PRECISION,&
  &MPI_MAX,0,MPI_COMM_WORLD,ierr)
CALL MPI_REDUCE(fmax,fmaxall,1,MPI_DOUBLE_PRECISION,&
  &MPI_MAX,0,MPI_COMM_WORLD,ierr)
!
CALL MPI_GATHER(maxtemp_zval,1,MPI_DOUBLE_PRECISION,&
  &mtempvalall,1,MPI_DOUBLE_PRECISION,0,MPI_COMM_WORLD,ierr)
!
CALL MPI_GATHER(mtempavg_zval,1,MPI_DOUBLE_PRECISION,&
  &mtempavgvalall,1,MPI_DOUBLE_PRECISION,0,MPI_COMM_WORLD,ierr)
!

```

```

err_all = err_all/(nx1*nx2*nx3*1.d0)
if (id==0) then
  mind = max_temp_all(2)+1
  mind2 = mtempavg_all(2)+1
  print 111, curr_time,err_all,max_temp_all(1),mtempvalall(mind),&
    &mtempavg_all(1),mtempavgvalall(mind2),qmaxall
  write(222,111) curr_time,err_all,max_temp_all(1),mtempvalall(mind)&
    &,mtempavg_all(1),mtempavgvalall(mind2)
end if
!
111  format(1x,1f10.5,2f10.6,1f6.3,1f10.6,1f6.3,2f10.6)
!
  End Subroutine track_error
!
!=====
!=====
!
!
! Subroutine ERROR
!
  USE vkvar
!
  IMPLICIT NONE
!
  INTEGER :: stat
!
  if (err_chk == 1) print *, 'Number of grid pts in all directions must be >= 5'
  if (err_chk == 2) print *, 'Number of time steps cannot be < 0'
  if (err_chk == 3) print *, 'ikutta is < 1'
  if (err_chk == 4) print *, 'All parameter values (Pr, Le... ) must be > 0'
  if (err_chk == 5) print *, 'Irestart must be 0 or 1'
  if (err_chk == 6) print *, 'Proc allocation error, pls check if nprocs > npts'
!
  if (err_chk > 0) CALL MPI_ABORT(MPI_COMM_WORLD,stat,ierr)
!
  End Subroutine ERROR
!=====
!=====
!
END MODULE vk_in

```

Grid Generation

```

MODULE gen_grid
contains
  SUBROUTINE grid
!
  USE vkvar
!
  IMPLICIT NONE
!
  INTEGER, target :: i,j,k
  INTEGER, pointer :: ii,jj,kk

```

```

INTEGER, dimension(2) :: indi,indj,indk
REAL*8 :: s1, s2, s3
REAL*8, dimension(3) :: dom,dx
REAL*8, pointer, dimension(:) :: v1,v2,v3
!
  ALLOCATE(x1(0:nx1-1),xx1(0:nx1-1))
  ALLOCATE(x2(0:nx2-1),xx2(0:nx2-1))
!
!   SUBROUTINE sets up the grid for the 3D problem
!===== 20
!
!   Caculate the min grid spacing for X1, X2 and X3
!=====
!
!   If dimension is periodic set value of boundary
!=====
!
!   if (x1max==0.)x1max = 2.*acos(-1.)
!   if (x2max==0.)x2max = 2.*acos(-1.)
!   if (x3max==0.)x3max = 2.*acos(-1.) 30
!
!
111 format(2x,3f6.3)
!
  dom(1) = (x1max-x1min)
  dom(2) = (x2max-x2min)
  dom(3) = (x3max-x3min)
!
  s1 = 1.
  s2 = 1. 40
!
  do j=1,nx1-2
    s1 = s1+STRETCH1**(j)
  end do
!
  do k=1,nx2-2
    s2 = s2+STRETCH2**(k)
  end do
!
  s1 = dom(1)/s1 50
  s2 = dom(2)/s2
!
  if (nx1.gt.0) then
    dx1 = dom(1)/((nx1-1.d0)*1.d0)
  else
    dx1 = 1.d0
  end if
!
  if (nx2.gt.0) then 60
    dx2 = dom(2)/((nx2-1.d0)*1.d0)
  else
    dx2 = 1.d0
  end if

```

```

!
  if (nx3.gt.0) then
    dx3 = dom(3)/((nx3-1.d0)*1.d0)
  else
    dx3 = 1.d0
  end if
!
! print *, 'dx', dx1,dx2,dx3
! print *, nx1,nx2,nx3
! if (id ==0) print *, 'dx3=', dx3
!
DO i=0,nx1-1
  x1(i) = i*dx1*1.d0
END DO
!
DO j=0,nx2-1
  x2(j) = j*dx2*1.d0
END DO
!
xx1(0) = x1min
do i = 1,nx1-1
  xx1(i) = xx1(i-1)+s1*STRETCH1**(i-1)
end do
!
xx2(0) = x2min
do i = 1,nx2-1
  xx2(i) = xx2(i-1)+s2*STRETCH2**(i-1)
end do
!
dx(1) = dx1
dx(2) = dx2
dx(3) = dx3
!
do i = 1,3
  sndx(i) = dx(sndim(i,2))
end do
!
DO k =0,nx3-1
  x3(k) = k*dx3
END DO
do i = 1,2
  indi(i) = loci(i)-dom_bound(1,i)
  indj(i) = locj(i)-dom_bound(2,i)
  indk(i) = lock(i)-dom_bound(3,i)
end do
!
!
do k = lock(1)-dom_bound(3,1),lock(2)-dom_bound(3,2)
  do j = locj(1)-dom_bound(2,1),locj(2)-dom_bound(2,2)
    do i = loci(1)-dom_bound(1,1),loci(2)-dom_bound(1,2)
!
      if (sndim(1,2) == 1) ii => i
      if (sndim(2,2) == 1) ii => j
!

```

```

        if (sndim(3,2) == 1) ii => k
        if (sndim(1,2) == 2) jj => i
        if (sndim(2,2) == 2) jj => j
        if (sndim(3,2) == 2) jj => k
        if (sndim(1,2) == 3) kk => i
        if (sndim(2,2) == 3) kk => j
        if (sndim(3,2) == 3) kk => k
!
        f(nvar+1,k,j,i) = xx1(ii)
        f(nvar+2,k,j,i) = xx2(jj)
        f(nvar+3,k,j,i) = x3(kk)
!
!           if (id==0) print 100, kk,jj,ii,f(nvar+1,k,j,i),f(nvar+2,k,j,i),f(nvar+3,k,j,i)
!           end do
        end do
    end do
!
    100 format(2x,3i5,6f10.5)
    DEALLOCATE(x1,x2,x3)
!
    CONTAINS
!
!     Functions
!=====
!
    FUNCTION BLOCK_LOW(proc_id,num_proc,num_elem)
        INTEGER :: BLOCK_LOW
        INTEGER, INTENT(IN) :: proc_id, num_proc
        REAL, INTENT(IN) :: num_elem
        BLOCK_LOW = proc_id*num_elem/num_proc
    END FUNCTION BLOCK_LOW
!
    FUNCTION BLOCK_HIGH(proc_id,num_proc,num_elem)
        INTEGER :: BLOCK_HIGH
        INTEGER, INTENT(IN) :: proc_id, num_proc, num_elem
        BLOCK_HIGH = (proc_id+1)*num_elem/num_proc-1
    END FUNCTION BLOCK_HIGH
!
    FUNCTION BLOCK_SIZE(proc_id,num_proc,num_elem)
        INTEGER :: BLOCK_SIZE
        INTEGER, INTENT(IN) :: proc_id, num_proc
        REAL, INTENT(IN) :: num_elem
        BLOCK_SIZE = (proc_id+1)*num_elem/num_proc &
            &-proc_id*num_elem/num_proc
    END FUNCTION BLOCK_SIZE
!
    END SUBROUTINE grid
!
!
!*****
!
!

```

120

130

140

150

160

```

END MODULE gen_grid 170

!
! NONUNIFORM GRID
! X1
!
!   xx1(0) = x1min
!   do i=1,nx1
!     xx1(i) = xx1(i-1)+s1*STRETCH1**(i-1)
!   end do
!
!
! X2 180
!
!   xx2(0) = x2min
!   do i=1,nx2
!     xx2(i) = xx2(i-1)+s2*STRETCH2**(i-1)
!   end do
!
!
! X3 190
!
!   xx3(0) = x3min
!   do i=1,nx3
!     xx3(i) = xx3(i-1)+s3*STRETCH3**(i-1)
!   end do
!
! end if
!
! 200

```

```

MODULE grid_map
!
! contains
!
! SUBROUTINE der_map
!
!   USE vkvar
!   USE der_ord_4
!
! IMPLICIT NONE 10
!
! INTEGER :: i, j, k, l, ind
! INTEGER, dimension(3) :: indi, indj, indk
! REAL*8 :: a1, a2
!
! do i = 1,2
!   indi(i) = loci(i) - dom_bound(1,i)
!   indj(i) = locj(i) - dom_bound(2,i)
!   indk(i) = lock(i) - dom_bound(3,i)
!

```

```

    end do
!
!   do l = 1,nvar
!
!       CALL prime(1,nvar+sndim(1,2))
!       CALL pprime(1,nvar+sndim(1,2))
!
!       do k = indk(1),indk(2)
!           do j = indj(1), indj(2)
!               do i = indi(1),indi(2)
!
!                   cc1(1,l,k,j,i) = 1.d0/(f_prime(1,nvar+sndim(1,2),k,j,i))
!                   cc1(2,l,k,j,i) = -f_pprime(1,nvar+sndim(1,2),k,j,i)/&
!                       &((f_prime(1,nvar+sndim(1,2),k,j,i))**3)
!
!                   a1 = abs(1.0d0 - cc1(1,l,k,j,i))
!                   a2 = abs(0.0d0 - cc1(2,l,k,j,i))
!
!                   if (a1.lt.1.0d-3) cc1(1,l,k,j,i) = 1.0d0
!                   if (a2.lt.1.0d-3) cc1(2,l,k,j,i) = 0.0d0
!
!                       end do
!                   end do
!               end do
!
!               deallocate(f_prime,f_pprime)
!
!           end do
!
!           CALL MPI_BARRIER(MPI_COMM_WORLD,ierr)
!
!           12 format(a10,4f12.8)
!
!       END SUBROUTINE der_map
!
!=====
!=====
!
!   END MODULE grid_map

```

MPI Assignments and Domain Decomposition

```

MODULE vkpar
!
! CONTAINS
!
! SUBROUTINE grid_assign
!
! This subroutine initiates and completes all necessary allocations and
! functions needed for the parallel routine
!=====
!
! USE vkvar

```

```

USE vk_in
!
IMPLICIT NONE
!
INTEGER :: i,end_index,plc_hld,mid
INTEGER, dimension(3) :: max_pts,min_pts
INTEGER, dimension(3,3) :: ndim
INTEGER, dimension(6) :: nrange
!
! In this subroutine, the procs are allocated such that the direction with the
! highest number of grid points is always assigned to the index i and the direction
! with the lowest number of grid points is assigned to the index k
! This was done to make the code perform faster, especially in terms of do loops
!
! The array sndim is crucial in identifying the direction each index corresponds to
! The sndim(*,1) correspond the indices: 1=i, 2=j, 3=k
! The sndim(*,2) elements store the value of the directions: 1=r, 2=theta, 3=z
!=====
!
! ndim(1,1) = nx1          ! ndim stores the no. of grid pts and the periodicity info
! ndim(2,1) = nx2
! ndim(3,1) = nx3
!
! ndim(1,3) = grd1
! ndim(2,3) = grd2
! ndim(3,3) = grd3
! do i=1,3
!   ndim(i,2) = 0
! end do
!
! if (x1max==0.) ndim(1,2) = 1
! if (x2max==0.) ndim(2,2) = 1
! if (x3max==0.) ndim(3,2) = 1
!
! if (nx1.ne.nx2.or.nx1.ne.nx3.or.nx2.ne.nx3) then
!   max_pts = maxloc(ndim,1) ! identify the directions which have max and min grid pts
!   min_pts = minloc(ndim,1)
! else
!   max_pts(1) = 3
!   min_pts(1) = 1
! end if
!
! mid = 0
!
! do i = 1,3
!   if (i.ne.min_pts(1).and.i.ne.max_pts(1)) mid = i
!   periodic(i) = 0
! end do
!
! sndim(1,1) = ndim(max_pts(1),1) ! sndim(1) = i, sndim(2) = j, sndim(3) = k
! sndim(1,2) = max_pts(1)          ! sndim(2) stores the corresponding directions
! periodic(1) = ndim(max_pts(1),2) ! (r,theta,z) that above indices point to

```



```

sndim(2,1) = ndim(mid,1)
sndim(2,2) = mid
periodic(2) = ndim(mid,2)
sndim(3,1) = ndim(min_pts(1),1)
sndim(3,2) = min_pts(1)
periodic(3) = ndim(min_pts(1),2)
!
if (grd1.eq.0.and.grd2.eq.0.and.grd3.eq.0) then
  if (mod(nprocs,8).eq.0) then
    dims(1) = 0
    dims(2) = 0
    dims(3) = 0
  else
    if (mod(nprocs,4).eq.0) then
      dims(2) = 0
      dims(3) = 1
    else
      dims(2) = 1
      dims(3) = 1
    end if
  end if
!
else
  dims(1) = ndim(max_pts(1),3)
  dims(2) = ndim(mid,3)
  dims(3) = ndim(min_pts(1),3)
end if
!
ghostlayer = 2
mpilayer = 1
!
call MPI_DIMS_CREATE(nprocs,3,dims,ierr)
call MPI_CART_CREATE(MPI_COMM_WORLD,3,dims,periodic,1,cart_comm,ierr)
call MPI_COMM_RANK(cart_comm,id,ierr)
call MPI_CART_SHIFT(cart_comm,0,1,idnbr(1),idnbr(2),ierr)
call MPI_CART_SHIFT(cart_comm,1,1,idnbr(3),idnbr(4),ierr)
call MPI_CART_SHIFT(cart_comm,2,1,idnbr(5),idnbr(6),ierr)
call MPL_CART_COORDS(cart_comm,id,3,coords,ierr)
!
do i = 1,3
  if (sndim(i,1).le.dims(i)) then
    err_chk = 6
    CALL ERROR
  end if
end do
!
! Assign vectors for identifying boundary processors
!=====
!
do i = 1,3
  dom_bound(i,1) = -ghostlayer
  dom_bound(i,2) = ghostlayer
end do

```

70

80

90

100

110

```

!
  if (coords(1) == 0 .and. periodic(1) == 0) dom_bound(1,1) = 0
  if (coords(1) == dims(1)-1 .and. periodic(1) == 0) dom_bound(1,2) = 0
  if (coords(2) == 0 .and. periodic(2) == 0) dom_bound(2,1) = 0
  if (coords(2) == dims(2)-1 .and. periodic(2) == 0) dom_bound(2,2) = 0
  if (coords(3) == 0 .and. periodic(3) == 0 ) dom_bound(3,1) = 0
  if (coords(3) == dims(3)-1 .and. periodic(3) == 0) dom_bound(3,2) = 0
!
! Set up sub communicators for each dimension
!=====
!
  free(1) = 1
  free(2) = 0
  free(3) = 0
!
  call MPI_CART_SUB(cart_comm,free,comm(1),ierr)
  call MPI_COMM_RANK(comm(1),rid(1),ierr)
  call MPI_COMM_SIZE(comm(1),rsize(1),ierr)
!
  free(1) = 0
  free(2) = 1
  free(3) = 0
!
  call MPI_CART_SUB(cart_comm,free,comm(2),ierr)
  call MPI_COMM_RANK(comm(2),rid(2),ierr)
  call MPI_COMM_SIZE(comm(2),rsize(2),ierr)
!
  free(1) = 0
  free(2) = 0
  free(3) = 1
!
  call MPI_CART_SUB(cart_comm,free,comm(3),ierr)
  call MPI_COMM_RANK(comm(3),rid(3),ierr)
  call MPI_COMM_SIZE(comm(3),rsize(3),ierr)
!
! Determine the start and end index for each processor in each dim
!=====
!
  loci(1) = BLOCK_LOW(rid(1),rsize(1),sndim(1,1))
  loci(2) = BLOCK_HIGH(rid(1),rsize(1),sndim(1,1))
  locj(1) = BLOCK_LOW(rid(2),rsize(2),sndim(2,1))
  locj(2) = BLOCK_HIGH(rid(2),rsize(2),sndim(2,1))
  lock(1) = BLOCK_LOW(rid(3),rsize(3),sndim(3,1))
  lock(2) = BLOCK_HIGH(rid(3),rsize(3),sndim(3,1))
!
!
  x1size = BLOCK_SIZE(rid(1),rsize(1),sndim(1,1))
  x2size = BLOCK_SIZE(rid(2),rsize(2),sndim(2,1))
  x3size = BLOCK_SIZE(rid(3),rsize(3),sndim(3,1))
!
!
  totsize = x1size*x2size*x3size
!

```

```

! Buffers for Gathering
!=====
!
  allocate(allsize(nprocs))
  allocate(dispatch(nprocs))
  allocate(allrange(6*nprocs))
!
  nrange(1) = lock(1)
  nrange(2) = lock(2)
  nrange(3) = locj(1)
  nrange(4) = locj(2)
  nrange(5) = loci(1)
  nrange(6) = loci(2)
!
  CALL MPI_ALLGATHER(totsize,1,MPI_INTEGER,allsize,1,&
    &MPI_INTEGER,cart_comm,ierr)
  CALL MPI_ALLGATHER(nrange,6,MPI_INTEGER,allrange,6,&
    &MPI_INTEGER,cart_comm,ierr)
!
  disp(1) = 0
  do i = 2,nprocs
    disp(i) = allsize(i-1) + disp(i-1)
  end do
!
! Account for the ghost layers in the Boundary Processors
!=====
!
  if (dom_bound(1,1).ne.0) then
    loci(1) = loci(1) - ghostlayer
  end if
!
  if (dom_bound(1,2).ne.0) then
    loci(2) = loci(2) + ghostlayer
  end if
!
  if (dom_bound(2,1).ne.0) then
    locj(1) = locj(1) - ghostlayer
  end if
!
  if (dom_bound(2,2).ne.0) then
    locj(2) = locj(2) + ghostlayer
  end if
!
  if (dom_bound(3,1).ne.0) then
    lock(1) = lock(1) - ghostlayer
  end if
!
  if (dom_bound(3,2).ne.0) then
    lock(2) = lock(2) + ghostlayer
  end if
!
! Allocate buffers for final communications
!=====

```

180

190

200

210

220

```

!
end_index = allsize(nprocs) + disp(nprocs)
ALLOCATE(myres(totsize))
ALLOCATE(allres(end_index))
! ALLOCATE(out_f(1:fsize,0:x3size*rsz(3)-1,0:x2size*rsz(2)-1,0:x1size*rsz(1)-1))
!
! Print Decomposition information:
!=====
!
! if (id == 0) then
!   print *, 'dim',sdim(1,2),':',dims(1),' dim',sdim(2,2),':', dims(2),&
!     &' dim',sdim(3,2),':',dims(3)
!   print *, 'Grid points / proc- nx1:', x1size,' nx2:',x2size,' nx3:',x3size
!   print *, 'Total no of grid points :', nx1,'X',nx2,'X',nx3
! end if
!
CONTAINS
!
! FUNCTION BLOCK_LOW(proc_id,num_proc,num_elem)
!   INTEGER :: BLOCK_LOW
!   INTEGER, INTENT(IN) :: proc_id, num_proc, num_elem
!   BLOCK_LOW = proc_id*num_elem/num_proc
! END FUNCTION BLOCK_LOW
!
! FUNCTION BLOCK_HIGH(proc_id,num_proc,num_elem)
!   INTEGER :: BLOCK_HIGH
!   INTEGER, INTENT(IN) :: proc_id, num_proc, num_elem
!   BLOCK_HIGH = (proc_id+1)*num_elem/num_proc-1
! END FUNCTION BLOCK_HIGH
!
! FUNCTION BLOCK_SIZE(proc_id,num_proc,num_elem)
!   INTEGER :: BLOCK_SIZE
!   INTEGER, INTENT(IN) :: proc_id, num_proc, num_elem
!   BLOCK_SIZE = (proc_id+1)*num_elem/num_proc &
!     &-proc_id*num_elem/num_proc
! END FUNCTION BLOCK_SIZE
!
!
!
!
!
!=====
!=====
!
!
! SUBROUTINE vk_communication(ind1,ind2)
!
!   USE vkvar
!
!   IMPLICIT NONE
!
!   INTEGER :: i,j,k,index,procs,el,n
!   INTEGER, INTENT(IN) :: ind1,ind2
!
!   ALLOCATE(out_f(ind1:ind2,0:sdim(3,1)-1,0:sdim(2,1)-1,0:sdim(1,1)-1))
!   do n = ind1,ind2

```

230

240

250

260

270

```

!
!   index = 1
!
!   do k = lock(1)-dom_bound(3,1),lock(2)-dom_bound(3,2)
!       do j = locj(1)-dom_bound(2,1),locj(2)-dom_bound(2,2)
!           do i = loci(1)-dom_bound(1,1),loci(2)-dom_bound(1,2)
!
!               myres(index) = f(n,k,j,i)
!               index = index+1
!
!           end do
!       end do
!   end do
!
!   CALL MPI_ALLGATHERV(myres,totsize,MPI_REAL8,&
!       &allres,allsize,disp,MPI_REAL8,&
!       &MPI_COMM_WORLD,ierr)
!
!   index = 1
!
!   do procs = 0,nprocs-1
!       el = 1 + procs*6
!       do k = allrange(el),allrange(el+1)
!           do j = allrange(el+2),allrange(el+3)
!               do i = allrange(el+4),allrange(el+5)
!                   out_f(n,k,j,i) = allres(index)
!                   index = index+1
!               end do
!           end do
!       end do
!   end do
!
!   end do
!
!   END SUBROUTINE vk_communication
!
!   =====
!   =====
!
!   SUBROUTINE vk_buffer_comm(ind1,ind2)
!
!       This subroutine facilitates the communication
!       between adjacent processors
!
!   =====
!
!   USE vkvar
!
!   IMPLICIT NONE
!
!   INTEGER :: ind,n,k,j,i,ii,jj,kk,arg1,arg2,p,tag1,tag2,dummy1, dummy2,stat
!   real*8 :: test1, test2

```

```

INTEGER, INTENT(IN) :: ind1,ind2
!
! Allocate the send and receive buffers
!=====
!
sbx1_size = (ind2-ind1+1)*(lock(2)-lock(1)+1+dom_bound(3,1)-dom_bound(3,2))&
&*(locj(2)-locj(1)+1+dom_bound(2,1)-dom_bound(2,2))*ghostlayer
sbx2_size = (ind2-ind1+1)*(lock(2)-lock(1)+1+dom_bound(3,1)-dom_bound(3,2))&
&*(loci(2)-loci(1)+1+dom_bound(1,1)-dom_bound(1,2))*ghostlayer
sbx3_size = (ind2-ind1+1)*(locj(2)-locj(1)+1+dom_bound(2,1)-dom_bound(2,2))&
&*(loci(2)-loci(1)+1+dom_bound(1,1)-dom_bound(1,2))*ghostlayer
!
!
ALLOCATE(send_buffx1_l(sbx1_size),recv_buffx1_r(sbx1_size))
ALLOCATE(send_buffx1_r(sbx1_size),recv_buffx1_l(sbx1_size))
ALLOCATE(send_buffx2_l(sbx2_size),recv_buffx2_r(sbx2_size))
ALLOCATE(send_buffx2_r(sbx2_size),recv_buffx2_l(sbx2_size))
ALLOCATE(send_buffx3_l(sbx3_size),recv_buffx3_r(sbx3_size))
ALLOCATE(send_buffx3_r(sbx3_size),recv_buffx3_l(sbx3_size))
!
!
! Communication in the i direction
!=====
!
!
if (dims(1).gt.1.and.idnbr(2).gt.id.and.idnbr(2).gt.-1) then
  i = 1
!
  do ii = 2*ghostlayer-1,ghostlayer,-1
    do n = ind1,ind2
      do k = lock(1)-dom_bound(3,1),lock(2)-dom_bound(3,2)
        do j = locj(1)-dom_bound(2,1),locj(2)-dom_bound(2,2)
!
          send_buffx1_r(i) = f(n,k,j,loci(2)-ii)
          i = i+1
!
        end do
      end do
    end do
  end do
!
CALL MPI_SENDRECV(send_buffx1_r,sbx1_size,&
&MPI_REAL8,idnbr(2),0,recv_buffx1_r,sbx1_size,&
&MPI_REAL8,idnbr(2),1,MPI_COMM_WORLD,stat,ierr)
!
i = 1
!
do ii = ghostlayer-1,0,-1
  do n = ind1,ind2
    do k = lock(1)-dom_bound(3,1),lock(2)-dom_bound(3,2)
      do j = locj(1)-dom_bound(2,1),locj(2)-dom_bound(2,2)
!
        f(n,k,j,loci(2)-ii) = recv_buffx1_r(i)
!

```

```

                i = i+1
!
                end do
            end do
        end do
    end do
!
end if
!
!
if (dims(1).gt.1.and.idnbr(1).lt.id.and.idnbr(1).gt.-1) then
!
    i = 1
!
    do ii = loci(1)+ghostlayer,loci(1)+2*ghostlayer-1
        do n = ind1,ind2
            do k = lock(1)-dom_bound(3,1),lock(2)-dom_bound(3,2)
                do j = locj(1)-dom_bound(2,1),locj(2)-dom_bound(2,2)
!
                    send_buffx1_l(i) = f(n,k,j,ii)
                    i = i+1
!
                end do
            end do
        end do
    end do
!
    CALL MPI_SENDRECV(send_buffx1_l,sbx1_size,&
        &MPI_REAL8,idnbr(1),1,recv_buffx1_l,sbx1_size,&
        &MPI_REAL8,idnbr(1),0,MPI_COMM_WORLD,stat,ierr)
!
    i = 1
!
    do ii = loci(1),loci(1)+1
        do n = ind1,ind2
            do k = lock(1)-dom_bound(3,1),lock(2)-dom_bound(3,2)
                do j = locj(1)-dom_bound(2,1),locj(2)-dom_bound(2,2)
!
                    f(n,k,j,ii) = recv_buffx1_l(i)
                    i = i+1
!
                end do
            end do
        end do
    end do
!
end if
!
!
call MPI_BARRIER(MPI_COMM_WORLD,ierr)
!
if (dims(1).gt.1.and.periodic(1)==1.and.idnbr(2).lt.id) then
    i = 1

```

390

400

410

420

430

```

!
  do ii = 2*ghostlayer,ghostlayer+1,-1
    do n = ind1,ind2
      do k = lock(1)-dom_bound(3,1),lock(2)-dom_bound(3,2)
        do j = locj(1)-dom_bound(2,1),locj(2)-dom_bound(2,2)
!
          send_buffx1_r(i) = f(n,k,j,loci(2)-ii)
          i = i+1
!
        end do
      end do
    end do
  end do
!
CALL MPI_SENDRECV(send_buffx1_r,sbx1_size,&
                  &MPI_REAL8,idnbr(2),4,recv_buffx1_r,sbx1_size,&
                  &MPI_REAL8,idnbr(2),5,MPL_COMM_WORLD,stat,ierr)
!
i = 1
!
do ii = ghostlayer-1,0,-1
  do n = ind1,ind2
    do k = lock(1)-dom_bound(3,1),lock(2)-dom_bound(3,2)
      do j = locj(1)-dom_bound(2,1),locj(2)-dom_bound(2,2)
!
        f(n,k,j,loci(2)-ii) = recv_buffx1_r(i)
        i = i+1
!
      end do
    end do
  end do
end do
!
end if
!
if (dims(1).gt.1.and.periodic(1)==1.and.idnbr(1).gt.id) then
  i = 1
!
  do ii = loci(1)+ghostlayer+1,loci(1)+2*ghostlayer
    do n = ind1,ind2
      do k = lock(1)-dom_bound(3,1),lock(2)-dom_bound(3,2)
        do j = locj(1)-dom_bound(2,1),locj(2)-dom_bound(2,2)
!
          send_buffx1_l(i) = f(n,k,j,ii)
          i = i+1
!
        end do
      end do
    end do
  end do
!
CALL MPI_SENDRECV(send_buffx1_l,sbx1_size,&
                  &MPI_REAL8,idnbr(1),5,recv_buffx1_l,sbx1_size,&

```



```

        &MPI_REAL8,idnbr(1),4,MPI_COMM_WORLD,stat,ierr)
!
i = 1
!
do ii = loci(1),loci(1)+1
  do n = ind1,ind2
    do k = lock(1)-dom_bound(3,1),lock(2)-dom_bound(3,2)
      do j = locj(1)-dom_bound(2,1),locj(2)-dom_bound(2,2)
!
          f(n,k,j,ii) = recv_buffx1_l(i)
          i = i+1
!
!
          end do
        end do
      end do
    end do
  end if
!
  call MPI_BARRIER(MPI_COMM_WORLD,ierr)
!
! Communication in the j direction
!=====
!
!
  if (dims(2).gt.1.and.idnbr(4).gt.id.and.idnbr(4).gt.-1) then
!
  j = 1
!
  do ii = 2*ghostlayer-1,ghostlayer,-1
!
    do n = ind1,ind2
      do k = lock(1)-dom_bound(3,1),lock(2)-dom_bound(3,2)
        do i = loci(1)-dom_bound(1,1),loci(2)-dom_bound(1,2)
!
          send_buffx2_r(j) = f(n,k,locj(2)-ii,i)
          j = j+1
!
          end do
        end do
      end do
    end do
!
    CALL MPI_SENDRECV(send_buffx2_r,sbx2_size,&
      &MPI_REAL8,idnbr(4),id,recv_buffx2_r,sbx2_size,&
      &MPI_REAL8,idnbr(4),idnbr(4),MPI_COMM_WORLD,stat,ierr)
!
  j = 1
!
  do ii = ghostlayer-1,0,-1
    do n = ind1,ind2
      do k = lock(1)-dom_bound(3,1),lock(2)-dom_bound(3,2)
        do i = loci(1)-dom_bound(1,1),loci(2)-dom_bound(1,2)
!

```

```

                f(n,k,locj(2)-ii,i) = recv_buffx2_r(j)
                j = j+1
!
                end do
            end do
        end do
    end do
end if
!
if (dims(2).gt.1.and.idnbr(3).lt.id.and.idnbr(3).gt.-1) then
!
    j = 1
!
    do ii = locj(1)+ghostlayer,locj(1)+2*ghostlayer-1
        do n = ind1,ind2
            do k = lock(1)-dom_bound(3,1),lock(2)-dom_bound(3,2)
                do i = loci(1)-dom_bound(1,1),loci(2)-dom_bound(1,2)
!
                    send_buffx2_l(j) = f(n,k,ii,i)
                    j = j+1
!
                end do
            end do
        end do
    end do
!
    CALL MPI_SENDRECV(send_buffx2_l,sbx2_size,&
        &MPI_REAL8,idnbr(3),id,recv_buffx2_l,sbx2_size,&
        &MPI_REAL8,idnbr(3),idnbr(3),MPI_COMM_WORLD,stat,ierr)
!
    j = 1
!
    do ii = locj(1),locj(1)+1
        do n = ind1,ind2
            do k = lock(1)-dom_bound(3,1),lock(2)-dom_bound(3,2)
                do i = loci(1)-dom_bound(1,1),loci(2)-dom_bound(1,2)
!
                    f(n,k,ii,i) = recv_buffx2_l(j)
                    j = j+1
!
                end do
            end do
        end do
!
    end do
!
end if
!
CALL MPI_BARRIER(MPI_COMM_WORLD,ierr)
!
if (dims(2).gt.1.and.periodic(2)==1.and.idnbr(4).lt.id) then
    j = 1
!

```

```

do ii = 2*ghostlayer,ghostlayer+1,-1
  do n = ind1,ind2
    do k = lock(1)-dom_bound(3,1),lock(2)-dom_bound(3,2)
      do i = loci(1)-dom_bound(1,1),loci(2)-dom_bound(1,2)
!
          send_buffx2_r(j) = f(n,k,locj(2)-ii,i)
          j = j+1
!
          end do
        end do
      end do
    end do
!
CALL MPLSENDRECV(send_buffx2_r,sbx2_size,&
  &MPI_REAL8,idnbr(4),4,recv_buffx2_r,sbx2_size,&
  &MPI_REAL8,idnbr(4),5,MPL_COMM_WORLD,stat,ierr)
!
j = 1
!
do ii = ghostlayer-1,0,-1
  do n = ind1,ind2
    do k = lock(1)-dom_bound(3,1),lock(2)-dom_bound(3,2)
      do i = loci(1)-dom_bound(1,1),loci(2)-dom_bound(1,2)
!
          f(n,k,locj(2)-ii,i) = recv_buffx2_r(j)
          j = j+1
!
          end do
        end do
      end do
    end do
!
end if
!
if (dims(2).gt.1.and.periodic(2)==1.and.idnbr(3).gt.id) then
!
j = 1
!
do ii = locj(1)+ghostlayer+1,locj(1)+2*ghostlayer
  do n = ind1,ind2
    do k = lock(1)-dom_bound(3,1),lock(2)-dom_bound(3,2)
      do i = loci(1)-dom_bound(1,1),loci(2)-dom_bound(1,2)
!
          send_buffx2_l(j) = f(n,k,ii,i)
          j = j+1
!
          end do
        end do
      end do
    end do
!
CALL MPLSENDRECV(send_buffx2_l,sbx2_size,&
  &MPI_REAL8,idnbr(3),5,recv_buffx2_l,sbx2_size,&

```

```

        &MPI_REAL8,idnbr(3),4,MPI_COMM_WORLD,stat,ierr)
!
j = 1
!
do ii = locj(1),locj(1)+1
  do n = ind1,ind2
    do k = lock(1)-dom_bound(3,1),lock(2)-dom_bound(3,2)
      do i = loci(1)-dom_bound(1,1),loci(2)-dom_bound(1,2)
!
          f(n,k,ii,i) = recv_buffx2_l(j)
          j = j+1
!
      end do
    end do
  end do
end do
end if
!
call MPI_BARRIER(MPI_COMM_WORLD,ierr)
!
!
!   Communication in the k direction
!===== 670
!
if (dims(3).gt.1.and.idnbr(6).gt.id.and.idnbr(6).gt.-1) then
  k = 1
!
  do ii = 2*ghostlayer-1,ghostlayer,-1
    do n = ind1,ind2
      do j = locj(1)-dom_bound(2,1),locj(2)-dom_bound(2,2)
        do i = loci(1)-dom_bound(1,1),loci(2)-dom_bound(1,2)
!
            send_buffx3_r(k) = f(n,lock(2)-ii,j,i)
            k = k+1
!
        end do
      end do
    end do
  end do
!
CALL MPI_SENDRECV(send_buffx3_r,sbx3_size,&
  &MPI_REAL8,idnbr(6),4,recv_buffx3_r,sbx3_size,&
  &MPI_REAL8,idnbr(6),5,MPI_COMM_WORLD,stat,ierr)
!
k = 1
!
do ii = ghostlayer-1,0,-1
  do n = ind1,ind2
    do j = locj(1)-dom_bound(2,1),locj(2)-dom_bound(2,2)
      do i = loci(1)-dom_bound(1,1),loci(2)-dom_bound(1,2)
!
          f(n,lock(2)-ii,j,i) = recv_buffx3_r(k)
          k = k+1
!

```

```

!
!           end do
!           end do
!           end do
!           end do
!
! end if
!
! if (dims(3).gt.1.and.idnbr(5).lt.id.and.idnbr(5).gt.-1) then
!           k = 1
!
!           do ii = lock(1)+ghostlayer,lock(1)+2*ghostlayer-1
!             do n = ind1,ind2
!               do j = locj(1)-dom_bound(2,1),locj(2)-dom_bound(2,2)
!                 do i = loci(1)-dom_bound(1,1),loci(2)-dom_bound(1,2)
!
!                   send_buffx3_l(k) = f(n,ii,j,i)
!                   k = k+1
!
!                 end do
!               end do
!             end do
!           end do
!
!           CALL MPI_SENDRECV(send_buffx3_l,sbx3_size,&
!             &MPI_REAL8,idnbr(5),5,recv_buffx3_l,sbx3_size,&
!             &MPI_REAL8,idnbr(5),4,MPI_COMM_WORLD,stat,ierr)
!
!           k = 1
!
!           do ii = lock(1),lock(1)+1
!             do n = ind1,ind2
!               do j = locj(1)-dom_bound(2,1),locj(2)-dom_bound(2,2)
!                 do i = loci(1)-dom_bound(1,1),loci(2)-dom_bound(1,2)
!
!                   f(n,ii,j,i) = recv_buffx3_l(k)
!                   k = k+1
!
!                 end do
!               end do
!             end do
!           end do
!
! end if
!
! call MPI_BARRIER(MPI_COMM_WORLD,ierr)
!
! if (dims(3).gt.1.and.periodic(3)==1.and.idnbr(6).lt.id) then
!           k = 1
!
!           do ii = 2*ghostlayer,ghostlayer+1,-1
!             do n = ind1,ind2
!               do j = locj(1)-dom_bound(2,1),locj(2)-dom_bound(2,2)

```

710

720

730

740

750

```

        do i = loci(1)-dom_bound(1,1),loci(2)-dom_bound(1,2)
!
            send_buffx3_r(k) = f(n,lock(2)-ii,j,i)
            k = k+1
!
        end do
    end do
end do
!
CALL MPL_SENDRECV(send_buffx3_r,sbx3_size,&
    &MPI_REAL8,idnbr(6),4,recv_buffx3_r,sbx3_size,&
    &MPI_REAL8,idnbr(6),5,MPL_COMM_WORLD,stat,ierr)
!
k = 1
!
do ii = ghostlayer-1,0,-1
!
    do n = ind1,ind2
!
        do j = locj(1)-dom_bound(2,1),locj(2)-dom_bound(2,2)
!
            do i = loci(1)-dom_bound(1,1),loci(2)-dom_bound(1,2)
!
                f(n,lock(2)-ii,j,i) = recv_buffx3_r(k)
                k = k+1
!
            end do
        end do
    end do
end do
!
end if
!
if (dims(3).gt.1.and.periodic(3)==1.and.idnbr(5).gt.id) then
!
    k = 1
!
    do ii = lock(1)+ghostlayer+1,lock(1)+2*ghostlayer
!
        do n = ind1,ind2
!
            do j = locj(1)-dom_bound(2,1),locj(2)-dom_bound(2,2)
!
                do i = loci(1)-dom_bound(1,1),loci(2)-dom_bound(1,2)
!
                    send_buffx3_l(k) = f(n,ii,j,i)
                    k = k+1
!
                end do
            end do
        end do
    end do
!
CALL MPL_SENDRECV(send_buffx3_l,sbx3_size,&
    &MPI_REAL8,idnbr(5),5,recv_buffx3_l,sbx3_size,&
    &MPI_REAL8,idnbr(5),4,MPL_COMM_WORLD,stat,ierr)
!
k = 1
!

```

760

770

780

790

800

```

do ii = lock(1),lock(1)+1
  do n = ind1,ind2
    do j = locj(1)-dom_bound(2,1),locj(2)-dom_bound(2,2)
      do i = loci(1)-dom_bound(1,1),loci(2)-dom_bound(1,2)
!
!         f(n,ii,j,i) = recv_buffx3_l(k)
!         k = k+1
!
!       end do
!     end do
!   end do
! end do
! end if
!
! call MPI_BARRIER(MPI_COMM_WORLD,ierr)
!
! Deallocate all send and recv buffers
!=====
!
! DEALLOCATE(send_buffx1_l,recv_buffx1_r)
! DEALLOCATE(send_buffx1_r,recv_buffx1_l)
! DEALLOCATE(send_buffx2_l,recv_buffx2_r)
! DEALLOCATE(send_buffx2_r,recv_buffx2_l)
! DEALLOCATE(send_buffx3_l,recv_buffx3_r)
! DEALLOCATE(send_buffx3_r,recv_buffx3_l)
!
! END SUBROUTINE vk_buffer_comm
!
!=====
!=====
!
END MODULE vkpar

```

Derivative Routines

```

!
!   This package has the derivative routines and the
!   Runge-Kutta routines for parallel implementation
!
!
!=====
!=====
!
MODULE der_ord_4
  contains
!
!   SUBROUTINE prime(ivar,nvec)
!   This subroutine calculates first derivatives
!   The following format should be used when calling this subroutine
!   f_prime(Independent variable,Dependent variable,x3loc,x2loc,x1loc)
!   Independent variable: x1=1
!                       x2=2
!

```

```

!                               x3=3
!   Dependent variable: The variable for which the derivative is being calculated (T,Yi,u,v,w....)
!   x3loc:                   The x3 location
!   x2loc:                   The x2 location
!   x1loc:                   The x1 location
!
!   USE vkvar
!
!   IMPLICIT NONE
!
!   INTEGER :: a1,b1,c1, i, j, k,ii,jj,kk
!   INTEGER, DIMENSION(:) :: indi(2),indj(2),indk(2)
!   INTEGER, INTENT(IN) :: ivar, nvec
!   REAL*8 :: h, h1, gl
!
!   ALLOCATE(f_prime(ivar:ivar,nvec:nvec,lock(1):lock(2),locj(1):locj(2),loci(1):loci(2)))
!
! Calculate dfdx1
!=====
!
!   if (ivar == 1) then
!       h = sndx(ivar)
!       ! print *, 'h', h,ivar,sndim(3,2),sndx(3)
!       h1 = 1.0/(12.0*h)
!       a1 = 1
!       b1 = 0
!       c1 = 0
!
!       do k = lock(1)-dom_bound(3,1),lock(2)-dom_bound(3,2)
!           do j = locj(1)-dom_bound(2,1),locj(2)-dom_bound(2,2)
!
!               kk = k - lock(1)
!               jj = j - locj(1)
!               indi(1) = loci(1)-dom_bound(1,1) - loci(1)
!               indi(2) = loci(2)-dom_bound(1,2) - loci(1)
!
!               if (dom_bound(1,1) == 0) then
!                   ii = 0;i = 0;
!                   f_prime(ivar,nvec,k,j,i) = bnd_0(f,nvec,ii,jj,kk,a1,b1,c1,h1)
!                   ii = 1;i = 1;
!                   f_prime(ivar,nvec,k,j,i) = bnd_1(f,nvec,ii,jj,kk,a1,b1,c1,h1)
!                   indi(1) = indi(1)+ghostlayer;
!               end if
!
!               if (dom_bound(1,2) == 0) then
!                   ii = loci(2)-loci(1)-1;i = loci(2)-1
!                   f_prime(ivar,nvec,k,j,i) = bnd_n1(f,nvec,ii,jj,kk,a1,b1,c1,h1)
!                   ii = loci(2)-loci(1);i = loci(2)
!                   f_prime(ivar,nvec,k,j,i) = bnd_n(f,nvec,ii,jj,kk,a1,b1,c1,h1)
!                   indi(2) = indi(2)-ghostlayer;
!               end if
!
!               do ii = indi(1),indi(2)

```



```

        i = ii+loci(1)
        f_prime(ivar,nvec,k,j,i) = mid(f,nvec,ii,jj,kk,a1,b1,c1,h1)
    end do
!
        end do
    end do
!
    else
!
! Calculate dfdx2
!=====*
        if (ivar==2) then
            h = sndx(ivar)
            h1 = 1.0/(12.0*h)
            a1 = 0
            b1 = 1
            c1 = 0
!
            do k = lock(1) - dom_bound(3,1), lock(2) - dom_bound(3,2)
                do i = loci(1) - dom_bound(1,1), loci(2) - dom_bound(1,2)
!
                    kk = k - lock(1)
                    ii = i - loci(1)
                    indj(1) = locj(1)-dom_bound(2,1) - locj(1)
                    indj(2) = locj(2)-dom_bound(2,2) - locj(1)
!
                    if (dom_bound(2,1) == 0) then
                        jj = 0;j = 0;
                        f_prime(ivar,nvec,k,j,i) = bnd_0(f,nvec,ii,jj,kk,a1,b1,c1,h1)
                        jj = 1;j = 1;
                        f_prime(ivar,nvec,k,j,i) = bnd_1(f,nvec,ii,jj,kk,a1,b1,c1,h1)
                        indj(1) = indj(1) + ghostlayer
                    end if
!
                    if (dom_bound(2,2) == 0) then
                        jj = locj(2)-locj(1)-1;j = locj(2)-1;
                        f_prime(ivar,nvec,k,j,i) = bnd_n1(f,nvec,ii,jj,kk,a1,b1,c1,h1)
                        jj = locj(2)-locj(1);j = locj(2)
                        f_prime(ivar,nvec,k,j,i) = bnd_n(f,nvec,ii,jj,kk,a1,b1,c1,h1)
                        indj(2) = indj(2) - ghostlayer
                    end if
!
                    do jj = indj(1),indj(2)
                        j = jj+locj(1)
                        f_prime(ivar,nvec,k,j,i) = mid(f,nvec,ii,jj,kk,a1,b1,c1,h1)
                    end do
!
                end do
            end do
        else
!
! Calculate dfdx3
!=====*

```

```

    if (ivar==3) then
      h = sndx(ivar)
      h1 = 1.0/(12.0*h)
      a1 = 0
      b1 = 0
      c1 = 1
      do j = locj(1) - dom_bound(2,1), locj(2) - dom_bound(2,2)
        do i = loci(1) - dom_bound(1,1), loci(2) - dom_bound(1,2)
!
          jj = j - locj(1)
          ii = i - loci(1)
          indk(1) = lock(1)-dom_bound(3,1) - lock(1)
          indk(2) = lock(2)-dom_bound(3,2) - lock(1)
!
          if (dom_bound(3,1) == 0) then
            kk = 0;k = 0;
            f_prime(ivar,nvec,k,j,i) = bnd_0(f,nvec,ii,jj,kk,a1,b1,c1,h1)
            kk = 1;k = 1;
            f_prime(ivar,nvec,k,j,i) = bnd_1(f,nvec,ii,jj,kk,a1,b1,c1,h1)
            indk(1) = indk(1) + ghostlayer
          end if
!
          if (dom_bound(3,2) == 0) then
            kk = lock(2)-lock(1)-1;k = lock(2)-1;
            f_prime(ivar,nvec,k,j,i) = bnd_n1(f,nvec,ii,jj,kk,a1,b1,c1,h1)
            kk = lock(2)-lock(1);k = lock(2);
            f_prime(ivar,nvec,k,j,i) = bnd_n(f,nvec,ii,jj,kk,a1,b1,c1,h1)
            indk(2) = indk(2) - ghostlayer
          end if
!
          do kk = indk(1),indk(2)
            k = kk + lock(1)
            f_prime(ivar,nvec,k,j,i) = mid(f,nvec,ii,jj,kk,a1,b1,c1,h1)
          end do
!
        end do
      end do
    endif
  end if
end if
CONTAINS
!=====
! Functions for calculating the above derivatives
!=====
!
! 0 th Boundary
!-----
function bnd_0(p,nv1,ll1,mm1,nn1,r,s,t,u)
  REAL*8::bnd_0
  INTEGER :: ll1, m1,n1
  REAL*8,intent(in),dimension(:, :, :,:) :: p
  INTEGER, intent(in) :: nv1,ll1,mm1,nn1,r,s,t
  real*8, intent(in) :: u

```

130

140

150

160

170

```

!
!
! ll = ll1+1;m1=mm1+1;n1=nn1+1
!
!
! bnd_0=(-3.0*p(nv1,n1+4*t,m1+4*s,ll+4*r)&
! &+16.0*p(nv1,n1+3*t,m1+3*s,ll+3*r)&
! &-36.0*p(nv1,n1+2*t,m1+2*s,ll+2*r)&
! &+48.0*p(nv1,n1+t,m1+s,ll+r)&
! &-25.0*p(nv1,n1,m1,ll))*u
!
! end function bnd_0
!
! 0-1 Boundary
! -----
! function bnd_1(p,nv1,ll1,mm1,nn1,r,s,t,u)
!
! ! Declare variables
!
! REAL*8 :: bnd_1
! REAL*8,intent(in),dimension(:,:,:): p
! INTEGER, intent(in) :: nv1,ll1,mm1,nn1,r,s,t
! INTEGER :: ll, m1, n1
! real*8, intent(in) :: u
!
! ll = ll1+1;m1=mm1+1;n1=nn1+1
!
! bnd_1 = (-3.0*p(nv1,n1-t,m1-s,ll-r)&
! &-10.0*p(nv1,n1,m1,ll)&
! &+18.0*p(nv1,n1+t,m1+s,ll+r)&
! &-6.0*p(nv1,n1+2*t,m1+2*s,ll+2*r)&
! &+p(nv1,n1+3*t,m1+3*s,ll+3*r))*u
!
! end function bnd_1
!
! Middle
! -----
! function mid(p,nv1,ll1,mm1,nn1,r,s,t,u)
!
! REAL*8 :: mid
! REAL*8, intent(in), dimension(:,:,:): p
! INTEGER, intent(in) :: nv1,ll1,mm1,nn1,r,s,t
! INTEGER :: ll, m1, n1
! real*8, intent(in) :: u
!
! ll = ll1+1;m1=mm1+1;n1=nn1+1
!
! mid = (p(nv1,n1-2*t,m1-2*s,ll-2*r)&
! &-8.0*p(nv1,n1-t,m1-s,ll-r)&
! &+8.0*p(nv1,n1+t,m1+s,ll+r)&
! &-p(nv1,n1+2*t,m1+2*s,ll+2*r))*u
!
! end function mid
!
! N-1 boundary
! -----
! function bnd_n1(p,nv1,ll1,mm1,nn1,r,s,t,u)

```

180

190

200

210

220

```

REAL*8::bnd_n1
REAL*8,intent(in),dimension(:,:,:) :: p
INTEGER, intent(in) :: nv1,ll1,mm1,nn1,r,s,t
INTEGER :: l1, m1, n1
real*8, intent(in) :: u
!
!
l1 = ll1+1;m1=mm1+1;n1=nn1+1
!
!
bnd_n1=-(-3.0*p(nv1,n1+t,m1+s,l1+r)&
&-10.0*p(nv1,n1,m1,l1)&
&+18.0*p(nv1,n1-t,m1-s,l1-r)&
&-6.0*p(nv1,n1-2*t,m1-2*s,l1-2*r)&
&+p(nv1,n1-3*t,m1-3*s,l1-3*r))*u
!
end function bnd_n1
!
! Nth Boundary
!-----
function bnd_n(p,nv1,ll1,mm1,nn1,r,s,t,u)
REAL*8 :: bnd_n
REAL*8,intent(in),dimension(:,:,:) :: p
INTEGER, intent(in) :: nv1,ll1,mm1,nn1,r,s,t
real*8, intent(in) :: u
INTEGER :: l1, m1, n1
!
!
l1 = ll1+1;m1=mm1+1;n1=nn1+1
!
!
bnd_n = -(-3.0*p(nv1,n1-4*t,m1-4*s,l1-4*r)&
&+16.0*p(nv1,n1-3*t,m1-3*s,l1-3*r)&
&-36.0*p(nv1,n1-2*t,m1-2*s,l1-2*r)&
&+48.0*p(nv1,n1-t,m1-s,l1-r)&
&-25.0*p(nv1,n1,m1,l1))*u
!
end function bnd_n
!
END SUBROUTINE prime
!
!=====
!=====
SUBROUTINE pprime(ivar,nvec)
! This subroutine calculates second derivatives
! The following format should be used when calling this subroutine
! dfdx(Independent variable,Dependent variable,x3loc,x2loc,x1loc)
! Independent variable: x1=1
! x2=2
! x3=3
! Dependent variable: The variable for which the derivative is being calculated (T,Yi,u,v,w....)
! x3loc: The x3 location
! x2loc: The x2 location
! x1loc: The x1 location
!
USE vkvar
!

```

230

240

250

260

270

280

```

    IMPLICIT NONE
!
    REAL*8 :: h, h1
    INTEGER :: a1,b1,c1,i,j,k,ii,jj,kk
    INTEGER, DIMENSION(:) :: gl(6),indi(2),indj(2),indk(2)
    INTEGER, INTENT(IN) :: ivar,nvec
!
    ALLOCATE(f_pprime(ivar:ivar,nvec:nvec,lock(1):lock(2),locj(1):locj(2),loci(1):loci(2)))
!
    df2dx1dx1
    290
    if (ivar==1) then
        h = sndx(ivar)
        h1 = 1.0/(12.0*h*h)
        a1 = 1
        b1 = 0
        c1 = 0
!
        do k = lock(1) - dom_bound(3,1), lock(2) - dom_bound(3,2)
            do j = locj(1) - dom_bound(2,1), locj(2) - dom_bound(2,2)
!
                kk = k - lock(1)
                jj = j - locj(1)
                indi(1) = loci(1) - dom_bound(1,1) - loci(1)
                indi(2) = loci(2) - dom_bound(1,2) - loci(1)
!
                if (dom_bound(1,1) == 0) then
                    ii = 0; i = 0;
                    f_pprime(ivar,nvec,k,j,i) = bnd_0(f,nvec,ii,jj,kk,a1,b1,c1,h1)
                    ii = 1; i = 1;
                    310
                    f_pprime(ivar,nvec,k,j,i) = bnd_1(f,nvec,ii,jj,kk,a1,b1,c1,h1)
                    indi(1) = indi(1) + ghostlayer
                end if
!
                if (dom_bound(1,2) == 0) then
                    ii = loci(2) - loci(1) - 1; i = loci(2) - 1;
                    f_pprime(ivar,nvec,k,j,i) = bnd_n1(f,nvec,ii,jj,kk,a1,b1,c1,h1)
                    ii = loci(2) - loci(1); i = loci(2)
                    f_pprime(ivar,nvec,k,j,i) = bnd_n(f,nvec,ii,jj,kk,a1,b1,c1,h1)
                    320
                    indi(2) = indi(2) - ghostlayer
                end if
!
                do ii = indi(1),indi(2)
                    i = ii + loci(1)
                    f_pprime(ivar,nvec,k,j,i) = mid(f,nvec,ii,jj,kk,a1,b1,c1,h1)
                end do
!
            end do
        end do
!
    else
        if (ivar==2) then
!
            df2dx2dx2
            h = sndx(ivar)
            h1 = 1.0/(12.0*h*h)

```

```

a1 = 0
b1 = 1
c1 = 0
!
do k = lock(1) - dom_bound(3,1), lock(2) - dom_bound(3,2)
do i = loci(1) - dom_bound(1,1), loci(2) - dom_bound(1,2)
!
kk = k - lock(1)
ii = i - loci(1)
indj(1) = locj(1) - dom_bound(2,1) - locj(1)
indj(2) = locj(2) - dom_bound(2,2) - locj(1)
!
if (dom_bound(2,1) == 0) then
jj = 0; j = 0;
f_pprime(ivar,nvec,k,j,i) = bnd_0(f,nvec,ii,jj,kk,a1,b1,c1,h1)
jj = 1; j = 1;
f_pprime(ivar,nvec,k,j,i) = bnd_1(f,nvec,ii,jj,kk,a1,b1,c1,h1)
indj(1) = indj(1) + ghostlayer
!
end if
!
if (dom_bound(2,2) == 0) then
jj = locj(2) - locj(1) - 1; j = locj(2) - 1
f_pprime(ivar,nvec,k,j,i) = bnd_n1(f,nvec,ii,jj,kk,a1,b1,c1,h1)
jj = locj(2) - locj(1); j = locj(2)
f_pprime(ivar,nvec,k,j,i) = bnd_n(f,nvec,ii,jj,kk,a1,b1,c1,h1)
indj(2) = indj(2) - ghostlayer
!
end if
!
do jj = indj(1),indj(2)
j = jj + locj(1)
f_pprime(ivar,nvec,k,j,i) = mid(f,nvec,ii,jj,kk,a1,b1,c1,h1)
end do
!
end do
end do
!
else
!
if (ivar == 3) then
df2dx3dx3
h = sndx(ivar)
h1 = 1.0/(12.0*h*h)
a1 = 0
b1 = 0
c1 = 1
!
do j = locj(1) - dom_bound(2,1), locj(2) - dom_bound(2,2)
do i = loci(1) - dom_bound(1,1), loci(2) - dom_bound(1,2)
!
jj = j - locj(1)
ii = i - loci(1)
indk(1) = lock(1) - dom_bound(3,1) - lock(1)

```

```

                                indk(2) = lock(2)-dom_bound(3,2) - lock(1)
!
                                if (dom_bound(3,1) == 0) then
                                    kk = 0; k = 0;
                                    f_pprime(ivar,nvec,k,j,i) = bnd_0(f,nvec,ii,jj,kk,a1,b1,c1,h1)
                                    kk = 1; k = 1;
                                    f_pprime(ivar,nvec,k,j,i) = bnd_1(f,nvec,ii,jj,kk,a1,b1,c1,h1)
                                    indk(1) = indk(1) + ghostlayer
                                end if
!
                                if (dom_bound(3,2) == 0) then
                                    kk = lock(2)-lock(1)-1; k = lock(2)-1
                                    f_pprime(ivar,nvec,k,j,i) = bnd_n1(f,nvec,ii,jj,kk,a1,b1,c1,h1)
                                    kk = lock(2)-lock(1); k = lock(2)
                                    f_pprime(ivar,nvec,k,j,i) = bnd_n(f,nvec,ii,jj,kk,a1,b1,c1,h1)
                                    indk(2) = indk(2) - ghostlayer
                                end if
!
                                do kk = indk(1),indk(2)
                                    k = kk+lock(1)
                                    f_pprime(ivar,nvec,k,j,i) = mid(f,nvec,ii,jj,kk,a1,b1,c1,h1)
                                end do
!
                                end do
                                end do
!
                                end if
                                end if
                                end if
!
CONTAINS
===== 4
!
! 0th Boundary
!-----
function bnd_0(p,nv1,ll1,mm1,nn1,r,s,t,u)
    REAL*8::bnd_0
    REAL*8,intent(in),dimension(:, :, :) :: p
    INTEGER, intent(in) :: nv1,ll1,mm1,nn1,r,s,t
    real*8, intent(in) :: u
    INTEGER :: ll, m1, n1
!
    ll = ll1+1;m1=mm1+1;n1=nn1+1
!
    bnd_0=(11.0*p(nv1,n1+4*t,m1+4*s,ll+4*r)&
        &-56.0*p(nv1,n1+3*t,m1+3*s,ll+3*r)&
        &+114.0*p(nv1,n1+2*t,m1+2*s,ll+2*r)&
        &-104.0*p(nv1,n1+t,m1+s,ll+r)&
        &+35.0*p(nv1,n1,m1,ll))*u
!
end function bnd_0
!
! 0-1 Boundary

```

390

400

410

430

440

```

!-----
function bnd_1(p,nv1,ll1,mm1,nn1,r,s,t,u)
  REAL*8 :: bnd_1
  REAL*8,intent(in),dimension(:,:,:): p
  INTEGER, intent(in) :: nv1,ll1,mm1,nn1,r,s,t
  real*8, intent(in) :: u
  INTEGER :: ll, m1, n1
!
  ll = ll1+1;m1=mm1+1;n1=nn1+1
!
  bnd_1 = (11.0*p(nv1,n1-1*t,m1-1*s,ll-1*r)&
    &-20.0*p(nv1,n1,m1,ll)&
    &+6.0*p(nv1,n1+t,m1+s,ll+r)&
    &+4.0*p(nv1,n1+2*t,m1+2*s,ll+2*r)&
    &-p(nv1,n1+3*t,m1+3*s,ll+3*r))*u
!
end function bnd_1
!
! Middle
!-----
function mid(p,nv1,ll1,mm1,nn1,r,s,t,u)
  REAL*8 :: mid
  REAL*8, intent(in), dimension(:,:,:): p
  INTEGER, intent(in) :: nv1,ll1,mm1,nn1,r,s,t
  real*8, intent(in) :: u
  INTEGER :: ll, m1, n1
!
  ll = ll1+1;m1=mm1+1;n1=nn1+1
!
  mid = (-p(nv1,n1-2*t,m1-2*s,ll-2*r)&
    &+16.0*p(nv1,n1-t,m1-s,ll-r)&
    &-30.0*p(nv1,n1,m1,ll)&
    &+16.0*p(nv1,n1+t,m1+s,ll+r)&
    &-p(nv1,n1+2*t,m1+2*s,ll+2*r))*u
!
end function mid
!
! N-1 Boundary
!-----
function bnd_n1(p,nv1,ll1,mm1,nn1,r,s,t,u)
  REAL*8::bnd_n1
  REAL*8,intent(in),dimension(:,:,:): p
  INTEGER, intent(in) :: nv1,ll1,mm1,nn1,r,s,t
  real*8, intent(in) :: u
  INTEGER :: ll, m1, n1
!
  ll = ll1+1;m1=mm1+1;n1=nn1+1
!
  bnd_n1=(11.0*p(nv1,n1+t,m1+s,ll+r)&
    &-20.0*p(nv1,n1,m1,ll)&
    &+6.0*p(nv1,n1-t,m1-s,ll-r)&
    &+4.0*p(nv1,n1-2*t,m1-2*s,ll-2*r)&
    &-p(nv1,n1-3*t,m1-3*s,ll-3*r))*u

```



```

!
end function bnd_n1
!
! Nth Boundary
!-----
function bnd_n(p,nv1,ll1,mm1,nn1,r,s,t,u)
REAL*8 :: bnd_n
REAL*8,intent(in),dimension(:,:,:) :: p
INTEGER, intent(in) :: nv1,ll1,mm1,nn1,r,s,t
real*8, intent(in) :: u
INTEGER :: ll, m1, n1
!
! ll = ll1+1;m1=mm1+1;n1=nn1+1
!
bnd_n = (11.0*p(nv1,n1-4*t,m1-4*s,ll-4*r)&
&+35.0*p(nv1,n1,m1,ll)&
&-104.0*p(nv1,n1-t,m1-s,ll-r)&
&+114.0*p(nv1,n1-2*t,m1-2*s,ll-2*r)&
&-56.0*p(nv1,n1-3*t,m1-3*s,ll-3*r))*u
!
end function bnd_n
!
END SUBROUTINE pprime
!
=====
=====
SUBROUTINE flf2prime(ivar1,ivar2,nvec)
! This subroutine calculates cross derivatives
! The following format should be used when calling this subroutine
! dfdx(Independent variable1,Independent variable2,Dependent variable,x3loc,x2loc,x1loc)
! Independent variable: x1=1
! x2=2
! x3=3
! Dependent variable: The variable for which the derivative is being calculated (T,Yi,u,v,w....)
! x3loc: The x3 location
! x2loc: The x2 location
! x1loc: The x1 location
!
USE vkvar
!
IMPLICIT NONE
!
INTEGER :: a1,b1,c1,var,i,j,k
INTEGER, DIMENSION(:) :: gl(6),indi(2),indj(2),indk(2)
INTEGER, INTENT(IN) :: ivar1,ivar2,nvec
REAL*8 :: h,h1
!
ALLOCATE(f_cpprime(ivar1:ivar1,ivar2:ivar2,nvec:nvec,lock(1):lock(2),locj(1):locj(2),loci(1):loci(2)))
call prime(ivar1,nvec)
! df2dx1dx2
if (ivar1==1 .and. ivar2==2) then
h = sndx(ivar1)
h1 = 1.0/(12.0*h)

```

```

a1 = 0
b1 = 1
c1 = 0
do k = lock(1) - dom_bound(3,1), lock(2) - dom_bound(3,2)
  do i = loci(1) - dom_bound(1,1), loci(2) - dom_bound(1,2)
!
    if (dom_bound(2,1) == 0) then
      j = 0
      f_cpprime(ivar1,ivar2,nvec,k,j,i) = bnd_0(f_prime,ivar1,nvec,i,j,k,a1,b1,c1,h1)
      j = 1
      f_cpprime(ivar1,ivar2,nvec,k,j,i) = bnd_1(f_prime,ivar1,nvec,i,j,k,a1,b1,c1,h1)
    end if
!
    do j = locj(1) - dom_bound(2,1), locj(2) - dom_bound(2,2)
      f_cpprime(ivar1,ivar2,nvec,k,j,i) = mid(f_prime,ivar1,nvec,i,j,k,a1,b1,c1,h1)
    end do
!
    if (dom_bound(2,2) == 0) then
      j = locj(2)-1
      f_cpprime(ivar1,ivar2,nvec,k,j,i) = bnd_n1(f_prime,ivar1,nvec,i,j,k,a1,b1,c1,h1)
      j = locj(2)
      f_cpprime(ivar1,ivar2,nvec,k,j,i) = bnd_n(f_prime,ivar1,nvec,i,j,k,a1,b1,c1,h1)
    end if
!
  end do
end do
deallocate(f_prime)
end if
if (ivar2==3 .and. ivar1==1 .or. ivar1==2 ) then
!
  var = 1
!   df2dx1dx3
do k = lock(1) - dom_bound(3,1), lock(2) - dom_bound(3,2)
  do j = locj(1) - dom_bound(2,1), locj(2) - dom_bound(2,2)
    do i = loci(1) - dom_bound(1,1), loci(2) - dom_bound(1,2)
      end do
    end do
  end do
end do
h = sndx(ivar2)
h1 = 1.0/(12.0*h)
a1 = 0
b1 = 0
c1 = 1
do j = locj(1) - dom_bound(2,1), locj(2) - dom_bound(2,2)
  do i = loci(1) - dom_bound(1,1), loci(2) - dom_bound(1,2)
!
    if (dom_bound(3,1) == 0) then
      k = 0
      f_cpprime(ivar1,ivar2,nvec,k,j,i) = bnd_0(f_prime,var,nvec,i,j,k,a1,b1,c1,h1)
      k = 1
      f_cpprime(ivar1,ivar2,nvec,k,j,i) = bnd_1(f_prime,var,nvec,i,j,k,a1,b1,c1,h1)
    end if
!

```

```

do k = lock(1) - dom_bound(3,1), lock(2) - dom_bound(3,2)
  f_cpprime(ivar1,ivar2,nvec,k,j,i) = mid(f_prime,var,nvec,i,j,k,a1,b1,c1,h1)
end do
!
  if (dom_bound(3,2) == 0) then
    k = lock(2)-1
    f_cpprime(ivar1,ivar2,nvec,k,j,i) = bnd_n1(f_prime,var,nvec,i,j,k,a1,b1,c1,h1)
    k = lock(2)
    f_cpprime(ivar1,ivar2,nvec,k,j,i) = bnd_n(f_prime,var,nvec,i,j,k,a1,b1,c1,h1)
  end if
!
end do
end do
deallocate(f_prime)
end if
CONTAINS
=====
!
! 0th Boundary
!-----
function bnd_0(p,q,nv1,ll1,mm1,nn1,r,s,t,u)
  REAL*8::bnd_0
  INTEGER :: ll1, m1,n1
  REAL*8,intent(in),dimension(:,:,:,:) :: p
  INTEGER, intent(in) :: nv1,q,ll1,mm1,nn1,r,s,t
  real*8, intent(in) :: u
!
  ll1 = ll1+1;m1=mm1+1;n1=nn1+1
!
  bnd_0=(-3.0*p(q,nv1,n1+4*t,m1+4*s,ll1+4*r)&
    &+16.0*p(q,nv1,n1+3*t,m1+3*s,ll1+3*r)&
    &-36.0*p(q,nv1,n1+2*t,m1+2*s,ll1+2*r)&
    &+48.0*p(q,nv1,n1+t,m1+s,ll1+r)&
    &-25.0*p(q,nv1,n1,m1,ll1))*u
!
end function bnd_0
!
! 0-1 Boundary
!-----
function bnd_1(p,q,nv1,ll1,mm1,nn1,r,s,t,u)
  REAL*8 :: bnd_1
  REAL*8,intent(in),dimension(:,:,:,:) :: p
  INTEGER, intent(in) :: nv1,q,ll1,mm1,nn1,r,s,t
  INTEGER :: ll1, m1, n1
  real*8, intent(in) :: u
!
  ll1 = ll1+1;m1=mm1+1;n1=nn1+1
!
  bnd_1 = (-3.0*p(q,nv1,n1-t,m1-s,ll1-r)&
    &-10.0*p(q,nv1,n1,m1,ll1)&
    &+18.0*p(q,nv1,n1+t,m1+s,ll1+r)&
    &-6.0*p(q,nv1,n1+2*t,m1+2*s,ll1+2*r)&
    &+p(q,nv1,n1+3*t,m1+3*s,ll1+3*r))*u
!

```

```

!
end function bnd_1
!
! Middle
!-----
function mid(p,q,nv1,ll1,mm1,nn1,r,s,t,u)
  REAL*8 :: mid
  REAL*8, intent(in), dimension(:,:,:,:) :: p
  INTEGER, intent(in) :: nv1,q,ll1,mm1,nn1,r,s,t
  INTEGER :: ll, m1, n1
  real*8, intent(in) :: u
!
  ll = ll1+1;m1=mm1+1;n1=nn1+1
!
  mid = (p(q,nv1,n1-2*t,m1-2*s,ll-2*r)&
    &-8.0*p(q,nv1,n1-t,m1-s,ll-r)&
    &+8.0*p(q,nv1,n1+t,m1+s,ll+r)&
    &-p(q,nv1,n1+2*t,m1+2*s,ll+2*r))*u
!
end function mid
!
! N-1 Boundary
!-----
function bnd_n1(p,q,nv1,ll1,mm1,nn1,r,s,t,u)
  REAL*8::bnd_n1
  REAL*8,intent(in),dimension(:,:,:,:) :: p
  INTEGER, intent(in) :: nv1,q,ll1,mm1,nn1,r,s,t
  INTEGER :: ll, m1, n1
  real*8, intent(in) :: u
!
  ll = ll1+1;m1=mm1+1;n1=nn1+1
!
  bnd_n1=-(-3.0*p(q,nv1,n1+t,m1+s,ll+r)&
    &-10.0*p(q,nv1,n1,m1,ll)&
    &+18.0*p(q,nv1,n1-t,m1-s,ll-r)&
    &-6.0*p(q,nv1,n1-2*t,m1-2*s,ll-2*r)&
    &+p(q,nv1,n1-3*t,m1-3*s,ll-3*r))*u
!
end function bnd_n1
!
! Nth Boundary
!-----
function bnd_n(p,q,nv1,ll1,mm1,nn1,r,s,t,u)
  REAL*8 :: bnd_n
  REAL*8,intent(in),dimension(:,:,:,:) :: p
  INTEGER, intent(in) :: nv1,q,ll1,mm1,nn1,r,s,t
  INTEGER :: ll, m1, n1
  real*8, intent(in) :: u
!
  ll = ll1+1;m1=mm1+1;n1=nn1+1
!
  bnd_n = -(-3.0*p(q,nv1,n1-4*t,m1-4*s,ll-4*r)&
    &+16.0*p(q,nv1,n1-3*t,m1-3*s,ll-3*r)&

```

```

&-36.0*p(q,nv1,n1-2*t,m1-2*s,l1-2*r)&
&+48.0*p(q,nv1,n1-t,m1-s,l1-r)&
&-25.0*p(q,nv1,n1,m1,l1))*u
!
end function bnd_n
!=====
!
END SUBROUTINE flf2prime
!=====
SUBROUTINE prime_periodic(ivar,nvec)
! This subroutine calculates first derivatives
! The following format should be used when calling this subroutine
! f_prime(Independent variable,Dependent variable,x3loc,x2loc,x1loc)
! Independent variable: x1=1
! x2=2
! x3=3
! Dependent variable: The variable for which the derivative is being calculated (T,Yi,u,v,w....)
! x3loc: The x3 location
! x2loc: The x2 location
! x1loc: The x1 location
!
USE vkvar
!
IMPLICIT NONE
!
INTEGER :: a1,b1,c1,i,j,k,ii,jj,kk
INTEGER, DIMENSION(:) :: gl(6),indi(2),indj(2),indk(2)
INTEGER, INTENT(IN) :: ivar,nvec
REAL*8 :: h, h1, test1
!
ALLOCATE(f_prime_periodic(ivar:ivar,nvec:nvec,lock(1):lock(2),locj(1):locj(2),loci(1):loci(2)))
!
! Calculate dfdx
!=====
if (ivar==1) then
h = sndx(ivar)
h1 = 1.0/(12.0*h)
a1 = 1
b1 = 0
c1 = 0
!
do k = lock(1) - dom_bound(3,1), lock(2) - dom_bound(3,2)
do j = locj(1) - dom_bound(2,1), locj(2) - dom_bound(2,2)
do i = loci(1)-dom_bound(1,1),loci(2)-dom_bound(1,2)
!
kk = k - lock(1)
jj = j - locj(1)
ii = i - loci(1)
!
f_prime_periodic(ivar,nvec,k,j,i) = &
& bnd_0(f,nvec,ii,jj,kk,a1,b1,c1,h1,nx3,nx2,nx1)
!

```

710

720

730

740

750

```

                end do
            end do
        end do
    else
!
! Calculate dfdx2
!=====*
        if (ivar==2) then
            h = sndx(ivar)
            h1 = 1.0/(12.0*h)
            a1 = 0
            b1 = 1
            c1 = 0
!
            do k = lock(1) - dom_bound(3,1), lock(2) - dom_bound(3,2)
                do j = locj(1) - dom_bound(2,1), locj(2) - dom_bound(2,2)
                    do i = loci(1)-dom_bound(1,1),loci(2)-dom_bound(1,2)
!
                        kk = k - lock(1)
                        jj = j - locj(1)
                        ii = i - loci(1)
!
                        f_prime_periodic(ivar,nvec,k,j,i) = &
                            & bnd_0(f,nvec,ii,jj,kk,a1,b1,c1,h1,nx3,nx2,nx1)
!
                    end do
                end do
            end do
!
        else
!
! Calculate dfdx3
!=====
            if (ivar==3) then
                h = sndx(ivar)
                h1 = 1.0/(12.0*h)
                a1 = 0
                b1 = 0
                c1 = 1
!
                do k = lock(1) - dom_bound(3,1), lock(2) - dom_bound(3,2)
                    do j = locj(1) - dom_bound(2,1), locj(2) - dom_bound(2,2)
                        do i = loci(1)-dom_bound(1,1),loci(2)-dom_bound(1,2)
!
                            kk = k - lock(1)
                            jj = j - locj(1)
                            ii = i - loci(1)
!
                            f_prime_periodic(ivar,nvec,k,j,i) = &
                                & bnd_0(f,nvec,ii,jj,kk,a1,b1,c1,h1,nx3,nx2,nx1)
!
                        end do
                    end do
                end do
!
            end do
        end do
    end do

```

760

770

780

790

800

810

```

                end do
!
                end if
            end if
        end if

CONTAINS
=====
        ! Functions for calculating the above derivatives
=====
        !
        ! 0 th Boundary
        !-----
        function bnd_0(p,nv1,ll1,mm1,nn1,r,s,t,u,nxx3,nxx2,nxx1)
            REAL*8::bnd_0
            INTEGER :: ll1, m1,n1
            REAL*8,intent(in),dimension(:,:,:) :: p
            INTEGER, intent(in) :: nv1,ll1,mm1,nn1,r,s,t,nxx3,nxx2,nxx1
            real*8, intent(in) :: u
!
            ll1 = ll1+1;m1=mm1+1;n1=nn1+1
!
            bnd_0=(-p(nv1,n1+2*t,m1+2*s,ll1+2*r)&
                &+8.0*p(nv1,n1+t,m1+s,ll1+r)&
                &-8.0*p(nv1,n1-1*t,&
                &m1-1*s,ll1-1*r)&
                &+p(nv1,n1-2*t,&
                &m1-2*s,ll1-2*r))*u
!
        end function bnd_0
!
        END SUBROUTINE prime-periodic
!
=====
!
SUBROUTINE pprime_per(ivar,nvec)
! This subroutine calculates first derivatives
! The following format should be used when calling this subroutine
! f_prime(Independent variable,Dependent variable,x3loc,x2loc,x1loc)
! Independent variable: x1=1
!                       x2=2
!                       x3=3
! Dependent variable: The variable for which the derivative is being calculated (T,Yi,u,v,w....)
! x3loc:               The x3 location
! x2loc:               The x2 location
! x1loc:               The x1 location
!
        USE vkvar
!
        IMPLICIT NONE
!
        INTEGER :: a1,b1,c1,i,j,k,ii,jj,kk
        INTEGER, INTENT(IN) :: ivar,nvec
        REAL*8 :: h, h1

```

820

830

840

850

860

```

      INTEGER, DIMENSION(:) :: gl(6),indi(2),indj(2),indk(2)
!
      ALLOCATE(f_pprime_per(ivar:ivar,nvec:nvec,lock(1):lock(2),locj(1):locj(2),loci(1):loci(2)))
!
      ! Calculate dfdx
=====
      if (ivar==1) then
        h = sndx(ivar)
        h1 = 1.0/(12.0*h*h)
        a1 = 1
        b1 = 0
        c1 = 0
!
        do k = lock(1) - dom_bound(3,1), lock(2) - dom_bound(3,2)
          do j = locj(1) - dom_bound(2,1), locj(2) - dom_bound(2,2)
            do i = loci(1) - dom_bound(1,1), loci(2) - dom_bound(1,2)
!
              kk = k - lock(1)
              jj = j - locj(1)
              ii = i - loci(1)
!
              f_pprime_per(ivar,nvec,k,j,i) = &
                & bnd_0(f,nvec,ii,jj,kk,a1,b1,c1,h1,nx3,nx2,nx1)
            end do
          end do
        end do
      else
!
      ! Calculate dfdx2
=====
      if (ivar==2) then
        h = sndx(ivar)
        h1 = 1.0/(12.0*h*h)
        a1 = 0
        b1 = 1
        c1 = 0
        do k = lock(1) - dom_bound(3,1), lock(2) - dom_bound(3,2)
          do j = locj(1) - dom_bound(2,1), locj(2) - dom_bound(2,2)
            do i = loci(1) - dom_bound(1,1), loci(2) - dom_bound(1,2)
!
              kk = k - lock(1)
              jj = j - locj(1)
              ii = i - loci(1)
!
              f_pprime_per(ivar,nvec,k,j,i) = &
                & bnd_0(f,nvec,ii,jj,kk,a1,b1,c1,h1,nx3,nx2,nx1)
            end do
          end do
        end do
      else
!
      ! Calculate dfdx3
=====

```



```

    if (ivar==3) then
        h = sndx(ivar)
        h1 = 1.0/(12.0*h*h)
        a1 = 0
        b1 = 0
        c1 = 1
        do k = lock(1) - dom_bound(3,1), lock(2) - dom_bound(3,2)
            do j = locj(1) - dom_bound(2,1), locj(2) - dom_bound(2,2)
                do i = loci(1) - dom_bound(1,1), loci(2) - dom_bound(1,2)
!
                    kk = k - lock(1)
                    jj = j - locj(1)
                    ii = i - loci(1)
!
                    f_pprime_per(ivar,nvec,k,j,i) = &
                        & bnd_0(f,nvec,ii,jj,kk,a1,b1,c1,h1,nx3,nx2,nx1)
                end do
            end do
        end do
!
    endif
end if
end if
!
CONTAINS
!=====
! Functions for calculating the above derivatives
!=====
!
! 0 th Boundary
!-----
function bnd_0(p,nv1,ll1,mm1,nn1,r,s,t,u,nxx3,nxx2,nxx1)
    REAL*8::bnd_0
    INTEGER :: ll1, m1,n1
    REAL*8,intent(in),dimension(:, :, :) :: p
    INTEGER, intent(in) :: nv1,ll1,mm1,nn1,r,s,t,nxx3,nxx2,nxx1
    real*8, intent(in) :: u
!
    ll1 = ll1+1;m1=mm1+1;n1=nn1+1
!
    bnd_0=(-p(nv1,n1+2*t,m1+2*s,ll1+2*r)&
        &+16.0*p(nv1,n1+t,m1+s,ll1+r)&
        &-30.*p(nv1,n1,m1,ll1)&
        &+16.0*p(nv1,n1-t,m1-s,ll1-r)&
        &-p(nv1,n1-2*t,m1-2*s,ll1-2*r))*u
    end function bnd_0
!
END SUBROUTINE pprime_per
!=====
!=====
SUBROUTINE init_runge
!
USE vkvar

```

920

930

940

950

960

970

```

!
!   IMPLICIT NONE
!
!   allocate(ack(ikutta),bck(ikutta),cck(ikutta))
!
!   if (ikutta==1) then
!
!       1st order backward scheme
!=====
!
!       nstage = 1
!
!       ack(1) = 0.0d0
!
!       bck(1) = 1.0d0
!
!       cck(1) = 1.0d0
!
!   end if
!
!   if (ikutta==3) then
!
!       (3,3) scheme of Williamson
!=====
!
!       nstage = 3
!
!       ack(1) = 0.0d0
!       ack(2) = -5.0d0/9.0d0
!       ack(3) = -153.0d0/128.0d0
!
!       bck(1) = 1.0d0/3.0d0
!       bck(2) = 15.0d0/16.0d0
!       bck(3) = 8.0d0/15.0d0
!
!       cck(1) = 0.0d0
!       cck(2) = 1.0d0/3.0d0
!       cck(3) = 3.0d0/4.0d0
!
!   end if
!
!   if (ikutta==5) then
!
!       (5,4) scheme of Carpenter
!=====
!
!       nstage = 5
!
!       ack(1) = 0.0d0
!       ack(2) = -0.417890474500d0
!       ack(3) = -1.192151694643d0
!       ack(4) = -1.697784692471d0
!       ack(5) = -1.514183444257d0

```

980

990

1000

1010

1020

```

!
!   bck(1) = 0.1496590219993d0
!   bck(2) = 0.3792103129999d0
!   bck(3) = 0.8229550293869d0
!   bck(4) = 0.6994504559488d0
!   bck(5) = 0.1530572479681d0
!
!   cck(1) = 0.0d0
!   cck(2) = 0.1496590219993d0
!   cck(3) = 0.3704009573644d0
!   cck(4) = 0.6222557631345d0
!   cck(5) = 0.9582821306748d0
!
!   end if
!
!   END SUBROUTINE init_runge
!
!=====
!=====
!
END MODULE der_ord_4

```

Integration

```

MODULE vk_cf
CONTAINS
!
!   SUBROUTINE rk54(tin,tout)
!
!   USE vkvar
!   USE vkpar
!
!   IMPLICIT NONE
!
!   Runge–Kutta
!
!   INTEGER :: i, j, k, n, ns
!   REAL*8, INTENT(IN) :: tin, tout
!   REAL*8 :: time_n, h
!   INTEGER, dimension(2) :: indi,indj,indk
!
!   h = tout-tin
!
!   DO ns=1,ikutta
!
!       time_n = tin + cck(ns)*h
!
!       CALL per_corr
!       CALL vk_buffer_comm(1,nvar)
!       CALL rhs(time_n)
!
!       DO n=1,nvar

```

```

DO k = lock(1)-dom_bound(3,1),lock(2)-dom_bound(3,2)
  DO j = locj(1)-dom_bound(2,1),locj(2)-dom_bound(2,2)
    DO i = loci(1)-dom_bound(1,1),loci(2)-dom_bound(1,2)
!
      rkj(n,k,j,i) = ack(ns)*rkj(n,k,j,i) + h*fprime(n,k,j,i)
      f(n,k,j,i) = f(n,k,j,i) + bck(ns)*rkj(n,k,j,i)
!
      if (f(n,k,j,i).lt.1.d-20) f(n,k,j,i) = 1.d-20
!
      END DO
    END DO
  END DO
END DO
!
CALL MPL_BARRIER(MPL_COMM_WORLD,ierr)
!
!
! Set boundary conditions
!=====
!
CALL bc(n)
!
! Check if temperature or species values go below 0 or above 100
! and set the floor at 0.0 and the ceiling at 100.0
!=====
!
END DO
!
CALL MPL_BARRIER(MPL_COMM_WORLD,ierr)
!
t = tout
!
END SUBROUTINE rk54
!
!=====
!=====
!
SUBROUTINE rhs(time_curr)
!
USE vkvar
USE der_ord_4
!
IMPLICIT NONE
!
INTEGER :: i, j, k, l, n,zpos
INTEGER, dimension(2) :: indi,indj,indk
REAL*8, INTENT(IN) :: time_curr
!
! Compute and assign respective derivative values
!=====
!
indi(1) = loci(1) - dom_bound(1,1)
indi(2) = loci(2) - dom_bound(1,2)

```

```

indj(1) = locj(1) - dom_bound(2,1)
indj(2) = locj(2) - dom_bound(2,2)
indk(1) = lock(1) - dom_bound(3,1)
indk(2) = lock(2) - dom_bound(3,2)
!
DO n = 1,nvar
  DO l = 1,3
    IF (periodic(l)==0) then
!
!
      CALL prime(1,n)
      CALL pprime(1,n)
!
      DO k = indk(1),indk(2)
        DO j = indj(1),indj(2)
          DO i = indi(1),indi(2)
!
            cc(n,sndim(1,2),k,j,i) = &
              &f_pprime(1,n,k,j,i)*(cc1(1,1,k,j,i)**2)&
              &+f_prime(1,n,k,j,i)*cc1(2,1,k,j,i)
!
            cc(n+nvar,sndim(1,2),k,j,i) = f_prime(1,n,k,j,i)*cc1(1,1,k,j,i)
!
!
          END DO
        END DO
      END DO
!
      DEALLOCATE(f_prime,f_pprime)
!
    else
!
      call prime_periodic(1,n)
      call pprime_per(1,n)
!
      DO k = indk(1),indk(2)
        DO j = indj(1),indj(2)
          DO i = indi(1),indi(2)
!
            cc(n,sndim(1,2),k,j,i) = f_pprime_per(1,n,k,j,i)
            cc(n+nvar,sndim(1,2),k,j,i) = f_prime_periodic(1,n,k,j,i)
!
!
          END DO
        END DO
      END DO
!
      DEALLOCATE(f_prime_periodic,f_pprime_per)
!
    END IF
  END DO
END DO
!
! Set domain boundary limits for the r direction since the
! singularities arise at boundary pts
!=====

```

```

!
!
  if (sndim(1,2) == 1.and.dom_bound(1,1) == 0) indi(1) = loci(1)+1
  if (sndim(1,2) == 1.and.dom_bound(1,2) == 0) indi(2) = loci(2)-1
  if (sndim(2,2) == 1.and.dom_bound(2,1) == 0) indj(1) = locj(1)+1
  if (sndim(2,2) == 1.and.dom_bound(2,2) == 0) indj(2) = locj(2)-1
  if (sndim(3,2) == 1.and.dom_bound(3,1) == 0) indk(1) = lock(1)+1
  if (sndim(3,2) == 1.and.dom_bound(3,2) == 0) indk(2) = lock(2)-1
!
!   Compute the d/dt for all the variables
!=====
!
DO k = indk(1),indk(2)
  DO j = indj(1),indj(2)
    DO i = indi(1),indi(2)
!
!                                     150
      if (sndim(1,2) == 3) zpos = i
      if (sndim(2,2) == 3) zpos = j
      if (sndim(3,2) == 3) zpos = k
!
      Q1(k,j,i) = Damk * (eps**3) / ((tstar*zstar)**2) &
        &* f(2,k,j,i)*f(3,k,j,i) * &
        &exp (eps*(dfloat(1)/tstar - 1.d0 / f(1,k,j,i) ) )
!
      fprime(1,k,j,i) =(1.d0/Pr)*(cc(1,1,k,j,i)+&
        &cc(1,2,k,j,i)/(f(nvar+1,k,j,i)**2)&
        &+cc(1,3,k,j,i))+&
        &(1.d0/(f(nvar+1,k,j,i)*Pr)-&
        &f(nvar+1,k,j,i)*VEL(1,zpos))*cc(4,1,k,j,i)&
        &-VEL(2,zpos)*cc(4,2,k,j,i)&
        &-VEL(3,zpos)*cc(4,3,k,j,i)&
        &+beta*Q1(k,j,i)
!
      fprime(2,k,j,i) = (1.d0/Pr/Le1)*(cc(2,1,k,j,i)+&
        &cc(2,2,k,j,i)/(f(nvar+1,k,j,i)**2)&
        &+cc(2,3,k,j,i))+&
        &(1.d0/(f(nvar+1,k,j,i)*Le1*Pr)-&
        &f(nvar+1,k,j,i)*VEL(1,zpos))*cc(5,1,k,j,i)&
        &-VEL(2,zpos)*cc(5,2,k,j,i)&
        &-VEL(3,zpos)*cc(5,3,k,j,i)&
        &-alpha1*Q1(k,j,i)
!                                     170
      fprime(3,k,j,i) = (1.d0/Pr/Le2)*(cc(3,1,k,j,i)+&
        &cc(3,2,k,j,i)/(f(nvar+1,k,j,i)**2)&
        &+cc(3,3,k,j,i))+&
        &(1.d0/(f(nvar+1,k,j,i)*Le2*Pr)-&
        &f(nvar+1,k,j,i)*VEL(1,zpos))*cc(6,1,k,j,i)&
        &-VEL(2,zpos)*cc(6,2,k,j,i)&
        &-VEL(3,zpos)*cc(6,3,k,j,i)&
        &-alpha2*Q1(k,j,i)
!                                     180
!
      print 11, fprime(1,k,j,i), fprime(2,k,j,i), fprime(3,k,j,i)
!
!

```

```

        END DO
        END DO
        END DO
!
11      format(2x,3f12.8)
!
      END SUBROUTINE rhs
!
!=====
!=====
!
      subroutine bc(invar)
!
          USE vkvar
!
          IMPLICIT NONE
!
          INTEGER :: i,j,k,n,a1,b1,c1,tsize,stat,ii,zpos,ffsize,r
          INTEGER, INTENT(IN) :: invar
          INTEGER, dimension(2) :: indi, indj, indk
          REAL*8,dimension(:),allocatable :: trans
          REAL*8,dimension(:,,:),allocatable :: ff
          REAL*8 :: h1, h2,y0
!
!      B.C at z = 0:
!=====
!
          indi(1) = loci(1) - dom_bound(1,1)
          indi(2) = loci(2) - dom_bound(1,2)
          indj(1) = locj(1) - dom_bound(2,1)
          indj(2) = locj(2) - dom_bound(2,2)
          indk(1) = lock(1) - dom_bound(3,1)
          indk(2) = lock(2) - dom_bound(3,2)
!
          a1 = 0; b1 = 0; c1 = 0;
          if (sndim(1,2) == 3) a1 = 1
          if (sndim(2,2) == 3) b1 = 1
          if (sndim(3,2) == 3) c1 = 1
          if (sndim(1,2) == 3) ii = 1
          if (sndim(2,2) == 3) ii = 2
          if (sndim(3,2) == 3) ii = 3
!
          y0 = 0.22d0
!
          h1 = 1.d0/(12.d0*dx3)&
             &*cc1(1,ii,indk(1),indj(1),indi(1))
!
          if (sndim(1,2) == 3.and.dom_bound(1,1) == 0) then
!
              DO k = lock(1)-dom_bound(3,1),lock(2)-dom_bound(3,2)
                  DO j = locj(1)-dom_bound(2,1),locj(2)-dom_bound(2,2)
!
                      f(1,k,j,loci(1)) = T0
!

```

```

f(2,k,j,loci(1)) = (h1*(-3.d0*f(2,k,j,loci(1)+4)+&
&16.d0*f(2,k,j,loci(1)+3)-36.d0*f(2,k,j,loci(1)+2)&
&+48.d0*f(2,k,j,loci(1)+1))+Le1*Pe)/(Le1*Pe+25.d0*h1)
!
f(3,k,j,loci(1)) = (h1*(-3.d0*f(3,k,j,loci(1)+4)+&
&16.d0*f(3,k,j,loci(1)+3)-36.d0*f(3,k,j,loci(1)+2)&
&+48.d0*f(3,k,j,loci(1)+1)))/(Le2*Pe+25.d0*h1)
!
END DO
END DO
END if
!
if (sndim(2,2) == 3.and.dom_bound(2,1) == 0) then
!
DO k = indk(1),indk(2)
DO i = indi(1),indi(2)
!
f(1,k,locj(1),i) = T0
f(2,k,locj(1),i) = (h1*(-3.d0*f(2,k,locj(1)+4,i)+&
&16.d0*f(2,k,locj(1)+3,i)-36.d0*f(2,k,locj(1)+2,i)&
&+48.d0*f(2,k,locj(1)+1,i))+Le1*Pe)/(Le1*Pe+25.d0*h1)
!
f(3,k,locj(1),i) = (h1*(-3.d0*f(3,k,locj(1)+4,i)+&
&16.d0*f(3,k,locj(1)+3,i)-36.d0*f(3,k,locj(1)+2,i)&
&+48.d0*f(3,k,locj(1)+1,i)))/(Le2*Pe+25.d0*h1)
!
END DO
END DO
END if
!
if (sndim(3,2) == 3.and.dom_bound(3,1) == 0) then
!
DO j = indj(1),indj(2)
DO i = indi(1),indi(2)
!
f(1,lock(1),j,i) = T0
f(2,lock(1),j,i) = (h1*(-3.d0*f(2,lock(1)+4,j,i)+&
&16.d0*f(2,lock(1)+3,j,i)-36.d0*f(2,lock(1)+2,j,i)&
&+48.d0*f(2,lock(1)+1,j,i))+Le1*Pe)/(Le1*Pe+25.d0*h1)
!
f(3,lock(1),j,i) = (h1*(-3.d0*f(3,lock(1)+4,j,i)+&
&16.d0*f(3,lock(1)+3,j,i)-36.d0*f(3,lock(1)+2,j,i)&
&+48.d0*f(3,lock(1)+1,j,i)))/(Le2*Pe+25.d0*h1)
!
END DO
END DO
END if
!
B.C at z = zinf
!=====
!
if (sndim(1,2)==3.and.dom_bound(1,2) == 0) then
!

```



```

DO k = lock(1)-dom_bound(3,1),lock(2)-dom_bound(3,2)
  DO j = locj(1)-dom_bound(2,1),locj(2)-dom_bound(2,2)
!
!       f(1,k,j,loci(2)) = f(1,k,j,loci(2)-1)
!       f(2,k,j,loci(2)) = f(2,k,j,loci(2)-1)
!       f(3,k,j,loci(2)) = f(3,k,j,loci(2)-1)
!       f(1,k,j,loci(2)) = TINF
!       f(2,k,j,loci(2)) = 0.0d0
!       f(3,k,j,loci(2)) = 1.0d0/eq1
!
!       END DO
!     END DO
!   END if
!
!   if (sndim(2,2)==3.and.dom_bound(2,2) == 0) then
!
!     DO k = indk(1),indk(2)
!       DO i = indi(1),indi(2)
!
!         f(1,k,locj(2),i) = f(1,k,locj(2)-1,i)
!         f(2,k,locj(2),i) = f(2,k,locj(2)-1,i)
!         f(3,k,locj(2),i) = f(3,k,locj(2)-1,i)
!         f(1,k,locj(2),i) = TINF
!         f(2,k,locj(2),i) = 0.0d0
!         f(3,k,locj(2),i) = 1.0d0/eq1
!
!       END DO
!     END DO
!   end if
!
!   if (sndim(3,2)==3.and.dom_bound(3,2) == 0) then
!
!     DO j = indj(1),indj(2)
!       DO i = indi(1),indi(2)
!
!         f(1,lock(2),j,i) = f(1,lock(2)-1,j,i)
!         f(2,lock(2),j,i) = f(2,lock(2)-1,j,i)
!         f(3,lock(2),j,i) = f(3,lock(2)-1,j,i)
!         f(1,lock(2),j,i) = TINF
!         f(2,lock(2),j,i) = 0.0d0
!         f(3,lock(2),j,i) = 1.0d0/eq1
!
!       END DO
!     END DO
!   end if
!
!   B.C at r = 0
!=====
!   indi(1) = loci(1) - dom_bound(1,1)
!   indi(2) = loci(2) - dom_bound(1,2)
!   indj(1) = locj(1) - dom_bound(2,1)
!   indj(2) = locj(2) - dom_bound(2,2)
!   indk(1) = lock(1) - dom_bound(3,1)

```

```

indk(2) = lock(2) - dom_bound(3,2)
!
ffsize=0
if (sndim(1,2)==1.and.dom_bound(1,1) == 0) then
!
    allocate(ff(3,indk(1):indk(2),indj(1):indj(2)))
    DO n = 1,nvar
        DO k = indk(1),indk(2)
            DO j = indj(1),indj(2)
                ff(n,k,j)=0.d0
!
                DO r = -2,2,1
                    if (sndim(2,2)==2) ff(n,k,j) = ff(n,k,j)+f(n,k,j+r,loci(1)+1)+f(n,k,j+r,loci(1))
                    if (sndim(3,2)==2) ff(n,k,j) = ff(n,k,j)+f(n,k+r,j,loci(1)+1)+f(n,k+r,j,loci(1))
!
                END DO
                ff(n,k,j) = ff(n,k,j)/dfloat(10)
                f(n,k,j,loci(1)) = ff(n,k,j)
!
            END DO
        END DO
    END DO
    deallocate(ff)
!
END if
!
if (sndim(2,2)==1.and.dom_bound(2,1) == 0) then
!
    allocate(ff(3,indk(1):indk(2),indi(1):indi(2)))
!
    DO n = 1,nvar
        DO k = indk(1),indk(2)
            DO i = indi(1),indi(2)
                ff(n,k,i)=0.d0
!
                DO r = -2,2,1
                    if (sndim(1,2)==2) ff(n,k,i) = ff(n,k,i)+f(n,k,locj(1)+1,i+r)+f(n,k,locj(1),i+r)
                    if (sndim(3,2)==2) ff(n,k,i) = ff(n,k,i)+f(n,k+r,locj(1)+1,i)+f(n,k+r,locj(1),i)
!
                END DO
                ff(n,k,i) = ff(n,k,i)/dfloat(10)
                f(n,k,locj(1),i) = ff(n,k,i)
!
            END DO
        END DO
    END DO
    deallocate(ff)
!
END if
!
if (sndim(3,2)==1.and.dom_bound(3,1) == 0) then
!
    allocate(ff(3,indj(1):indj(2),indi(1):indi(2)))
!
    DO n = 1,nvar
        DO j = indj(1),indj(2)

```

```

DO i = indi(1),indi(2)
  ff(n,j,i)=0.d0
!
  DO r = -2,2,1
    if (sndim(1,2)==2) ff(n,j,i) = ff(n,j,i)+f(n,lock(1)+1,j,i+r)+f(n,lock(1),j,i+r)
    if (sndim(2,2)==2) ff(n,j,i) = ff(n,j,i)+f(n,lock(1)+1,j+r,i)+f(n,lock(1),j+r,i)
  END DO
  ff(n,j,i) = ff(n,j,i)/dfloat(10)
  f(n,lock(1),j,i) = ff(n,j,i)
!
!
  END DO
  END DO
  END DO
  deallocate(ff)
END if
!
!   B.C. at r = x2max
!=====
!
  if (sndim(1,2) == 1) ii = 1
  if (sndim(2,2) == 1) ii = 2
  if (sndim(3,2) == 1) ii = 3
!
  h1 = 1.d0/(12.d0*dx1)&
    &*cc1(1,ii,indk(2),indj(2),indi(2))
!
  if (sndim(1,2) == 1.and.dom_bound(1,2) == 0) then
!   DO n = 1,nvar
!     DO k = indk(1),indk(2)
!       DO j = indj(1),indj(2)
!
!         if (sndim(2,2) == 3) zpos = j
!         if (sndim(3,2) == 3) zpos = k
!
!         f(1,k,j,loci(2)) = f(1,k,j,loci(2)-1)
!         f(2,k,j,loci(2)) = ((-3.d0*f(2,k,j,loci(2)-4)+&
!           &16.d0*f(2,k,j,loci(2)-3)-36.d0*f(2,k,j,loci(2)-2)&
!           &+48.d0*f(2,k,j,loci(2)-1)))/(25.d0)
!         f(3,k,j,loci(2)) = ((-3.d0*f(3,k,j,loci(2)-4)+&
!           &16.d0*f(3,k,j,loci(2)-3)-36.d0*f(3,k,j,loci(2)-2)&
!           &+48.d0*f(3,k,j,loci(2)-1)))/(25.d0)
!
!         END DO
!       END DO
!     END DO
!   END if
!
!   if (sndim(2,2) == 1.and.dom_bound(2,2) == 0) then
!     DO n = 1,nvar
!       DO k = indk(1),indk(2)
!         DO i = indi(1),indi(2)
!

```

```

      if (sndim(1,2) == 3) zpos = i
      if (sndim(3,2) == 3) zpos = k
!
      f(1,k,locj(2),i) = f(1,k,locj(2)-1,i)
      f(2,k,locj(2),i) = ((-3.d0*f(2,k,locj(2)-4,i)+&
        &16.d0*f(2,k,locj(2)-3,i)-36.d0*f(2,k,locj(2)-2,i)&
        &+48.d0*f(2,k,locj(2)-1,i)))/(25.d0)
      f(3,k,locj(2),i) = ((-3.d0*f(3,k,locj(2)-4,i)+&
        &16.d0*f(3,k,locj(2)-3,i)-36.d0*f(3,k,locj(2)-2,i)&
        &+48.d0*f(3,k,locj(2)-1,i)))/(25.d0)
!
      END DO
      END DO
!
      END DO
      END if
!
      if (sndim(3,2) == 1.and.dom_bound(3,2) == 0) then
!
      DO n = 1,nvar
!
      DO j = indj(1),indj(2)
!
      DO i = indi(1),indi(2)
!
      if (sndim(1,2) == 3) zpos = i
      if (sndim(2,2) == 3) zpos = j
!
      f(1,lock(2),j,i) = f(1,lock(2)-1,j,i)
      f(2,lock(2),j,i) = ((-3.d0*f(2,lock(2)-4,j,i)+&
        &16.d0*f(2,lock(2)-3,j,i)-36.d0*f(2,lock(2)-2,j,i)&
        &+48.d0*f(2,lock(2)-1,j,i)))/(25.d0)
      f(3,lock(2),j,i) = ((-3.d0*f(3,lock(2)-4,j,i)+&
        &16.d0*f(3,lock(2)-3,j,i)-36.d0*f(3,lock(2)-2,j,i)&
        &+48.d0*f(3,lock(2)-1,j,i)))/(25.d0)
!
      END DO
      END DO
!
      END DO
      END if
!
!
!
      END SUBROUTINE bc
!
=====
=====
!
      Subroutine per_corr
!
      USE vkvar
!
      IMPLICIT NONE
!
      INTEGER :: i,j,k,n
!
      if (periodic(1).ne.0.and.dims(1)==1) then

```

460

470

480

490

500

```

do n = 1,nvar
  do k = lock(1) - dom_bound(3,1), lock(2) - dom_bound(3,2)
    do j = locj(1) - dom_bound(2,1), locj(2) - dom_bound(2,2)
!
      f(n,k,j,loci(1)) = f(n,k,j,loci(2)-ghostlayer-2)
      f(n,k,j,loci(1)+1) = f(n,k,j,loci(2)-ghostlayer-1)
      f(n,k,j,loci(2)) = f(n,k,j,loci(1)+ghostlayer+2)
      f(n,k,j,loci(2)-1) = f(n,k,j,loci(1)+ghostlayer+1)
!
    end do
  end do
end do
!
end if
!
if (periodic(2).ne.0.and.dims(2)==1) then
!
  do n = 1,nvar
    do k = lock(1) - dom_bound(3,1), lock(2) - dom_bound(3,2)
      do i = loci(1) - dom_bound(1,1), loci(2) - dom_bound(1,2)
!
        f(n,k,locj(1),i) = f(n,k,locj(2)-ghostlayer-2,i)
        f(n,k,locj(1)+1,i) = f(n,k,locj(2)-ghostlayer-1,i)
        f(n,k,locj(2),i) = f(n,k,locj(1)+ghostlayer+2,i)
        f(n,k,locj(2)-1,i) = f(n,k,locj(1)+ghostlayer+1,i)
!
      end do
    end do
  end do
!
end if
!
if (periodic(3).ne.0.and.dims(3)==1) then
  do n = 1,nvar
    do j = locj(1) - dom_bound(2,1), locj(2) - dom_bound(2,2)
      do i = loci(1) - dom_bound(1,1), loci(2) - dom_bound(1,2)
!
        f(n,lock(1),j,i) = f(n,lock(2)-ghostlayer-2,j,i)
        f(n,lock(1)+1,j,i) = f(n,lock(2)-ghostlayer-1,j,i)
        f(n,lock(2),j,i) = f(n,lock(1)+ghostlayer+2,j,i)
        f(n,lock(2)-1,j,i) = f(n,lock(1)+ghostlayer+1,j,i)
!
      end do
    end do
  end do
end if
!
End Subroutine per_corr
!
=====
=====
=====
!
Subroutine perturb

```

```

!
USE vkvar
USE vkpar
USE vk_in
!
IMPLICIT NONE
!
INTEGER :: i,j,k,n
INTEGER,dimension(2) :: indi,indj,indk
REAL*8 :: sp
sp = 1.d0
!
if (id==0) print *, 'Perturbing in Theta'
!
do i = 1,2
  indi(i) = loci(i)-dom_bound(1,i)
  indj(i) = locj(i)-dom_bound(2,i)
  indk(i) = lock(i)-dom_bound(3,i)
end do
!
if (wnum.gt.0.d0) sp = 0.d0
do n = 1,nvar
  do k = indk(1),indk(2)
    do j = indj(1),indj(2)
      do i = indi(1),indi(2)
        f(n,k,j,i) = f(n,k,j,i)*(1.d0+(1.d0-sp)*pert*(cos(wnum*f(5,k,j,i)))&
          &+sp*pert*(0.01*cos(f(5,k,j,i))+cos(acos(-1.))-f(4,k,j,i)/x1max*acos(-1.))))
        if (f(n,k,j,i).lt.1.d-20) f(n,k,j,i) = 1.d-20
      end do
    end do
  end do
end do
call track_error(t)
CALL vk_communication(1,fsize)
CALL output(t,1000)
!
end Subroutine perturb
!
!=====
!
END MODULE vk_cf

```

Sample Input

```

nvar  nstep  dt
3     10000 0.0002d0
ikutta iord
5     2
H0    b      eq1
0.1d0 1.     2.d0
rmin  thetmin zmin

```

```

0.0001 0.0 0.0
rmax  thetmax zmax
40.  0.0  25.
nr    ntheta  nz
64   64   64
St1  St2  St3
1.0  1.0  1.04
Pr   Le1  Le2  Damk      a1    a2    beta  Ze    bcval
1.0  1.0  1.0  1.90d0    .25d0 1.0   25.d0 40.   1.0
T0   TINF
1.0  1.0
Irestart      thetapert      wnum  err ouput freq  Contour_out_freq
3            0.01           0.0   100           25000
nproc1 nproc2 nproc3
0      0      0
tstar  zstar
7.43  1.54

```

Notes:

thetamax: **if 0**, direction is taken to be periodic

Irestart: 0 – Initial conditions given in
initial_conditions(nvar) in func_def.f90
1 – restart
2 – restart with time=0
3 – time=0, Initial conditions=temp_colsys.dat

therapert: Magnitude of perturbation (usually 0.01)

wnum: 0.0 – cos(r)
1.0 – cos(theta)
2.0 – cos(2theta)
3.0 – cos(3theta)
.
.
.

err_output_freq: Interval at which to print to screen

Contour_out_freq: Interval at which to write output

nproc: Number of processors assigned
to the respective direction.
If all are set to 0 then the optimal
combination is assigned.

References

- [1] V. Nayagam and F. A. Williams. Rotating Spiral Edges in Von Karman Swirling Flows, *Physical Review Letters* **84**, 3 (2000).
- [2] V. Nayagam and F. A. Williams. Pattern Formation in Diffusion Flames Embedded in Von Karman Swirling Flows, NASA/CP 2001-21082 (2001).
- [3] V. Nayagam and F. A. Williams. Pattern Formation in Diffusion flames Embedded in Von Karman Swirling Flows, NASA/CR 2006-214057 (2006).
- [4] M. H. Carpenter and C. A. Kennedy. Fourth-order 2N Storage Runge-Kutta Schemes, NASA Technical Memorandum 109112 (1994).
- [5] R. Vance, M. Miklavic, and I. S. Wichman. On the stability of one-dimensional diffusion flames established between plane, parallel, porous walls, *Combustion Theory and Modelling* **5**,, 147 (2001).
- [6] J. D. Buckmaster and G. S. S. Ludford, *Theory of Laminar Flames* (Cambridge University Press, 1982).
- [7] P. J. Zandbergen and D. Dijkstra. Von Karman Swirling Flows, *Annual Review of Fluid Mechanics* **19**, 456 (1987).
- [8] V. Nayagam and F. A. Williams. Diffusion Flame Extinction for a Spining Fuel Disk in an Oxidizer Counterflow, *Proceedings of the Combustion Institute* **28**, 2875 (2000).
- [9] M. L. Shay and P. D. Ronney. Nonpremixed Edge Flames in Spatially Varying Straining Flows, *Combustion and Flame* **112**, 117 (1998).
- [10] J. D. Buckmaster. Edge-Flames and their Stability, *Combustion Science and Technology* **115**, 1-3, 41 (1996).
- [11] J. D. Buckmaster. Edge-flames, *Progress in Energy and Combustion Science* **28**, 435 (2002).
- [12] G. L. Pellet, K. M. Isaac, W. M. J. Humphreys, L. R. Gartrell, W. L. Roberts, C. L. Dancey, and G. B. Northam. Velocity and Thermal Structure, and Strain-Induced Extinction of 14 to 100% Hydrogen-Air Counterflow Diffusion Flames, *Combustion and Flame* **112**, 575 (2002).

- [13] C. E. Frouzakis, A. G. Tomboulides, J. Lee, and K. Boulouchos. From Diffusion to Premixed Flames in an H₂/Air Opposed-Jet Burner: The Role of Edge Flames, *Combustion and Flame* **130**, 171 (2002).
- [14] Z. Lu and S. Ghoshal. Flame Holes and Flame Disks on the Surface of a Diffusion Flame, *Journal of Fluid Mechanics* **513**, 287 (2004).
- [15] J. D. Buckmaster, A. Nachman, and S. Taliaferro. The Fast-Time Instability of Diffusion Flames, *Physica D: Nonlinear Phenomena* **9**, **3**, 408 (1983).
- [16] J. S. Kim. Linear Analysis of Diffusional-Thermal Instability in Diffusion Flames with Lewis Numbers Close to Unity, *Combustion Theory and Modelling* **1**, 13 (1997).
- [17] S. Cheatham and M. Matalon. A General Asymptotic Theory of Diffusion Flames with Application to Cellular Instabilities, *Journal of Fluid Mechanics* **414**, 105 (2000).
- [18] S. Kukuck and M. Matalon. The Onset of Oscillations in Diffusion Flames, *Combustion Theory and Modelling* **5**, 217 (2001).
- [19] J. D. Buckmaster and T. L. Jackson. Holes in Flames, Flame Isolas, and Flame Edges, *Proceedings of the Combustion Institute* **28**, 1957 (2000).
- [20] M. Short and Y. Liu. Edge-flame Structure and Oscillations for Unit Lewis Numbers in a Non-premixed Counterflow, *Combustion Theory and Modelling* **8**, 425 (2004).
- [21] B. S. Margolis. Bifurcation Phenomena in Burner-Stabilized Premixed Flames, *Combustion Science and Technology* **22**, 143 (1979).
- [22] J. D. Buckmaster. Stability of the Porous Plug Burner Flame, *SIAM Journal on Applied Mathematics* **43**, **6**, 1335 (1983).
- [23] R. Chen, B. G. Mitchell, and P. D. Ronney. Diffusive-Thermal Instability and Flame Extinction in Nonpremixed Combustion, *Twenty-fourth Eighteenth Symposium (International) on Combustion* pp. 213–221 (1992).
- [24] S. P. Burke and T. E. W. Schumann. Diffusion Flames, 76th Meeting of the American Chemical Society **20**, **10**, 998 (1928).
- [25] M. Matalon. The Effect of Thermal Expansion on Flame Dynamics, 5th US Combustion Meeting (2007).
- [26] M. Matalon. Intrinsic Flame Instabilities in Premixed and Nonpremixed Combustion, *Annual Review of Fluid Mechanics* (2007).
- [27] M. Matalon and V. Kurdyumov. Effect of Thermal Expansion on Edge-Flames, 46th AIAA Aerospace Sciences Meeting and Exhibit (2008).
- [28] M. Smooke, C. McEnally, L. Pfefferle, R. Hall, and M. Colket. Computational and Experimental Study of Soot Formation in a Coflow, Laminar Diffusion Flame, *Combustion and Flame* **117**, **Issues 1-2**, 117 (1999).

- [29] G. Amantini and A. G. Jonathan H. Frank, Mitchell D. Smooke. Computational and Experimental Study of Standing Methane Edge Flames in the Two-Dimensional Axisymmetric Counterflow Geometry, *Combustion and Flame* **147**, 133 (2006).
- [30] U. Asher, J. Christiansen, and R. D. Russel. Collocation Software for Boundary Value ODEs, *ACM Transactions on Math Software* **7**, 223 (1981).
- [31] J. H. Williamson. Low Storage Runge-Kutta Schemes, *Journal of Computational Physics* (1980).
- [32] M. J. Quinn, *Parallel Programming in C with MPI and OpenMP* (McGraw-Hill, 2004).
- [33] A. Gray, *Modern Differential Geometry of Curves and Surfaces with Mathematica* (CRC Press, Boca Raton, FL, 1997).
- [34] R. W. Bilger. Turbulent Diffusion Flames, *Annual Review of Fluid Mechanics* **2**, 101 (1989).
- [35] R. W. Bilger. The Structure of Diffusion Flames, *Combustion Science and Technology* **13**, 155 (1976).
- [36] K. K. Kuo, *Principles of Combustion* (John Wiley and Sons, 1986).
- [37] N. Peters, *Turbulent Combustion* (Cambridge University Press, 2000).
- [38] V. Favier and L. Vervisch. Edge Flames and Partially Premixed Combustion in Diffusion Flame Quenching, *Combustion and Flame* **125**, 788 (2001).
- [39] N. Chakraborty and E. Mastorakos. Numerical Investigation of Edge Flame Propagation Characteristics in Turbulent Mixing Layers, *Physics of Fluids* **18**, 105103 (2006).

Curriculum Vitae

Kishwar Hossain

550 W Stocker St
Glendale, CA 91202
773-787-672

Education

5/2003 - Present

University of Illinois at Urbana Champaign, Department of Aerospace Engineering, Urbana, IL

§§ Doctorate

§§ GPA: 3.7, Minor: Computational Science and Engineering

5/2000 - 5/2003

University of Illinois - Urbana Champaign, Department of Aerospace Engineering, Urbana, IL

§§ Master's Degree

§§ GPA: 3.6

8/1997 - 5/2000

Lafayette College, Easton, PA

§§ Bachelor's Degree

§§ GPA: 3.5, Minor: Mathematics

§§ Graduated with Honors, Excel Scholar

Experience

Research Assistant

10/2007 – Present

Computational Science and Engineering, UIUC, Urbana, IL

§§ Member of the Combustion and Energetic Materials Group.

§§ Conducting a study on burn rates for heterogeneous solid-propellant packs using a 3-step kinetic model to evaluate the robustness of the model.

Researcher

5/2004 – Present

UIUC, Department of Aerospace Engineering, Urbana, IL

§§ Development of numerical algorithms to study flame dynamics.

§§ Conducting a study on the stability, and extinction characteristics of diffusion flames supported by a spinning methane burner. It is found that non-uniform flames, namely flame holes and spirals appear at near extinction conditions. These flames are simulated using a

three-dimensional parallel combustion code in cylindrical coordinates.

§§ Developed FORTRAN based computational code for solving three-dimensional combustion problems.

§§ Adapted the above code to run on a cluster of parallel computers using the MPI protocol.

Analyst – Graduate Assistant

8/2003 - 8/2006

Champaign Simulation Center, Caterpillar, Champaign, IL

§§ Structural analysis of earth moving vehicles using finite element methods. Generated finite element meshes using software such as IDEAS and Hypermesh and conducted analysis using NASTRAN and ABAQUS.

§§ Conducted modal analysis to identify critical frequencies in newly developed machines.

Analyst - CAT PRACTICUM Internship

5/2006 - 8/2006

CATERPILLAR INC., Champaign, IL

§§ Performed analysis for the Structural/Optimization group at the Champaign Simulation Center.

§§ Conducted non-linear structural analysis.

§§ Conducted fatigue analysis.

§§ Conducted linear static analysis using finite element models for different components of Caterpillar machines for validation of simulations with test results and for identifying weak spots in new designs.

§§ Conducted non-linear static analysis to identify structural weaknesses in designs during the development of new machines.

Analyst - CAT PRACTICUM Internship

5/2005 - 8/2005

CATERPILLAR INC., Champaign, IL

§§ Performed analysis for the Structural/Optimization group at the center.

§§ Conducted non-linear structural analysis.

§§ Conducted modal analysis.

Research Assistant

8/2000 - 5/2003

UIUC, Department of Aerospace Engineering, Urbana, IL

§§ Member of the Smart Icing Systems group, SIS, a multidisciplinary group dedicated to the development of a semi-autonomous icing protection system for small aircraft.

§§ Developed numerical algorithms to enhance the envelope protection systems of aircrafts impaired under icing conditions.

§§ Developed C code to implement the algorithms in a flight simulator.

§§ Developed a neural network in MATLAB to characterize icing effects as a function of aerodynamic coefficients.

Teaching Assistant

8/2000 - 12/2000

UIUC, Department of Aerospace Engineering, Urbana, IL

§§ Instructor for AAE 260, the undergraduate fluid dynamics lab course.

Instructor, Illinois Aerospace Institute Summer Camp

Summer 2001, Summer 2002, Summer 2003

UIUC, Department of Aerospace Engineering, Urbana, IL

§§ Instructor for aerodynamics sessions.

§§ Instructor for glider building sessions.

Research Assistant

8/1997 - 5/2000

Lafayette College, Easton, PA

§§ Conducted research on the behavior of viscoelastic materials under tensile loads.

§§ Developed a diagnostic setup to study thermoforming using thermocouples in conjunction with the Labview diagnostic interface.

§§ Designed and manufactured a pseudo fluidized bed for coating prepregs with microparticles.

Publications

§§ Hossain K., Jackson T., Buckmaster J., Numerical Simulations of Flame Patterns Supported by a Spinning Methane Burner, Submitted to the 32nd International Symposium on Combustion, 2008.

§§ Hossain K., Jackson T., Buckmaster J., Three-dimensional Simulations of Flames Supported by a Spinning Porous Plug Burner, AIAA 2008-1047, 2008.

§§ Wang, X., Hossain K., Jackson T., The Three-dimensional Numerical Simulation of Aluminized Composite Solid Propellant Combustion, Combustion Theory and Modelling, 11, 4, 2007.

§§ Hossain K., Sharma V., Bragg M., Voulgaris P., Envelope Protection and Control Adaptation in Icing Encounters, AIAA 2003-0025, 2003.

§§ Merret J., Hossain K., Bragg M., Envelope Protection and Atmospheric Disturbances in Icing Encounter, AIAA 2002-0814, 2002.

§§ Hummel, S. Hossain K., Hayes G., Biaxial Stress Relaxation of High Impact Polystyrene (HIPS) Above the Glass Transition Temperature, Polymer Engineering and Science, 41, 3, pg 566, 2001.

Activities

§§ Member of the Graduate Student Advisory Committee, Department of Aerospace Engineering, UIUC, 2006-2007